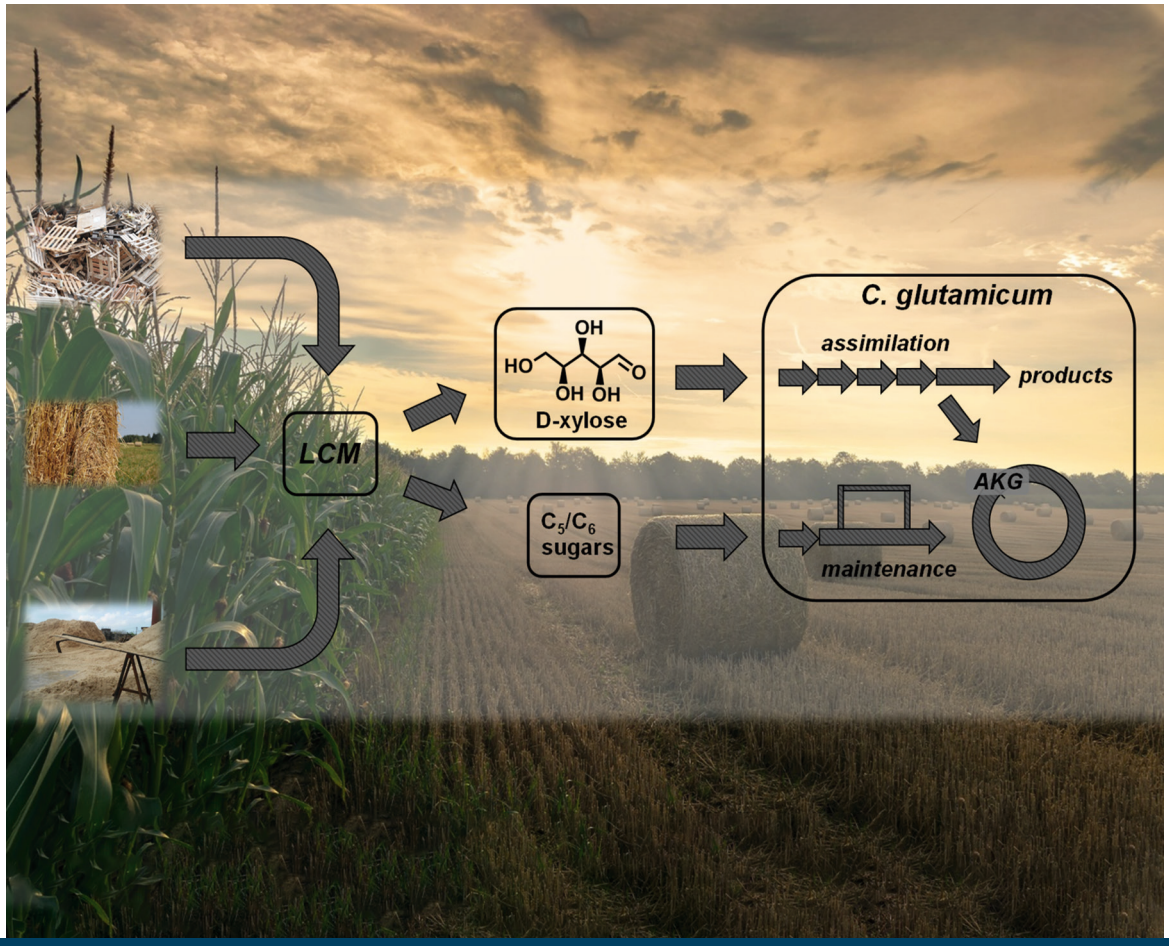

Shortcut to the carbon-efficient microbial production of chemical building blocks from lignocellulose-derived D-xylose

Christian Brüsseler

Schlüsseltechnologien / Key Technologies
Band / Volume 198
ISBN 978-3-95806-409-6

Mitglied der Helmholtz-Gemeinschaft

JÜLICH
Forschungszentrum

Shortcut to the carbon-efficient microbial production of chemical building blocks from lignocellulose-derived D-xylose

Inaugural Dissertation

submitted to
the Faculty of Mathematics and Natural Sciences
of the Heinrich Heine University Düsseldorf

presented by

Christian Brüsseler
born in Mönchengladbach

Jülich, February 2019

Forschungszentrum Jülich GmbH
Institut für Bio-und Geowissenschaften
Biotechnologie (IBG-1)

Shortcut to the carbon-efficient microbial production of chemical building blocks from lignocellulose-derived D-xylose

Christian Brüsseler

Schriften des Forschungszentrums Jülich
Reihe Schlüsseltechnologien / Key Technologies Band / Volume 198

ISSN 1866-1807 ISBN 978-3-95806-409-6

Bibliografische Information der Deutschen Nationalbibliothek.
Die Deutsche Nationalbibliothek verzeichnet diese Publikation in der
Deutschen Nationalbibliografie; detaillierte Bibliografische Daten
sind im Internet über http://dnb.d-nb.de abrufbar.

Herausgeber und Vertrieb:	Forschungszentrum Jülich GmbH Zentralbibliothek, Verlag 52425 Jülich Tel.: +49 2461 61-5368 Fax: +49 2461 61-6103 zb-publikation@fz-juelich.de www.fz-juelich.de/zb
Umschlaggestaltung:	Grafische Medien, Forschungszentrum Jülich GmbH
Druck:	Grafische Medien, Forschungszentrum Jülich GmbH
Copyright:	Forschungszentrum Jülich 2019

Schriften des Forschungszentrums Jülich
Reihe Schlüsseltechnologien / Key Technologies, Band / Volume 198

D 61 (Diss., Düsseldorf, Univ., 2019)

ISSN 1866-1807
ISBN 978-3-95806-409-6

Vollständig frei verfügbar über das Publikationsportal des Forschungszentrums Jülich (JuSER)
unter www.fz-juelich.de/zb/openaccess.

This is an Open Access publication distributed under the terms of the Creative Commons Attribution License 4.0, which permits unrestricted use, distribution, and reproduction in any medium, provided the original work is properly cited.

This thesis in hand has been performed at the Institute of Bio- and Geosciences, IBG-1: Biotechnology, Forschungszentrum Jülich GmbH, from November 2015 until February 2019 under the supervision of Prof. Dr. Michael Bott and Prof. Dr. Jan Marienhagen.

Printed with the permission of
the Faculty of Mathematics and Natural Sciences
of the Heinrich Heine University Düsseldorf

Examiner: **Prof. Dr. Michael Bott**
Institute of Bio- and Geosciences, IBG-1: Biotechnology
Forschungszentrum Jülich GmbH

Co-examiner: **Prof. Dr. Karl-Erich Jaeger**
Institute of Bio- and Geosciences, IBG-1: Biotechnology
Forschungszentrum Jülich GmbH

Date of oral examination: **27.05.2019**

„Zwei Dinge sind zu unserer Arbeit nötig. Unermüdliche Ausdauer und die Bereitschaft, etwas, in das man viel Zeit und Arbeit gesteckt hat, wieder wegzuwerfen.“

Albert Einstein, 1879 – 1955

deutscher Physiker

Results presented in this thesis have been published in three original publications. An additional manuscript has been submitted very recently:

Radek, A., Tenhaef, N., Müller, M. F., Brüsseler, C., Wiechert, W., Marienhagen, J., Polen, T., Noack, S. (2017). Miniaturized and automated adaptive laboratory evolution: Evolving *Corynebacterium glutamicum* towards an improved D-xylose utilization. *Bioresour. Technol.* 245: 1377 – 1385, permission to reuse in a thesis/ dissertation: license number 4517490894167

Brüsseler, C., Radek, A., Tenhaef, N., Krumbach, K., Noack, S., Marienhagen, J. (2018). The *myo*-inositol/proton symporter IolT1 contributes to D-xylose uptake in *Corynebacterium glutamicum*. *Bioresour. Technol.* 249: 953 – 961, permission to reuse in a thesis/dissertation: license number 4517490958577

Tenhaef, N., Brüsseler, C., Radek, A., Hilmes, R., Pornkamol, U., Marienhagen, J., Noack, S. (2018). Production of D-xylonic acid using a non-recombinant *Corynebacterium glutamicum* strain. *Bioresour. Technol.* 268: 332 – 339, permission to reuse in a thesis/dissertation: license number 4517491018872

Brüsseler, C., Späth, A., Sokolowsky, S., Marienhagen, J. (2019). Alone at last! – Heterologous expression of a single gene is sufficient for establishing the five-step Weimberg pathway in *Corynebacterium glutamicum*. Submitted in *Metabolic Engineering Communications* Submission no: MEC_2019_2; submitted January 27th, 2019

Table of contents

Abstract VII

Zusammenfassung VIII

Abbreviations IX

1. Scientific context and key results of this thesis ..... - 1 -

1.1 Society challenges and the bio-based economy ..... - 1 -

1.2 Lignocellulosic biomass ..... - 2 -

1.3 D-Xylose-utilizing pathways ..... - 4 -

1.4 *C. glutamicum* and its industrial relevance ..... - 6 -

1.6 Aims of the thesis ..... - 7 -

1.7 Key results on engineering *C. glutamicum* towards D-xylose utilization ..... - 8 -

1.7.1 Adaptive laboratory evolution improves D-xylose utilization ..... - 8 -

1.7.2 Rational engineering for improvement of D-xylose uptake ..... - 9 -

1.7.3 Production of the chemical building block D-xylonate ..... - 11 -

1.7.4 Reduction of the Weimberg pathway encoding operon ..... - 13 -

1.8 Conclusion and Outlook ..... - 16 -

2. Peer-reviewed publications ..... - 18 -

2.1 Evolution of a D-xylose metabolizing *C. glutamicum* strain ..... - 18 -

2.2 Discovery of a D-xylose transporter ..... - 27 -

2.3 Growth-decoupled production of D-xylonate ..... - 36 -

2.4 Discovery of an α-ketoglutarate semialdehyde dehydrogenase ..... - 44 -

3. References ..... - 51 -

4. Appendix ..... - 57 -

4.1 Authors‘ Contributions ..... - 57 -

4.2 Patent application ..... - 59 -

Danksagung ..... - 60 -

Erklärung ..... - 62 -

Abstract

In times of increasing scarcity of fossil raw materials, a growing world population and progressing climate change, more sustainable strategies are needed to secure global prosperity and to utilize available resources more responsibly. A bio-based economy can be part of the solution by transforming petrochemical-based processes into renewable, biomass-based processes. For establishing these large-scale microbial production processes metabolically versatile microorganisms, which can utilize a broad substrate spectrum, are required. In this context, the industrial workhorse *Corynebacterium glutamicum* was engineered for the efficient metabolization of the pentose D-xylose by systematic analysis and rational engineering of the metabolism. The following results have been obtained:

(1) The growth of a recently constructed *C. glutamicum* strain, which is able to utilize D-xylose via the Weimberg pathway, has been improved by an Adaptive laboratory Evolution strategy. Afterwards, beneficial mutations were identified by performing genome sequencing. Mutational studies revealed that loss of the transcriptional regulator IolR was mainly responsible for the observed improved growth on D-xylose. However, this result raised the question which of the 22 IolR-regulated genes contribute to D-xylose metabolization. Further investigations identified the *myo*-inositol/glucose symporter IolT1 to be involved in the transport of D-xylose, for which transcription of the respective gene is repressed by IolR.,. By rational disruption of a IolR-binding site in the chromosomal *iolT1* promoter, the repression could be abolished. Furthermore, it has been shown that the *myo*-inositol-2-dehydrogenase IolG, which is also transcriptionally repressed by IolR, contributes to the oxidation of D-xylose to D-xylonolactone, which is then hydrolyzed to D-xylonate spontaneously. By taking advantage of both effects, an efficient, non-GMO variant of *C. glutamicum* was constructed for the microbial production of D-xylonate from D-xylose. The achieved product yield matched the theoretical maximum yield of 1 mol mol^{-1}.

(2) A genome-wide search for additional endogenous genes potentially contributing to D-xylose utilization via the Weimberg pathway revealed a hitherto unknown α-ketoglutarate semialdehyde dehydrogenase capable of oxidizing α-ketoglutarate semialdehyde to α-ketoglutarate. This knowledge of endogenously encoded genes and enzymes catalyzing reactions of the Weimberg pathway allowed for the systematic reduction of the *xylXABCD*-operon from *Caulobacter crescentus*. In this context, it was demonstrated that expression of a heterologous 2-keto-3-deoxy-D-xylonate dehydratase or D-xylonate dehydratase is sufficient for establishing the five-step Weimberg pathway in *C. glutamicum*. Finally, application of the Weimberg pathway turned out to be more beneficial for the production of α-ketoglutarate from a D-glucose/D-xylose mixture compared to cultivations using D-glucose as sole substrate.

Zusammenfassung

In Zeiten zunehmender Verknappung fossiler Rohstoffe, einer wachsenden Weltbevölkerung und dem fortschreitenden Klimawandel werden nachhaltigere Strategien benötigt, um den erreichten Lebensstandard zu erhalten und gleichzeitig die verfügbaren Ressourcen verantwortungsvoller zu nutzen. Die Bioökonomie stellt hier eine vielversprechende Strategie dar, da sie Petrochemie-basierte Prozesse durch erneuerbare, Biomasse-basierte Prozesse ersetzt. Zur Etablierung solcher großtechnischen mikrobiellen Produktionsprozesse auf Basis nachwachsender Kohlenstoffquellen werden Mikroorganismen mit einem breiten Substratspektrum benötigt. Zu diesem Zweck wurde das in der industriellen Biotechnologie oft eingesetzte Bakterium *Corynebacterium glutamicum* durch systematische Analyse und rationales Engineering des Stoffwechsels in der Fähigkeit, die Pentose D-Xylose zu verstoffwechseln, verbessert. Dabei wurden die folgenden Ergebnisse erzielt:

(1) Das Wachstum eines kürzlich etablierten *C. glutamicum*-Stammes, der in der Lage ist D-Xylose über den Weimberg-Stoffwechselweg zu metabolisieren, wurde durch *Adaptive laboratory Evolution* verbessert. Die anschließende Genomsequenzierung isolierter Varianten zeigte, dass insbesondere der Verlust des transkriptionellen Regulators IolR für das verbesserte Wachstum verantwortlich war. Daraus ergab sich die Frage, welche der 22 durch IolR regulierten Gene zur Verstoffwechselung von D-Xylose beitragen. Weitere Untersuchungen identifizierten, dass der *myo*-Inositol/Glucose-Symporter IolT1, dessen Transkription durch IolR reprimiert ist, an der Aufnahme von D-Xylose beteiligt ist. Durch gezieltes Ausschalten einer IolR-Bindestelle im chromosomalen *iolT1*-Promotor konnte die Repression durch IolR verhindert werden. Weiterhin wurde gezeigt, dass die ebenfalls durch IolR regulierte *myo*-Inositol-2-Dehydrogenase IolG maßgeblich an der Oxidation von D-Xylose zu D-Xylonolacton beteiligt ist, das anschließend spontan zu D-Xylonat hydrolysiert. Mit dem Wissen um beide Effekte konnte ein als nicht genetisch modifiziert einzustufender *C. glutamicum*-Stamm für die mikrobielle Produktion von D-Xylonat aus D-Xylose konstruiert werden, dessen Produktausbeute dem theoretischen Maximum von 1 mol mol^{-1} entspricht.

(2) Weiterführende genomweite Untersuchungen ergaben, dass eine bisher unbekannte α-Ketoglutarat-Semialdehyd-Dehydrogenase in der Lage ist, α-Ketoglutarat-Semialdehyd zu α-Ketoglutarat zu oxidieren. Dieses Wissen über endogen kodierte Gene und Enzyme, die Reaktionen des Weimberg-Wegs katalysieren können, erlaubte die systematische Reduzierung des *xylXABCD*-Operon aus *Caulobacter crescentus*. Dabei zeigte sich, dass die heterologe Expression einer 2-Keto-3-Desoxy-D-Xylonat-Dehydratase oder einer D-Xylonat-Dehydratase für die Etablierung des fünfschrittigen Weimberg-Stoffwechselweges in *C. glutamicum* ausreichend ist. Abschließend wurde gezeigt, dass die Produktion von α-Ketoglutarat ausgehend von einem D-Glucose/D-Xylose-Gemisch vorteilhafter im Vergleich zur alleinigen Nutzung von D-Glucose ist.

Abbreviations

ALE	Adaptive laboratory Evolution
ATCC	American Type Culture Collection
BGR	Federal Institute for Geosciences and Raw Materials
BHI	brain heart infusion medium
bp	base pair
BS	backscatter
DNA	deoxyribonucleic acid
DO	dissolved oxygen
ESI	electro spray ionization
e.g.	(lat.) *exempli gratia* (for example)
et al.	(lat.) *et alii* (and others)
FACS	fluorescence activated cell sorting
FAO	Food and Agriculture Organization
GC-TOF-MS	gas chromatography coupled to time-of-flight mass spectrometry
GMO	genetically modified organism
GRAS	generally recognized as safe
IEA	International Energy Agency
IPCC	Intergovernmental Panel on Climate Change
IPTG	isopropyl-β-D-thiogalactopyranoside
Kan	kanamycin
KdxA	2-keto-3-deoxy-D-xylonate aldolase
KdxD	2-keto-3-deoxy-D-xylonate dehydratase
KgsaDh	α-ketoglutarate semialdehyde dehydrogenase
LB	lysogeny broth
MNP	multi nucleotide polymorphism
MOPS	3-morpholinopropanesulfonic acid
MPP	mini pilot plant
MTP	microtiter plate
µ	growth rate
NAD	nicotinamide adenine dinucleotide
NGS	Next Generation Sequencing
Ni-NTA	nickel-nitrilotriacetic acid
NOAA	National Centers for Environmental Information
nt	nucleotide
OD_{600}	optical density at a wavelength of 600 nm
ODHC	α-ketoglutarate dehydrogenase complex
ORF	open reading frame
PCR	polymerase chain reaction
pH	negative decimal logarithmic value of hydrogen ion concentration
RB	repetitive batch
rbs	ribosomal binding site
tRNA	transfer-ribonucleic acid
rpm	revolutions per minute
SNP	single nucleotide polymorphism
Spc	spectinomycin
TCA	tricarboxylic acid
TRIS	trishydroxymethylaminomethane
U	enzymatic activity unit (1 U = 1 µmol/min)
UN	United Nations

WMB1	expression plasmid pEKEx3-*xylXABCD*$_{Cc}$
WMB2	expression plasmid pEKEx3-*xylXABCD*$_{Cc}$-opt
WT	wild type
w/v	weight per volume
XDh	D-xylose dehydrogenase
XD	D-xylonate dehydratase
XI	D-xylose isomerase
XK	D-xylulose kinase
XL	D-xylonolactonase
XR	D-xylose reductase
XyDh	D-xylitol dehydrogenase

1. Scientific context and key results of this thesis

1.1 Society challenges and the bio-based economy

Over the past 43 years, the world's total primary energy consumption rose by more than 200 % from 25.54 x 10^4 PJ in 1973 to 57.62 x 10^4 PJ in 2016 (IEA 2018). This increase goes hand in hand with the exploitation and use of fossil raw materials (crude oil, natural gas and coal). Since the availability of these raw materials on earth is limited, the goal is to reduce the energy consumption by using more efficient technologies. However, the International Energy Agency (IEA) estimates that, if all actions to increase energy efficiency, which have been previously agreed to, will be implemented by 2040, the demand can only be reduced by 26 %. Without this reduction, the Federal Institute for Geosciences and Raw Materials (BGR) estimates in its annual report that the fossil raw materials, that are currently available on a reliable base, will only suffice for further 55 (crude oil), 59 (natural gas) and 113 (coal) years (BGR 2017). This situation is aggravated by the fact that, besides of their energetic use, these raw materials are also used in production of everyday commodities such as plastics, cosmetics or chemicals.

In addition to the limited availability, the combustion of these raw materials leads to high emissions of greenhouse gas, which contributes to climatic changes such as global warming. This was observed especially in the last twelve years of which nine have been considered to be the warmest years since the beginning of weather recordings (Gao *et al.,* 2018; NOAA 2018; IPCC 2014).

Furthermore, the global world population grows continuously and rose to its highest level of 7.63 billion people in October 2018. The United Nations (UN) estimate an increase to 9.7 billion people by 2050. Moreover, the UN evaluated that 821 million people already suffer from hunger (FAO 2018). This raises the question of how we are going to feed 9.7 billion people in the future.

To sum up, the increasing scarcity of fossil raw materials, the growing world population and the progressing climatic change pose major challenges for the global society. More sustainable strategies are needed to secure global prosperity and to utilize the available resources more responsibly.

The bio-based economy can provide promising assistance, as it tries to replace selected fossil raw material-dependent production processes with renewable biomass-based production processes (Langeveld *et al.,* 2010; Sanders *et al.,* 2007). One field of the bio-based economy is the industrial biotechnology, whose main goal is to convert renewable biomass with the use of microorganisms or enzymes derived thereof into food and feed, bio-based products or bio-energy, thus contributing to sustainable economic growth (FitzPatrick *et al.,* 2010).

1.2 Lignocellulosic biomass

Recently, the overall biomass composition of the biosphere was calculated to be 550 gigatons of carbon (Gt C), which consists of archaea (7 Gt C), viruses (0.2 Gt C), bacteria (70 Gt C), protists (4 Gt C), fungi (12 Gt C), animals (2 Gt C) and plants (primarily terrestrial) (450 Gt C) (Bar-on *et al.,* 2018).

More than 90 % of the terrestrial plants contain lignocellulose, which can further be subdivided into the three major components: cellulose (50 %), hemicellulose (24 %) and lignin (20 %) (Acatech 2012; Rubin 2008). Cellulose is the main structural component of cell walls and consists of a chain of β-1,4-linked D-glucose molecules. Hemicellulose, the second most abundant fraction is a polysaccharide, which contains a mixture of different C_5- and C_6-sugars (mainly D-xylose, but also D-glucose, D-arabinose, D-galactose and D-mannose). Finally, lignin is a phenolic three-dimensional macromolecule composed of different phenylpropanoid units (such as *p*-coumaryl alcohol, coniferyl alcohol or sinapyl alcohol) (Fig. 1) (Rubin 2008).

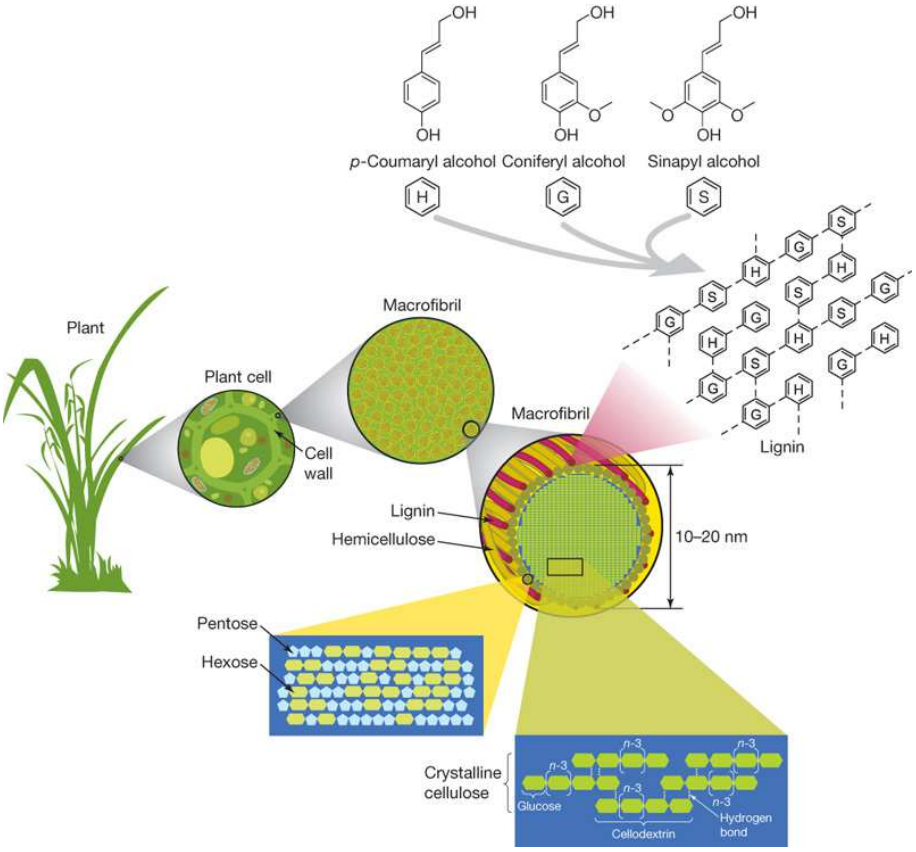

Fig. 1: Schematic overview of the composition of lignocellulosic biomass. Source: (Rubin 2008)

The economic significance of lignocellulosic biomass is reflected by the high abundance in many industrial waste streams. Consequently, this material has been identified as a potential source of fermentable sugars for the industrial biotechnology.

However, unprocessed lignocellulosic material cannot be used as feedstock in the microbial production due to the complex structures of lignin and cellulose. In a suitable procedure such as steam-, hot water-, acid-, lime or ammonia pretreatments, these structures first have to be disrupted (Mosier *et al.,* 2005). Ideally, after this procedure all monomers should be available for a potential production process.

In addition to substrate pretreatment, it has to be considered that many industrially relevant microorganisms have a limited substrate spectrum by nature. In these cases genetic engineering of the microorganisms is necessary to metabolize the complex sugar compositions derived from lignocellulosic biomass.

1.3 D-Xylose-utilizing pathways

Besides D-glucose, which can be readily metabolized by most organisms, D-xylose is the second most abundant fraction of lignocellulosic biomass. Several organisms such as bacteria, fungi and archaea are capable of utilizing D-xylose as carbon and energy source. In bacteria, usually the isomerase pathway is followed (Fig. 2). In this pathway, D-xylose is first isomerized to D-xylulose by a D-xylose isomerase (XI), which is subsequently phosphorylated by a xylulokinase (XK) yielding D-xylulose-5-phosphate (Anderson and Wood 1962; Chen 1980; Patrick and Lee 1968). As this compound is an intermediate of the pentose phosphate pathway it can be metabolized rapidly within the central carbon metabolism. In most fungi and yeast, D-xylose is first reduced to D-xylitol by a D-xylose reductase (XR) and subsequently oxidized to D-xylulose by a D-xylitol dehydrogenase (XyDh), which, similar to bacteria, is phosphorylated to D-xylulose-5-phosphate (Bolen *et al.,* 1986; Bruinenberg *et al.,* 1984; Rizzi *et al.,* 1988; Rizzi *et al.,* 1989; Wang and Jeffries 1990). In addition, yeast and filamentous fungi exhibiting a XI-activity have been reported (Banerjee *et al.,* 1994; Harhangi *et al.,* 2003; Vongsuvanlert and Tani 1988). In contrast, two oxidative and non-phosphorylating pathways have been discovered in most archaea and some bacterial and fungal strains. In these pathways, D-xylose is first oxidized by a D-xylose dehydrogenase (XDH) yielding D-xylonolactone, which is subsequently hydrolyzed by a D-xylonolactonase (XL) to D-xylonate. In case of the Weimberg pathway, two molecules of water are eliminated successively by a D-xylonate dehydratase (XD) and a 2-keto-3-deoxy-D-xylonate dehydratase (KdxD) yielding α-ketoglutarate semialdehyde, which is finally oxidized to α-ketoglutarate by an α-ketoglutarate semialdehyde dehydrogenase (KgsaDh). In case of the Dahms pathway, 2-keto-3-deoxy-D-xylonate is cleaved to pyruvate und glycolaldehyde by a 2-keto-3-deoxy-D-xylonate aldolase (KdxA) (Dahms and Donald 1982; Johnsen *et al.,* 2009; Stephens *et al.,* 2007; Weimberg 1961).

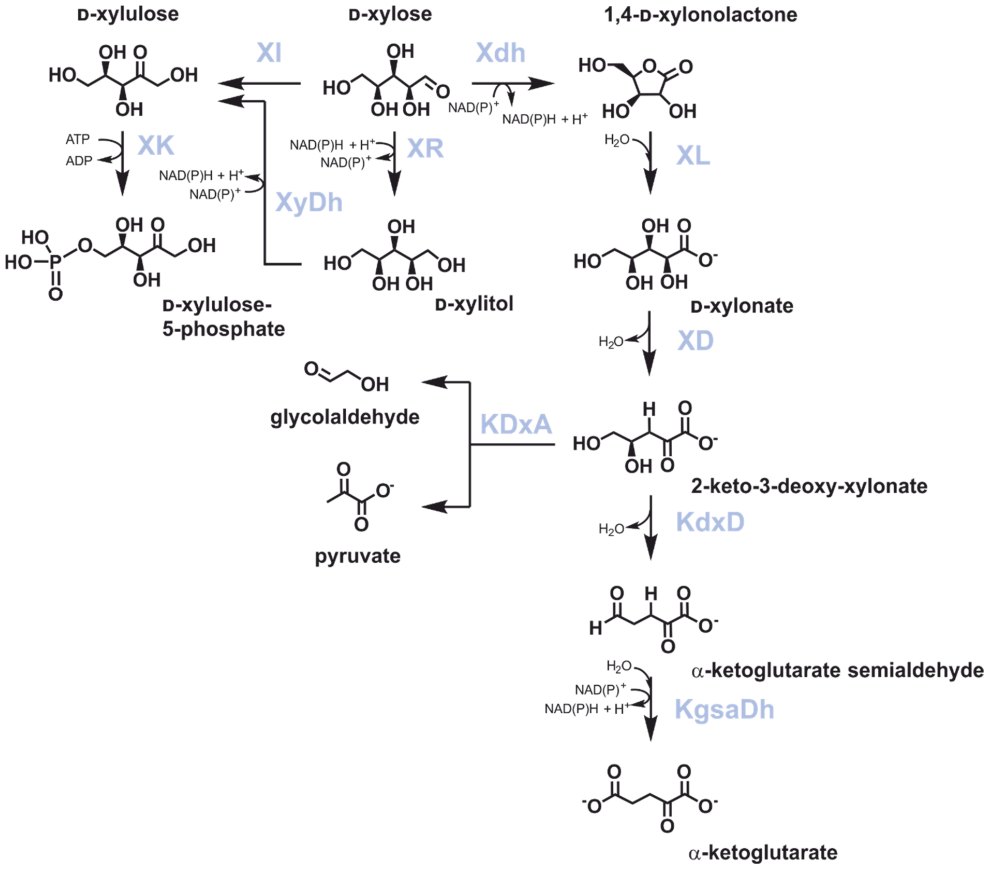

Fig. 2: Overview of different metabolic strategies for D-xylose utilization. Abbreviations: XDh: D-xylose dehydrogenase, XL: D-xylonolactonase, XD: D-xylonate dehydratase, KdxD: 2-keto-3-deoxy-D-xylonate dehydratase, KgsaDh: α-ketoglutarate semialdehyde dehydrogenase, KdxA: 2-keto-3-deoxy-D-xylonate aldolase, XR: D-xylose reductase, XyDh: D-xylitol dehydrogenase, XI: D-xylose isomerase, XK: D-xylulose kinase. **Weimberg pathway**: XDh, XL, XD, KdxD, KgsaDh. **Dahms pathway**: XDh, XL, XD, KdxA. **Oxido-reductase pathway**: XR, XyDh, XK. **Isomerase pathway**: XI, XK

1.4 *Corynebacterium glutamicum* and its industrial relevance

Corynebacterium glutamicum is a Gram-positive, non-pathogenic and biotin-auxotrophic soil bacterium, which was first discovered in 1957 when scientists were searching for a natural L-glutamate-producing microorganism (Kinoshita *et al.,* 1957). The isolated microorganism was first named *Micrococcus glutamicus* No. 534 and later renamed *Corynebacterium glutamicum* after a more detailed taxonomic characterization *(*Abe *et al.,* 1967*;* Eggeling and Bott 2005). Thenceforward, application of this organism changed the amino acid producing industry, enabling the microbial production of L-glutamate and L-lysine with *C. glutamicum* at a million ton-scale per year (Eggeling and Bott 2015; Wendisch *et al.,* 2014).

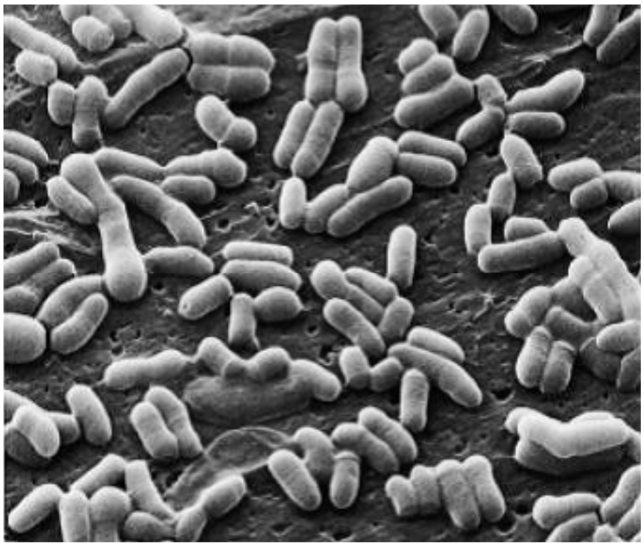

Fig. 3: Electron microscopic image of *C. glutamicum* ATCC13032 Source: (Sahm *et al.,* 2000)

Initially, strains have been optimized for amino acid production by mutagenesis and subsequent screening cycles and later by rational engineering (Becker et al., 2011; Ikeda 2006). Important milestones in the development of *C. glutamicum* as a model organism and industrial workhorse was the sequencing of the entire genome in 2003 and the construction of numerous tools for genetic engineering such as expression plasmids or promoters (Kalinowski *et al.,* 2003; Pátek and Nešvera 2013). During the

last years, *C. glutamicum* strains have been engineered for more than 70 biotechnologically interesting compounds such as alcohols, organic acids, biofuels or polyphenols (Becker *et al.,* 2018; Kallscheuer *et al.,* 2016; Kallscheuer *et al.,* 2017; Vogt *et al*., 2016; Wieschalka *et al.,* 2013). Apart from the capability to produce many different biotechnologically relevant compounds, all products obtained by *C. glutamicum* have GRAS (generally recognized as safe) status.

However, to date all large-scale applications for amino acid production with *C. glutamicum* use D-glucose from starch hydrolysates or D-fructose (and sucrose) from molasses. The substrate spectrum of *C. glutamicum* variants engineered for other small molecules is mostly limited to these hexoses (Blombach and Seibold 2010). For a more sustainable production using *C. glutamicum,* it is essential to expand its substrate spectrum with respect to the use of lignocellulose-containing material. In the recent past, some efforts have been made in engineering *C. glutamicum* for D-xylose metabolization, the key building block of the hemicellulose fraction. In 2006, the isomerase pathway was implemented in *C. glutamicum* by heterologous expression of a XI (encoded by *xylA*) from either *Escherichia coli* or *Xanthomonas campestris* with additional expression of the endogenous XK (encoded by *xylB*) yielding the pentose phosphate pathway intermediate xylulose-5-phosphate (Fig. 2) (Kawaguchi *et al.,* 2006; Kawaguchi *et al.,* 2008). In contrast, the oxidative five-step Weimberg pathway was established in 2014 by heterologous expression of genes coding for XDh (encoded by *xylB*), XL (encoded by *xylC*), XD (encoded by *xylD*), KdxD (encoded by *xylX*) and KgsaDh (encoded by *xylA*) from *Caulobacter crescentus* (Radek *et al.,* 2014).

1.6 Aims of this thesis

The major objective of this thesis is to identify and engineer key genetic targets for the improvement of D-xylose utilization in recently established, D-xylose-metabolizing *C. glutamicum* strains. This includes the detailed genome-wide search of genes potentially coding for enzymes involved in D-xylose utilization as well as engineering of the host metabolic network. Based on the knowledge gained, the strains were supposed to be improved for D-xylose utilization and engineered towards production of D-xylonate and α-ketoglutarate as biotechnologically interesting compounds.

1.7 Key results on engineering *C. glutamicum* towards D-xylose utilization

1.7.1 Adaptive laboratory evolution improves D-xylose utilization

(Radek et al., 2017, Bioresource Technology, cf. chapter 2.1)

C. glutamicum WMB1 was the first engineered strain for D-xylose utilization via the Weimberg pathway, but only reached a growth rate of $\mu = 0.07\ h^{-1}$ in medium containing only D-xylose as carbon and energy source. In this strain, the native pentacistronic operon from *C. crescentus* comprised of genes coding for XDh (encoded by *xylB*), XL (encoded by *xylC*), XD (encoded by *xylD*), KdxD (encoded by *xylX*) and KgsaDh (encoded by *xylA*) was heterologously expressed. With the aim to improve the overall performance of the pathway in *C. glutamicum*, gene variants, codon-optimized for expression in *C. glutamicum* were synthesized and organized as synthetic pentacistronic operon on the expression plasmid pEKEx3. Subsequently, the wild-type strain *C. glutamicum* ATCC13032 (WT) was transformed, using the resulting plasmid pEKEx3-*xylXABCD*$_{Cc}$-opt, and subsequently cultivated in defined CGXII minimal medium containing 40 g L^{-1} D-xylose as sole carbon and energy source. The obtained strain *C. glutamicum* WMB2 strain allowed for a growth rate of $\mu = 0.10\ h^{-1}$ corresponding to an improvement of 43 % compared to the strain *C. glutamicum* WMB1.

For further improving growth, an Adaptive laboratory Evolution (ALE) strategy was followed, in which faster-growing *C. glutamicum* variants in D-xylose containing medium were isolated. By using this technique, a strain was obtained that showed a maximum growth rate of $\mu_{max} = 0.26 \pm 0.01\ h^{-1}$ when cultivated in defined CGXII minimal medium containing 40 g L^{-1} D-xylose as sole carbon and energy source. The isolated strain was named *C. glutamicum* WMB2$_{evo}$.

In order to identify the underlying reasons for the improved growth phenotype, genome sequencing of *C. glutamicum* WMB2$_{evo}$ was performed. This analysis revealed that mainly genes coding for enzymes presumably involved in the metabolism of *myo*-inositol were affected. A deletion of 98 nucleotides (nt) from position 133 to 232 relative to the start codon in the open reading frame (ORF) of the transcriptional regulator gene *iolR* was identified, which most probably led to its inactivation. As this regulator is responsible for the regulation of 22 genes, it was assumed that this deletion had a large influence on cell metabolism. Furthermore, upstream of the *myo*-inositol

transporter gene *iolT1* different single nucleotide polymorphisms (SNP) and multi nucleotide polymorphisms (MNP) were found. However, since it is not known how the repression of *iolT1* through IolR can be prevented, it is unclear whether these mutations also have an effect on the expression of *iolT1*. Additional point mutations and partial gene deletions were identified in gene cg3388, which is assumed to encode a repressor controlling the expression of the putative *myo*-inositol transporter gene *iolT2*. Furthermore, mutations in gene cg0587 (*tuf*) coding for the elongation factor Tu (EF-TU) have been identified. This elongation factor enables binding of an aminoacyl-transfer ribonucleic acid (tRNA) to the ribosome during translation.

1.7.2 Rational engineering for improvement of D-xylose uptake

(Brüsseler et al., 2018, Bioresource Technology, cf. chapter 2.2)

After identification of different mutations in *C. glutamicum* WMB2$_{evo}$, a detailed characterization of these mutations was performed. Structural similarity between D-xylose and the cyclic polyol *myo*-inositol led to the assumption that mutations in genes coding for enzymes involved in the metabolism of *myo*-inositol might be responsible for improved growth. For this reason, the observed deletion of 98 nt in the ORF of the transcriptional regulator gene *iolR* was chosen as the most promising target as this regulator controls the expression of 22 genes (Klaffl *et al.,* 2013). Consequently, the *iolR* gene was deleted in *C. glutamicum* WT yielding *C. glutamicum* Δ*iolR,* which was subsequently transformed with the Weimberg pathway encoding plasmid pEKEx3-*xylXABCD*$_{Cc}$-opt. The constructed strain *C. glutamicum* Δ*iolR* WMB2 was cultivated in comparison to *C. glutamicum* WMB2 in defined CGXII medium supplemented with 40 g L^{-1} D-xylose as sole carbon and energy source. Astonishingly, the specific maximum growth rate of *C. glutamicum* Δ*iolR* WMB2 was μ_{max} = 0.28 h^{-1} which was twice as high as the growth rate of *C. glutamicum* WMB2 (μ_{max} = 0.13 h^{-1}). Beyond, growth of *C. glutamicum* Δ*iolR* WMB2 was characterized by a much shorter lag phase.

This observed improvement in growth encouraged further investigations for uncovering the underlying physiological consequences of the absence of the transcriptional regulator. Among the IolR-regulated genes, there are several gene products involved in the degradation and transport of *myo*-inositol, which could also contribute to the metabolization of D-xylose. The most promising candidates included *myo*-inositol

dehydrogenase (OxiA, encoded by *oxiA)*, aldehyde dehydrogenase (IolA, encoded by *iolA),* 2-keto-*myo*-inositol dehydratase (IolE, encoded by *iolE)*, efflux carrier (IolP, encoded by *iolP),* and glucose permease/*myo*-inositol transporter (IolT1, encoded by *iolT1*). Among these candidates, *iolT1* stood out as several mutations upstream of the *iolT1*-ORF were identified during the genome sequence analyses. In order to assess the contribution of these proteins during D-xylose utilization, all five genes were deleted individually in the strain background of *C. glutamicum* Δ*iolR* WMB2 and a comparative cultivation with respect to the parental strain was performed in defined CGXII medium with 40 g L^{-1} D-xylose as sole carbon and energy source. While the absence of *oxiA*, *iolE*, *iolP* or *iolA* led to the same growth behavior as the reference strain, deletion of *iolT1* resulted in a very similar growth to *C. glutamicum* WMB2 with intact regulation by IolR. Monitored D-xylose concentrations in the supernatant revealed that *C. glutamicum* Δ*iolR* WMB2 consumed nearly all of the available pentose within 30 h (residual concentration in the supernatant: 0.70 ± 0.12 g L^{-1} D-xylose). In comparison to this only 25 % of the initial D-xylose amount were consumed by *C. glutamicum* Δ*iolR* Δ*iolT1* WMB2 in the same time (residual concentration in the supernatant: 27.36 ± 0.24 g L^{-1} D-xylose). This shows that IolT1 indeed contributes to D-xylose uptake in *C. glutamicum*, which was hitherto unknown. However, potential negative effects could never be excluded because of the deregulation of all IolR-controlled genes. For this reason, a precise deregulation of the *iolT1* expression was desired. In a previous study, the consensus DNA binding motif of IolR was determined and two IolR-binding sites in the *iolT1*-promotor could be identified (Klaffl *et al.,* 2013). In context of this work, the IolR-binding site, designated as O6, was disrupted by substituting two highly conserved nucleotides at position -29 and -28 (A→G and C→G, respectively) relative to the transcriptional start site of *iolT1*. The resulting strain designated as *C. glutamicum* P_{O6} *iolT1* was subsequently transformed with the Weimberg pathway encoding plasmid pEKEx3-*xylXABCD*$_{Cc}$-opt and cultivated in comparison to *C. glutamicum* Δ*iolR* WMB2. Interestingly, both strains showed the same growth behavior indicating that mutation of the IolR-binding site O6 efficiently prohibits repression of *iolT1*.

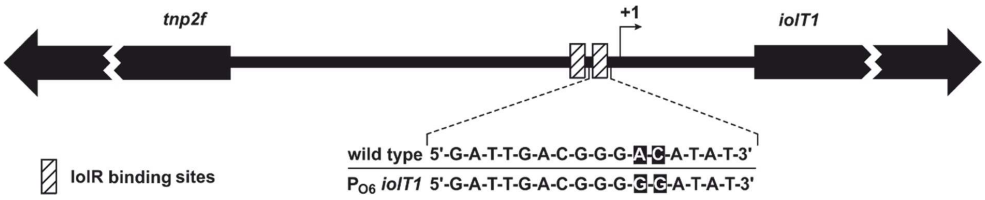

Fig. 4: Schematic representation of the intergenic region of *tnp2f* and *iolT1* on the chromosome of *C. glutamicum*. The two white boxes with diagonal black bars indicate the IolR binding sites. Furthermore, the transcriptional start site and the wild-type sequence in comparison to the engineered sequence of *C. glutamicum* P_{O6} *iolT1* are displayed.

1.7.3 Production of the chemical building block D-xylonate

(Tenhaef et al., 2018, Bioresource Technology, cf. chapter 2.3)

During growth studies of *C. glutamicum* Δ*iolR* WMB2, and *C. glutamicum* P_{O6} *iolT1* WMB2 it was observed that the control strains *C. glutamicum* Δ*iolR, C. glutamicum* P_{O6} *iolT1* and *C. glutamicum* WT already accumulated the Weimberg pathway intermediate D-xylonate in the supernatant. This commercially available C_5 sugar acid has a potential to replace or complement the available C_6 sugar acid D-gluconate, which is derived from D-glucose and already biotechnological produced in a scale of 100,000 t per year. In case of D-gluconate many applications are described, e.g. for production of pharmaceuticals, solvents, food and additional products (Climent *et al.,* 2011; Toivari *et al.,* 2012).

In contrast to *C. glutamicum* Δ*iolR, C. glutamicum* P_{O6} *iolT1* and *C. glutamicum* WT accumulated D-xylonate to a much lower extend. This observation indicates that the loss of the transcriptional regulator IolR does not only have an impact on D-xylose uptake but additionally also affects either i) D-xylose oxidation or ii) D-xylonate export or iii) both.

First, the gluconate permease (GntP, encoded by *gntP*) was identified as the most promising D-xylonate exporter candidate in *C. glutamicum*, as it has already been demonstrated in *Pseudomonas putida* that a similar gluconate permease is capable to export D-xylonate as a side activity. Furthermore, the putative *myo*-inositol permease (IolP, encoded by *iolP*) as second transport protein might contribute to D-xylonate export. In order to find out whether one or both permeases are involved in the export

of D-xylonate, the corresponding genes were deleted individually in *C. glutamicum* Δ*iolR* and a triple deletion strain was constructed by deleting both permease genes. All strains were examined in a comparative cultivation for their ability to accumulate D-xylonate in the supernatant. Therefore, defined CGXII minimal medium supplemented with 10 g L^{-1} D-glucose and 30 g L^{-1} D-xylose was chosen as cultivation medium since the constructed strains are not capable to use D-xylose as sole carbon and energy source due to the lack of the expression of genes coding for the Weimberg pathway. During this cultivation, no differences regarding D-xylonate formation were observable, indicating that neither the gluconate permease GntP nor the putative *myo*-inositol permease IolP are involved in D-xylonate export.

This reinforced the suspicion that the oxidation of D-xylose to D-xylonolactone is affected, which is usually catalyzed by dehydrogenases (Stephens *et al.,* 2007; Weimberg 1961). The expression of genes coding for aldehyde dehydrogenase (IolA, encoded by *iolA*), 5-deoxy-glucuronate isomerase (IolB, encoded by *iolB*), *myo*-inositol-2 dehydrogenase (IolG, encoded by *iolG*), *myo*-inositol dehydrogenase (OxiA, encoded by *oxiA*) and *myo*-inositol catabolism isomerase/epimerase (IolH, encoded by *iolH*) are under the transcriptional control of IolR and could potentially contribute to the oxidation of D-xylose (Klaffl *et al.,* 2013). Again, individual double-deletion strains were constructed and cultivated in defined CGXII minimal medium supplemented with 10 g L^{-1} D-glucose as carbon and energy source and 30 g L^{-1} D-xylose. While the deletion of *iolA*, *iolB*, *oxiA* and *iolH* had no influence on the D-xylonate accumulation capacity, the deletion of *iolG* resulted in a significant decrease in extracellular amounts of D-xylonate. *C. glutamicum* Δ*iolR* Δ*iolG* accumulated 7.8 g L^{-1} (47 mM) D-xylonate in the supernatant whereas *C. glutamicum* Δ*iolR* converted the entire D-xylose used. To validate the participation of IolG in the oxidation of D-xylose, plasmid-based complementation of the *iolG*-deletion was performed which indeed restored the ability to accumulate D-xylonate. These experiments revealed that IolG contributes to the oxidation of D-xylose in *C. glutamicum* Δ*iolR.*

Due to the high product titers, process development for the production of D-xylonate was started with *C. glutamicum* Δ*iolR*. In a first step, batch cultivation in a bioreactor (1L) was performed using defined CGXII minimal medium with 10 g L^{-1} D-glucose and 40 g L^{-1} D-xylose. In total, a final concentration of 24.0 ± 0.01 g L^{-1} D-xylonate with a yield of 1 mol mol^{-1} was achieved, which is also the theoretical maximum. Since the

production rate after D-glucose consumption was reduced significantly, it was assumed that the availability of the reduction equivalent nicotinamide adenine dinucleotide (NAD^+) was limiting. For this reason, the next step was to investigate production under fed-batch conditions. Therefore, the D-glucose concentration was increased to 20 g L^{-1} and after depletion of the initial D-glucose, a low feed rate of 7.5 ml h^{-1} with a 100 g L^{-1} D-glucose solution was started. At the end, the D-xylonate titer was increased by 50 % to 35.7 ± 0.10 g L^{-1}.

In order to make a potential D-xylonate production process more sustainable and cost-effective, the consumption of sugarcane bagasse instead of defined and purified sugar mixtures was investigated in a one-pot hydrolysis and fermentation process. First, optimization of the fermentation medium using sugarcane bagasse as carbon and energy source was investigated. In this context, it turned out that the optimal composition requires the addition of a nitrogen source (such as ammonium sulfate) and a phosphate source (such as dibasic potassium phosphate) as well as biotin. Based on these results, a one-pot process in a buffer system using 50 mM acetate was designed. After enzymatic hydrolysis (72 h), the nitrogen and phosphate sources as well as biotin were added and the cultivation was performed for 24 h. At the end, a D-xylonate concentration of 5.7 ± 0.03 g L^{-1} was achieved while the yield was close to the theoretical maximum.

1.7.4 Reduction of the Weimberg pathway encoding operon

(Brüsseler et al., 2019, Metabolic Engineering Communications, cf. chapter 2.4)

The presence of the endogenously encoded transport (IolT1) and oxidation of D-xylose (IolG) led to accumulation of the Weimberg pathway intermediate D-xylonate in the supernatant when *C. glutamicum* strains were cultivated in D-xylose-containing medium (Fig. 5). This indicated that the expression of the heterologous XDh (encoded by *xylB*) and the XL (encoded by *xylC*) from *C. crescentus* might not be required for establishing the Weimberg pathway. Therefore, a new, reduced synthetic operon comprised of the codon-optimized genes coding for KdxD (encoded by *xylX*), XD (encoded by *xylD*) and KgsaDh (encoded by *xylA*) was constructed. The resulting pEKEx3-*xylXAD*$_{Cc}$-opt expression plasmid was introduced in *C. glutamicum* P_{O6} *iolT1* yielding *C. glutamicum* P_{O6} *iolT1* pEKEx3-*xylXAD*$_{Cc}$-opt which was subsequently cultivated in comparison to *C. glutamicum* P_{O6} *iolT1* WMB2 in defined CGXII minimal

medium containing 40 g L^{-1} D-xylose as sole carbon and energy source. Astonishingly, growth of both strains was indistinguishable (μ_{max} = 0.26 ± 0.006 h^{-1}, μ_{max} = 0.26 ± 0.004 h^{-1}, respectively) indicating that the expression of genes coding for the heterologous XDh and XL was not necessary or beneficial for growth of *C. glutamicum*.

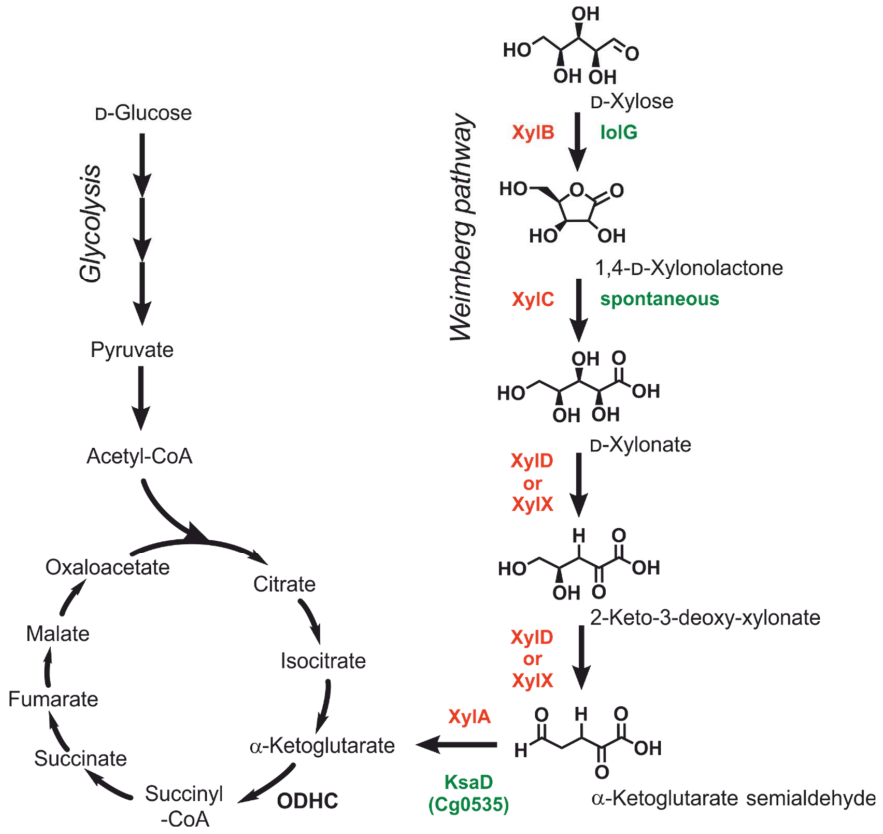

Fig. 5: Schematic overview of the metabolic connection of the Weimberg pathway to the central carbon metabolism of *C. glutamicum*. Endogenously encoded enzymes of *C. glutamicum* capable of catalyzing reactions in the Weimberg pathway are shown in green. The corresponding analogous enzymes obtained from *C. crescentus* are highlighted in red. Abbreviations: XylB, xylose dehydrogenase; XylC, D-1,4-xylono lactonase; XylD, D-xylonate dehydratase; XylX, 2-keto-3-deoxy-D-xylonate dehydratase; XylA, α-ketoglutarate semialdehyde dehydrogenase; IolG, *myo*-inositol-2-dehydrogenase; KsaD, α-ketoglutarate semialdehyde dehydrogenase; ODHC, α-ketoglutarate dehydrogenase complex

Motivated by these results, a genome-wide search was performed to identify additional endogenously encoded enzymes, which could potentially replace the activity of the heterologous XD (encoded by *xylD*), KdxD (encoded by *xylX*) or KgsaDh (encoded by

xylA). This analysis revealed a gene coding for a putative α-ketoglutarate semialdehyde dehydrogenase (encoded by cg0535). Although nothing was known about the regulation and natural expression conditions of cg0535, the synthetic Weimberg pathway encoding operon was reduced by the gene coding for the heterologous KgsaDh (encoded by *xylA)*. The resulting pEKEx3-*xylXD*$_{Cc}$-opt expression plasmid was introduced in *C. glutamicum* P_{O6} *iolT1* and a comparative cultivation of the resulting strain *C. glutamicum* P_{O6} *iolT1* pEKEx3-*xylXD*$_{Cc}$-opt with respect to *C. glutamicum* P_{O6} *iolT1* pEKEx3-*xylXAD*$_{Cc}$-opt was performed. This cultivation experiments revealed that *C. glutamicum* harbors an endogenous KgsaDh activity as both strains exhibited the same growth rate (μ_{max} = 0.26 ± 0.008 h^{-1}, μ_{max} = 0.26 ± 0.006 h^{-1}, respectively). Further experiments disclosed that the gene cg0535 indeed encodes for a KgsaDh, which prefers the co-substrate NAD^+. Therefore, the gene was designated as *ksaD* (α-ketoglutarate semialdehyde dehydrogenase).

Additional analysis of the *C. glutamicum* genome did not identify genes coding for dehydratases potentially catalyzing the dehydration reactions of the Weimberg pathway. However, enzyme assays performed with the KdxD and XD from *C. crescentus* showed that both dehydratases accept D-xylonate as substrate. Besides, the substrates of both dehydratases, D-xylonate and 2-keto-3-deoxy-xylonate, are very similar in their structures. Therefore, the Weimberg pathway encoding operon was further reduced by constructing the two expression plasmids pEKEx3-*xylX*$_{Cc}$-opt and pEKEx3-*xylD*$_{Cc}$-opt which were subsequently introduced individually into *C. glutamicum* P_{O6} *iolT1* yielding *C. glutamicum* P_{O6} *iolT1* pEKEx3-*xylX*$_{Cc}$-opt and *C. glutamicum* P_{O6} *iolT1* pEKEx3-*xylD*$_{Cc}$-opt. Comparative cultivation revealed that both strains could use D-xylose as sole carbon and energy source, whereas the control strain *C. glutamicum* P_{O6} *iolT1* could not. The growth rates of *C. glutamicum* P_{O6} *iolT1* pEKEx3-*xylX*$_{Cc}$-opt and *C. glutamicum* P_{O6} *iolT1* pEKEx3-*xylD*$_{Cc}$-opt were identical (μ_{max} = 0.25 ± 0.006 h^{-1}, μ_{max} = 0.25 ± 0.004 h^{-1}, respectively) indicating that expression of either *xylX* or *xylD* from *C. crescentus* is sufficient for enabling D-xylose utilization via the Weimberg pathway in *C. glutamicum* P_{O6} *iolT1*.

Although, the Weimberg pathway represents a shortcut to the biotechnologically interesting TCA cycle intermediate α-ketoglutarate when compared to synthesis starting from D-glucose, microbial production of this dicarboxylic acid from D-xylose has not been investigated yet (Fig. 5) (Jo *et al.,* 2012). Unfortunately, many competing

metabolic pathways use α-ketoglutarate. It is either consumed by the TCA cycle orserves as a direct precursor of L-glutamate and as an amino group acceptor for transamination reactions. It was already demonstrated that the deletion of the gene coding for the E1o subunit (OdhA, encoded by *odhA*) of the large multienzyme α-ketoglutarate dehydrogenase complex (ODHC) resulted in the accumulation of α-ketoglutarate in *C. glutamicum* (Asakura *et al.,* 2007; Bott 2007, Usuda *et al*., 1996). With the goal of establishing microbial α-ketoglutarate production from D-xylose via the Weimberg pathway in *C. glutamicum*, the gene *odhA* coding for this particular subunit was deleted in *C. glutamicum* P_{O6} *iolT1*. In an initial cultivation, the resulting strain *C. glutamicum* P_{O6} *iolT1* Δ*odhA* was able to accumulate 5.76 ± 0.06 g L^{-1} (39.43 ± 0.4 mM) α-ketoglutarate in the supernatant when cultivated in defined CGXII medium supplemented with 40 g L^{-1} D-glucose. In contrast, the parental strain *C. glutamicum* P_{O6} *iolT1* accumulated only 0.05 ± 0.00 g L^{-1} (0.37 ± 0.03 mM) α-ketoglutarate. Subsequently, *C. glutamicum* P_{O6} *iolT1* Δ*odhA* was transformed with the expression plasmid pEKEx3-*xylXABCD*$_{Cc}$-opt and subsequently cultivated in a mixture of D-glucose/D-xylose as the deletion of *odhA* interrupts the TCA cycle and renders cultivation on D-xylose as sole carbon and energy source with this strain impossible. *C. glutamicum* P_{O6} *iolT1* Δ*odhA* WMB2 accumulated 7.92 ± 0.13 g L^{-1} (54.21 ± 0.86 mM) α-ketoglutarate in the supernatant when cultivated in defined CGXII medium with 10 g L^{-1} D-glucose and 30 g L^{-1} D-xylose, which represents a 1.5-fold increase .

1.8 Conclusions and Outlook

The results obtained in this thesis demonstrate that *C. glutamicum* is an attractive host for the efficient utilization of D-xylose and therefore is a good candidate for establishing more sustainable microbial production processes with this pentose as substrate. Systematic analysis of constructed strains showed that *C. glutamicum* wild type, although not capable of D-xylose utilization via the Weimberg pathway or any other catabolic strategy by nature, already possess individual components enabling D-xylose transport, D-xylose oxidation and α-ketoglutarate semialdehyde oxidation. Beyond that, knowledge of genes and enzymes involved in this catabolic pathway could be used directly for the construction of a non-recombinant *C. glutamicum* strain capable of producing D-xylonate from D-xylose with a resulting yield matching the theoretical maximum. Secondly, it was shown that the utilization of D-xylose via the Weimberg

pathway combined with the utilization of D-glucose via the central carbon metabolism for the production of α-ketoglutarate leads to an increase in product yield compared to use of D-glucose alone.

Although α-ketoglutarate production from D-xylose was achieved in *C. glutamicum*, the observed titers are far away from any industrial application. With the aim of developing *C. glutamicum* strains suitable for large-scale applications, several challenges have to be tackled. The α-ketoglutarate consumption has to be prevented by engineering competitive pathways in the cell metabolism. Additionally, fine-tuning of the expression of the Weimberg pathway encoding genes is beneficial to avoid the accumulation of pathway intermediates (*e.g.* D-xylonate). Finally, improved production can be addressed by strain engineering towards efficient export of α-ketoglutarate since the transport of this dicarboxylic acid in *C. glutamicum* is unknown by now.

2. Peer-reviewed publications

2.1 Evolution of a D-xylose metabolizing *C. glutamicum* strain

Bioresource Technology 245 (2017) 1377–1385

Contents lists available at ScienceDirect

Bioresource Technology

journal homepage: www.elsevier.com/locate/biortech

Miniaturized and automated adaptive laboratory evolution: Evolving *Corynebacterium glutamicum* towards an improved D-xylose utilization

Andreas Radek [1], Niklas Tenhaef [1], Moritz Fabian Müller, Christian Brüsseler, Wolfgang Wiechert, Jan Marienhagen, Tino Polen, Stephan Noack *

Institute of Bio- and Geosciences, IBG-1: Biotechnology, Forschungszentrum Jülich GmbH, Jülich D-52425, Germany

HIGHLIGHTS

- Automated procedures for Adaptive Laboratory Evolution of microbial strains were developed.
- Growth rate of engineered *C. glutamicum* strain was increased by 260% on sole D-xylose.
- Results from small-scale ALE experiments were successfully transferred to lab-scale operation.
- Genome sequencing revealed up to 15 potential key mutations for improved D-xylose assimilation.

ARTICLE INFO

Article history:
Received 31 March 2017
Received in revised form 8 May 2017
Accepted 10 May 2017
Available online 12 May 2017

Keywords:
Adaptive Laboratory Evolution
Untargeted strain optimization
Lab automation
Corynebacterium glutamicum
Xylose utilization

ABSTRACT

Adaptive Laboratory Evolution (ALE) is increasingly being used as a technique for untargeted strain optimization. This work aimed at developing an automated and miniaturized ALE approach based on repetitive batch cultivations in microtiter plates. The new method is applied to the recently published strain *Corynebacterium glutamicum* pEKEx3-*xylXABCD*$_{Cc}$, which is capable of utilizing D-xylose via the Weimberg (WMB) pathway. As a result, the significantly improved strain WMB2$_{evo}$ was obtained, showing a specific growth rate of 0.26 h^{-1} on D-xylose as sole carbon and energy source. WMB2$_{evo}$ grows stable during lab-scale bioreactor operation, demonstrating the high potential of this strain for future biorefinery applications. Genome sequencing of cell samples from two different ALE processes revealed potential key mutations, e.g. in the gene cg0196 (encoding for the transcriptional regulator lolR of the *myo*-inositol metabolism). These findings open up new perspectives for the rational engineering of *C. glutamicum* towards improved D-xylose utilization.

© 2017 Elsevier Ltd. All rights reserved.

1. Introduction

The ability to adapt quickly to different environmental conditions is vital for any microorganism. Adaptive Laboratory Evolution (ALE) exploits this characteristic and is increasingly being used as a technique for untargeted strain optimization (Portnoy et al., 2011). ALE was successfully applied to adapt biotechnologically relevant organisms to lignocellulosic material (Qin et al., 2016; Wang et al., 2014), to improve biodegradation capabilities (Lasik et al., 2010; Wang et al., 2016a) or to enhance growth performance (Cheng et al., 2014; Li et al., 2015; Wang et al., 2016b). Furthermore, strategies were developed to increase productivity, i.e. by using stress conditions (Reyes et al., 2014; Yu et al., 2013), by selection using a biosensor and FACS (Mahr et al., 2015) or by enhancing tolerance against the target product (Mundhada et al., 2017).

Key principle of ALE is the application of a selection criterion to the culture. In most cases, this criterion is increased growth rate, since cells with a higher growth rate inherently prevail during cultivation. ALE experiments are routinely performed in shaking flasks or laboratory bioreactors either in continuous cultivation or repetitive batch mode (Dragosits and Mattanovich, 2013; Portnoy et al., 2011). Due to long experimentation times and many manual handling steps these approaches are laborious and prone to errors. Therefore recent developments aim for a miniaturization and automation of ALE approaches, and first microfluidic systems have already been developed (Sjostrom et al., 2014). However, no system is currently available that enables to run ALE experiments under process conditions similar to lab-scale bioreactors and in a fully automated manner without any user intervention.

* Corresponding author.
E-mail address: s.noack@fz-juelich.de (S. Noack).
[1] These authors contributed equally to this work.

http://dx.doi.org/10.1016/j.biortech.2017.05.055
0960-8524/© 2017 Elsevier Ltd. All rights reserved.

Table 1
Strains and plasmids used in this study.

Strain or plasmid	Relevant characteristics[a]	Source or reference
C. glutamicum		
ATCC 13032 (WT)	Biotin auxotroph wild-type strain	(Abe et al., 1967)
WMB2	*C. glutamicum* pEKEx3-*xylXABCD*$_{Cc}$-opt	This work
E. coli		
DH5α	F⁻ Φ80*lacZ*ΔM15 Δ(*lacZ*YA-*arg*F)U169 *recA1 endA1 hsd*R17 (r_K^-, m_K^+) *pho*A *sup*E44 λ– *thi*-1 *gyr*A96 *rel*A1	Invitrogen (Karlsruhe, Germany)
Plasmids		
pEKEx3	Spec^R; *C. glutamicum*/ *E. coli* shuttle vector for regulated gene expression; (P_{tac}, lacI^q, pBL1 *ori*VCg, pUC18 *ori*VEc)	(Hoffelder et al., 2010)
pEKEx3-*xylXABCD*$_{Cc}$-opt	Spec^R; pEKEx3 derivative for the regulated expression of *xylXABCD* of *C. crescentus*. All five genes were codon optimized for a heterologous expression in *C. glutamicum*	This work

[a] Spec^r; spectinomycin resistance.

Currently established large-scale microbial production processes rely on feedstock containing primarily D-glucose, D-fructose or sucrose as carbon sources. However, when taking costs and competition with food production for arable land into account (Ekman et al., 2013; Viikari et al., 2012), so called 2nd generation feedstocks based on lignocellulosic biomass represent promising alternatives (Straathof, 2014). Lignocellulosic biomass is composed of up to 40% hemicellulose, whose key building block is the pentose D-xylose. Unfortunately, D-xylose cannot be directly utilized by important microbial platform organisms such as *Saccharomyces cerevisiae* (Bettiga et al., 2009) and *Corynebacterium glutamicum* (Meiswinkel et al., 2013), since both are missing assimilation pathways for this carbon source.

In this study, the development of an automated ALE approach is presented, which is based on repetitive batch cultivations in milliliter-scale using the recently introduced Mini Pilot Plant (MPP) technology (Unthan et al., 2015b). Essentially, the MPP combines a liquid handling robot with a BioLector® cultivation device. The latter enables to online monitor pH, dissolved oxygen and backscatter-biomass in all 48-wells of a FlowerPlate® and, thus, provides an instantaneous recording of metabolic adaptation events during ALE experimentation. Sophisticated workflows, employing automated liquid handling operations for sample transfer and processing, were developed that offer detailed characterization of growth and production performances of evolved strains.

In a proof of concept study, the novel ALE technique is applied to a recently constructed *C. glutamicum* strain harboring the Weimberg pathway from *Caulobacter crescentus* for D-xylose assimilation (Radek et al., 2014). As a starting point, this strain showed a comparable low specific growth rate of 0.07 ± 0.01 h^{-1} on defined medium with D-xylose as sole carbon and energy source.

Firstly, codon optimization increased the growth rate by 43%. Secondly, untargeted strain optimization in two different ALE approaches further increased the growth rate by 260%, which was also verified in subsequent lab-scale bioreactors cultivations. Transient sampling during the ALE process followed by genome sequencing led to the identification of several mutations, which are potentially responsible for the improved growth phenotype and build the basis for future rational strain development.

2. Materials and methods

2.1. Construction of strains and plasmids

All used bacterial strains and plasmids are listed in Table 1. *Escherichia coli* DH5α was used for cloning purposes and was grown aerobically on a rotary shaker (170 rpm) at 37 °C in 5 mL Lysis Broth (LB) medium (Bertani, 1951) or on LB agar plates (LB medium with 1.8% [wt vol^{-1}] agar). *C. glutamicum* strains are derived from *C. glutamicum* ATCC 13032 (Abe et al., 1967) and were routinely cultivated aerobically in 500 mL baffled shake flasks with 50 mL medium on a rotary shaker (130 rpm) at 30 °C. All used enzymes for performing cloning methods were purchased from Thermo Scientific (Schwerte, Germany). Synthetic genes were obtained in codon-optimized version for expression in *C. glutamicum* from LifeTechnologies (Darmstadt, Germany). Standard protocols for molecular cloning, such as PCR, DNA restriction, and ligation were carried out for recombinant DNA work (Sambrook and Russell, 2001). *C. glutamicum* strains were transformed by electroporation as described previously (Eggeling and Bott, 2005) and constructed plasmids were finally verified by DNA sequencing at Eurofins MWG Operon (Ebersberg, Germany).

2.2. Cultivation media and conditions

Cultivations in complex media were performed on Brain-heart infusion (BHI) supplied by Sigma-Aldrich (Steinheim, Germany). CGXII medium (Eggeling and Bott, 2005) was used for cultivations in defined medium. It contained per liter of deionized water: 1 g K_2HPO_4, 1 g KH_2PO_4, 5 g urea, 13.25 mg $CaCl_2 \cdot 2\,H_2O$, 0.25 g $MgSO_4 \cdot 7\,H_2O$, 10 mg $FeSO_4 \cdot 7\,H_2O$, 10 mg $MnSO_4 \cdot H_2O$, 0.02 mg $NiCl_2 \cdot 6\,H_2O$, 0.313 mg $CuSO_4 \cdot 5\,H_2O$, 1 mg $ZnSO_4 \cdot 7\,H_2O$, 0.2 mg biotin, 30 mg protocatechuate and 42 g MOPS. D-glucose and D-xylose were added in varying amounts. Certain components were added sterile after autoclaving (D-xylose, D-glucose, protocatechuate, trace elements). All chemicals were purchased from Sigma-Aldrich (Steinheim, Germany) or Carl Roth GmbH (Karlsruhe, Germany). Strain storage was done via cryo-conservation as described elsewhere (Unthan et al., 2015a).

Microtiter plate cultivations were performed in specialized, disposable FlowerPlates® (m2plabs GmbH, Baesweiler, Germany), which provide increased mass transfer and enable online measurement of pH and dissolved oxygen via optodes. The following conditions were applied: Shaking frequency 1200 rpm, temperature 30 °C, humidity > 80%, backscatter gain 15, filling volume 1000 or 800 µL. Cultures were started at OD_{600} = 0.2 by inoculation from a cryo-culture.

Bioreactor cultivations were done in a parallel cultivation platform (Eppendorf/DASGIP, Jülich, Germany). A pH of 7 was held constant during the cultivation by feeding 5 M H_3PO_4 and 5 M NH_4OH on demand. Temperature and air flow was set to 30 °C and 0.5 vvm, respectively. Aerobic process conditions were maintained by controlling the stirrer speed (400–1.200 rpm) to achieve a dissolved oxygen concentration (DO) of at least 30%. Online measurements were taken for pH (405-DPAS-SC-K80/225, Mettler Toledo), DO (Visiferm DO 225, Hamilton) and exhaust gas compo-

sition (GA4, DASGIP AG). The vessels were inoculated from an exponential growing pre-culture to a final OD_{600} of 1. Pre-cultures were inoculated from cryo-cultures.

2.3. Automated repetitive batch procedures

Automated repetitive batch procedures were carried out using the "Mini Pilot Plant" (MPP) described in detail by (Unthan et al., 2015b) or in a similar setup using a Freedom Evo 200 (Tecan, Switzerland) robotic platform. Both robotic workstations employ a liquid handling arm using eight steel needles and a gripper arm for transport of plates. Additionally, BioLector cultivation devices are embedded in both workstations.

The BioLector uses 48-well FlowerPlates® for high-throughput cultivations. During the cultivation, each well was monitored using the RoboLector agent software to perform automated inoculation and media filling. The RoboLector software checks if predefined triggers are fulfilled. An exemplary trigger condition was "backscatter signal greater than 250". If the condition was satisfied, the robotic workstation transferred 250 μL or 50 μL of culture liquid to the next empty well on the same Flowerplate. Subsequently, this well was filled with fresh CGXII media stored at 4 °C on the robotic platform.

Some wells were harvested after the first trigger or at the end of cultivation depending on the experimental layout. Harvesting was done by transferring the cultivation liquid into a deep well plate. The deep well plate was then centrifuged at 4000 rpm for 10 min to gain culture supernatants. The supernatant was pipetted into a sealed multititer plate and stored at 4 °C. The whole process was carried out fully automated by the robotic workstation.

2.4. Substrate and by-product analytics

Samples were prepared by passing the supernatants through a cellulose acetate syringe filter (0.2 μm, DIA-Nielsen, Düren, Germany).

By-product formation and carbohydrate content (except for D-xylose) was analyzed by high performance liquid chromatography (Agilent 1100 Infinity, Agilent Technologies, Santa Clara, CA) using isocratic ion exchange on an Organic Acid Resin HPLC Column 300 x 8 mm (CS Chromatography, Düren, Germany) as stationary phase and 0.1 M H_2SO_4 as mobile phase with a flow rate of 0.6 mL/min. The column temperature was 80 °C and the injection volume 10 μL. Carbohydrates were detected using a Refractive Index Detector. Organic acids were detected using UV light absorption at 230 nm with a Diode Array Detector. For external calibration, standards of organic acids or carbohydrates (D-xylonate supplied by Santa Cruz Biotechnology, Dallas, USA; other organic acids and carbohydrates suplied by Sigma-Aldrich, Steinheim, Germany) were applied in the dynamic linear range. Estimation of measurement errors was done by Gaussian error propagation.

D-xylose concentration was quantified by an enzymatic assay (D-xylose Assay Kit, Megazyme, Wicklow, Ireland). The protocol used was modified: One well of a 96-well plate contained 290 μL master mix and 10 μL sample or standard. Seven standard concentrations were measured to cover the linear range of 0.1–1 g/L. Master mix for one MTP consisted of 32 mL TRIS-maleate buffer (pH

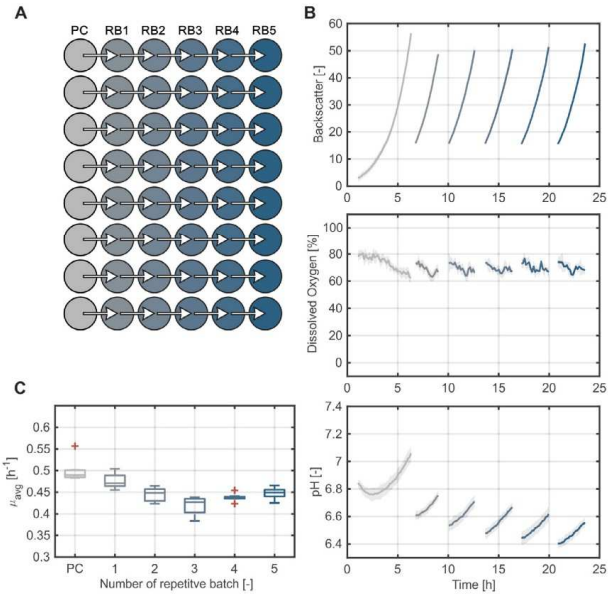

Fig. 1. Simple repetitive batch setup with prefilled defined media containing 10 g/L D-glucose and whole plate incubation at 30 °C. (A) Experimental layout in a 48-well FlowerPlate. (B) Time course of online backscatter, DO and pH signals. Mean values (thick lines) and standard deviations (grey areas) were estimated from eight independent replicate cultures, respectively. (C) Average specific growth rates, estimated from eight independent replicate cultures (see Supplementary Material for more details). Red crosses mark outliers. (For interpretation of the references to colour in this figure legend, the reader is referred to the web version of this article.)

6.8), 1 mL 100 mM $MgCl_2$ solution, 0.5 mL 50 g/L NAD solution and 0.1 mL XDH/XMR solution (from kit). After incubation for 30 min, absorption at 340 nm was measured using an Infinite 200 (Tecan, Switzerland) microplate reader. External standards were used for linear regression within the linear range. Estimation of measurement errors was done by Gaussian error propagation.

2.5. Genome sequencing

Sequencing libraries of genomic DNA from relevant cell samples were prepared using the TruSeq DNA PCR-free sample preparation kit (Illumina). To obtain an average DNA fragment size of 550 bp, genomic DNA (4 μg) was fragmented using the ultrasonic device Bioruptor® Pico (Diagenode). Then, 2 μg of fragmented DNA was end-repaired and size-selected using magnetic beads, followed by the ligation of a single A nucleotide to the 3′ end. Illumina PE index adapters were ligated to the fragments and the indexed libraries were quantified *via* qPCR using the KAPA library quantification kit (Peqlab). Normalized libraries (2 nM) were pooled, diluted to an average final concentration of 10 pM and paired-end sequenced on a MiSeq desktop sequencer (Illumina) with a read length of 2 × 150 nt. An automated workflow for read data analysis and variant detection was designed using tools of the CLC Genomics Workbench (Qiagen Aarhus A/S). The read data were preprocessed for removing adapter sequences and quality trimming to filter out reads or sequence ends having a Phred quality value < 30. Using default parameters, reads were mapped to the *C. glutamicum* ATCC 13032 reference genome BX927147. SNVs (single nucleotide variants), MNVs (multiple nucleotide variants), InDels and structural variants were detected using quality-based variant detection tools of the CLC Genomics Workbench. The individual variant lists of the samples were combined in Excel (Microsoft) and further analyzed to check the occurrence, frequencies and overlap of variants in all samples.

3. Results and discussion

3.1. Miniaturization and automation of ALE

For establishing an automated adaptive laboratory evolution (ALE) approach, the existing Mini Pilot Plant (MPP) was extended by implementing a repetitive batch process in microtiter plate (MTP) format.

As a starting point, a simple experimental setup was defined in which one FlowerPlate was prefilled with freshly prepared CGXII media containing 10 g/L D-glucose as sole carbon and energy source. The wells of the first column (pre-culture, PC) of the MTP was then inoculated with *C. glutamicum* wild type to an OD of 0.2 (Fig. 1A). By monitoring each well, the automated inoculation of the next batch was triggered when the backscatter (BS) signal reached a threshold of BS = 70, ensuring that the culture was in the middle of the exponential growth phase. 250 μL of each culture was then transferred to the wells of the next column (repetitive batch 1, RB1) of the MTP. In total, this setup allowed for five repetitive batches in eight replicates. By taking the online backscatter data, both average (μ_{avg}) and maximum (μ_{max}) specific growth

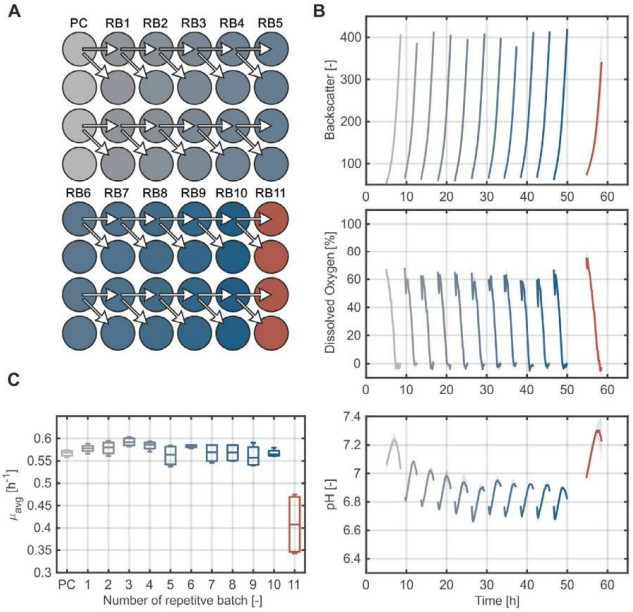

Fig. 2. Advanced repetitive batch setup with medium dosing at trigger time-point and untouched cultivations. Fresh defined medium containing 40 g/L D-glucose was stored at room temperature in the robotic workstation. (A) Experimental layout in a 48-well FlowerPlate. (B) Time course of online backscatter, DO and pH signals. Mean values (thick lines) and standard deviations (grey areas) were estimated from four independent replicate cultures, respectively. (C) Average specific growth rates, estimated from four independent replicate cultures.

rates were calculated for each batch culture. These calculations posed some challenges due to the noise inherited in the optical signal of freshly inoculated cultures and the amount of data to be analyzed. Hence, a new algorithm for the automated calculation of μ_{avg} and μ_{max} from online backscatter data was developed (see Supplementary Information for more details).

The first experiment demonstrated the feasibility of this approach to realize automated repetitive batch cultivations in microtiter plates. However, the pH significantly decreased over the course of the experiment (Fig. 1B), and this effect was accompanied by a decrease in specific growth rates (Fig. 1C). The decrease in pH is probably due to the prefilling and storage of the MTP at 30 °C long before the cultivation experiments starts. Thus, a more sophisticated inoculation sequence using external media storage at lower temperature is needed, in order to ensure stable growth conditions. For the determination of specific growth rates another challenge was revealed by this experiment: The removal of 25% of the cultivation broth alters the backscatter signal and renders it unsuitable for growth rate estimation beyond the trigger threshold.

Both challenges were addressed in the next setup with two major changes: Firstly, the medium to be used in the repetitive batch cultivations was stored separately at room temperature on the robotic platform. The filling of a next well with fresh medium and its inoculation is now both triggered when the predefined backscatter threshold of a running batch is reached. Secondly, two wells are inoculated from each previous well (Fig. 2A). One well is used for continuation of the repetitive batch series, the other one is left undisturbed for monitoring growth and increasing the number of measurements for growth rate estimation. Moreover, a higher concentration of D-glucose (40 g/L) was used in order to elongate the exponential phase of each culture. The last repetitive batch was carried out with CGXII medium lacking protocatechuate to investigate the effect of this component on the culture when the media is stored over several hours.

In total, two independent series of eleven repetitive batch cultivations were performed on one MTP (Fig. 2B and C). The highly reproducible growth rate over the course of ten batches demonstrates the feasibility of this setup to maintain stable conditions during the experiment. There is still a slight pH shift observable, but with negligible influence on growth. For the last batch cultivation on CGXII medium without protocatechuate a negative effect on growth was observed. This is in agreement with previous results where protocatechuate was found to serve as co-substrate for *C. glutamicum* wild type, enhancing the maximum specific growth up to $\mu_{avg} = 0.61 \pm 0.02\ h^{-1}$ (Unthan et al., 2014). It is likely that protocatechuate availability during the repetitive batches is higher due to the external storage of fresh medium at room temperature. This would explain the consistent average growth rate of $\mu_{avg} = 0.57 \pm 0.02\ h^{-1}$, which is significantly higher than the growth rate ($\mu_{avg} = 0.46 \pm 0.02\ h^{-1}$) of the second exponential phase when protocatechuate is depleted (Unthan et al., 2014).

In the following, the novel automated repetitive batch procedures were applied to evolve *C. glutamicum* towards an improved D-xylose utilization.

3.2. ALE of C. glutamicum WMB

Recently, the strain *C. glutamicum* pEKEx3-*xylXABCD*$_{Cc}$ which employs the Weimberg (WMB) pathway from *Caulobacter crescentus* was introduced (Radek et al., 2014). This pathway opens a metabolic route for the conversion of D-xylose into α-ketoglutarate without carbon loss and, thus, is particularly interesting for the production of TCA-cycle derived organic acids. The strain (here denoted as *C. glutamicum* WMB) showed a maximum specific growth rate of $\mu_{max} = 0.07 \pm 0.01\ h^{-1}$ on defined medium using D-xylose as sole carbon and energy source. Following codon optimization of all WMB genes increased the maximum growth rate only slightly to $\mu_{max} = 0.10 \pm 0.02\ h^{-1}$ (data not shown, strain henceforth denoted *as C. glutamicum* WMB2). By contrast, a strain harboring the alternative isomerase pathway was shown to grow with $\mu_{max} = 0.20\ h^{-1}$ (Meiswinkel et al., 2013). Therefore, it was assumed that there is still room for improvement of D-xylose assimilation in *C. glutamicum* WMB2.

With the aim to enhance the growth performance of *C. glutamicum* WMB2 on D-xylose, ALE experiments were initiated in two different ways as will be described in the following. In the first approach, six independent clones of *C. glutamicum* WMB2 were used, and these clones were individually picked from a BHI agar plate, to inoculate a FlowerPlate similar to the simple repetitive batch setup, but with medium dosing at trigger time-point (Fig. 3A) and fresh media stored separately at 4 °C. From a preculture (PC) using BHI medium, 50 µL of each culture was transferred to the first repetitive batch well (RB1). Clones A to C were cultivated in RB1 on CGXII medium containing 20 g/L D-xylose. For clones D to F, 2 g/L D-glucose was additionally added to aid expression of Weimberg proteins in the initial growth phase. For all following RBs, 20 g/L D-xylose was used as sole carbon and energy source. The backscatter threshold for all inoculation events was set to BS = 250 realizing biomass transfer in the late exponential phase of the cultivation. Together with the smaller transfer vol-

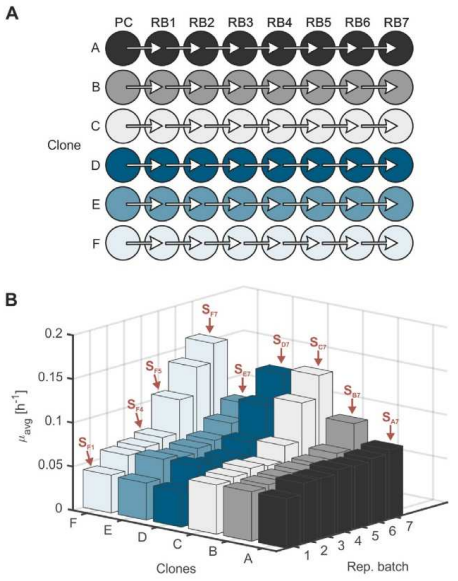

Fig. 3. ALE of *C. glutamicum* WMB2 starting from 6 independent clones and following automated repetitive batch cultivations in microtiter plates. Fresh defined medium containing 2 g/L D-glucose and 20 g/L D-xylose (for first batches of A, B and C) or 20 g/L D-xylose (for all other batches) was stored at 4 °C in the robotic workstation prior use. (A) Experimental layout. (B) Average specific growth rates, estimated from single cultures. Red arrows mark cultivations which were chosen for genome sequencing. (For interpretation of the references to colour in this figure legend, the reader is referred to the web version of this article.)

ume of 50 µL this enhanced the number of generations per RB. In total, the experiment ran for 13 days and provided 35 generations of growth-selection. This is notably shorter both in time and generations than in previously described *E. coli* ALE processes, which use e.g. 2000 generations in 261 days (Jantama et al., 2008) or 360 generations over 90 days (Qin et al., 2016).

As a result, five of the six clones showed an increasing average specific growth rate over the course of the experiment (Fig. 3B). The fastest-growing clone F showed a threefold increase in growth rate (up to $\mu_{avg} = 0.16 \pm 0.02\ h^{-1}$ and $\mu_{max} = 0.18\ h^{-1}$) along the ALE experiment. Notably, the time-point and extent of the growth rate increase varied from clone to clone, suggesting that individual mutation events occurred. For genome sequencing cell samples from relevant cultivations were used as indicated (Fig. 3B).

In the second approach, the ALE experiment was started from a cryo-culture of *C. glutamicum* WMB2. The cryo-culture was prepared from a shaking flask culture of *C. glutamicum* WMB2 grown on defined CGXII medium with D-xylose. Following the hypothesis that this step already had induced genetic heterogeneity in the culture, the subsequent repetitive batch process should enable an enrichment of cells with beneficial mutations for D-xylose assimilation.

The experimental design for this ALE experiment is shown in Fig. 4A. Similar to the advanced setup (cf. Fig. 2A), in every trigger event two cultures were inoculated from the previous batch and a total of two independent repetitive batch series were performed. In one of the series, the second inoculated well was harvested at the end of the cultivation in stationary phase (endpoint harvest, EH). In the other series, the second inoculated well was harvested when the first well reached the backscatter threshold (trigger harvest, TH). The supernatant resulting from these wells was used for by-product analysis. For all cultures defined media containing 40 g/L D-xylose was used.

As a result, the specific growth rate of *C. glutamicum* WMB2 showed a steady increase over the course of the ALE experiment and, eventually, reached a maximum at $\mu_{max} = 0.26 \pm 0.02\ h^{-1}$

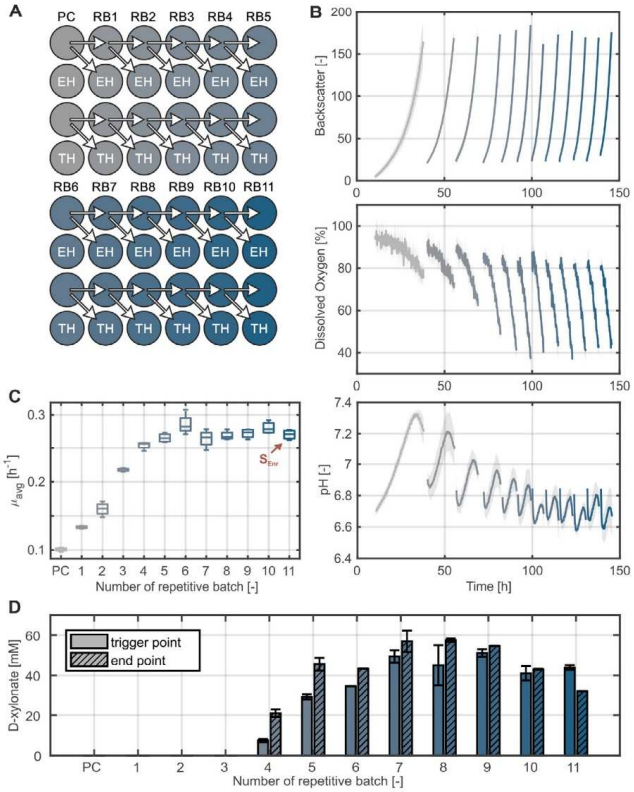

Fig. 4. ALE of *C. glutamicum* WMB2 starting from a common cryo-culture and following automated repetitive batch cultivations in microtiter plates. Fresh defined medium containing 40 g/L D-xylose was stored at room temperature in the robotic workstation. (A) Experimental layout. (B) Mean values (thick lines) and standard deviations (grey areas) of online backscatter, DO and pH signals were estimated from four independent replicate cultures, respectively. (C) Average specific growth rates, estimated from four independent replicate cultures. (D) D-xylonate concentrations in culture supernatant at trigger points and endpoints. Mean values and standard deviations were estimated from two analytical replicates, respectively.

(Fig. 4B and C). Most interestingly, the analysis of the supernatant samples gathered at the trigger points and endpoints, respectively, revealed significant by-product formation of D-xylonate (Fig. 4D). Accumulation of this Weimberg pathway intermediate was also found in a previous study (Radek et al., 2014), pointing to a still non-optimal carbon flow along this pathway into the TCA-cycle. Analogous to the prior experiment using single clones, here cells from RB11 were used for genome sequencing and the resulting strain is henceforth denoted $WMB2_{evo}$.

3.3. Verification of improved D-xylose utilization of $WMB2_{evo}$

To be used as a platform strain for industrially relevant bioprocesses, an evolved strain must be phenotypically stable, even under changing media conditions. In the following, a modified version of the presented ALE setup was used to test the stability of $WMB2_{evo}$ by following consecutive cultivations on CGXII medium containing 20 g/L of either D-glucose or D-xylose, respectively (Fig. 5A). The experiment was started by inoculating the first repetitive batch on D-glucose from an exponentially growing pre-culture on D-xylose. After the backscatter trigger in mid-exponential phase was reached, the next repetitive batch using D-glucose and a parallel batch using D-xylose were inoculated. From the latter, an average growth rate over all eight cultivations (each in three independent replicates) was estimated as $\mu_{avg} = 0.27 \pm 0.01\ h^{-1}$ (Fig. 5B), clearly demonstrating the stability of the evolved strain $WMB2_{evo}$ on D-xylose medium.

Moreover, in order to verify the results from the MTP-based ALE experiments under process relevant conditions, $WMB2_{evo}$ was cultivated in 1 L lab-scale bioreactors using defined media containing 20 g/L D-xylose as sole carbon and energy source (Fig. 5B). During cultivation, samples were withdrawn for analyzing specific substrate uptake, biomass growth and by-product formation. As a result, $WMB2_{evo}$ showed an specific average growth rate of $\mu_{avg} = 0.26 \pm 0.01\ h^{-1}$, verifying the improvement of D-xylose utilization under lab-scale conditions. The specific D-xylose uptake rate was estimated as $upt_{Xyl} = 5.7 \pm 0.1$ mmol/g/h. Additionally, formation of D-xylonate up to a concentration of 40 mM was observed, resulting in a carbon loss of 30%.

To the best of our knowledge, the evolved strain *C. glutamicum* $WMB2_{evo}$ is currently the fastest growing strain on pure D-xylose media gained from untargeted strain optimization experiments.

3.4. Genome sequencing during ALE

The underlying mutations in the cell cultures exhibiting increasingly improved growth rates with D-xylose in the course of the two ALE experiments (cf. Fig. 3B and Fig. 4C) were determined by sequencing of genomic DNA from relevant samples using the Illumina technology. Within the sequencing results and detected variants, a number of highly meaningful variants with various frequencies were found, suggesting some heterogeneity in the cultures (Table 2). In samples from both the first ALE approach using six independent clones of *C. glutamicum* WMB2 and the second one starting from a cryo-culture, two transcriptional regulators were found to be affected.

On one hand, a deletion and structural variants within cg0196 was found. This gene encodes the repressor IolR of the *iol* gene cluster for proteins involved in *myo*-inositol uptake and degradation (Klaffl et al., 2013). These variants in cg0196 most likely result in functional inactivation of IolR.

On the other hand, cg3388 was affected, which encodes a hitherto putative transcriptional regulator. The detected variants are partial gene deletions as well as point mutations resulting in amino acid exchanges or premature stop of translation. The partial deletions and the premature stop codon likely inactivate the encoded

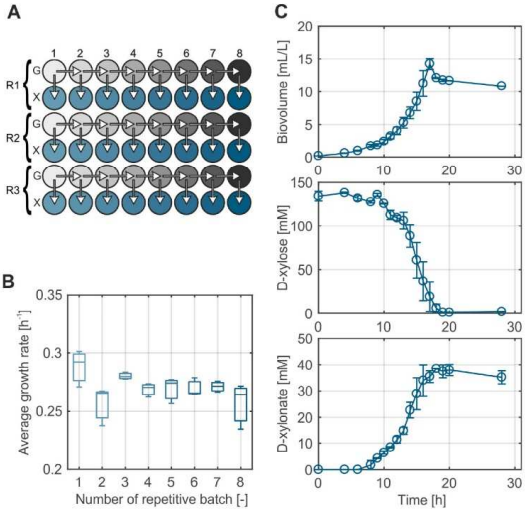

Fig. 5. Verification of improved D-xylose utilization of $WMB2_{evo}$. (A) Experimental layout for testing the phenotypic stability on changing carbon sources. Eight repetitive batches (each in three independent replicates R1 to R3) were performed using defined CGXII media with 20 g/L D-glucose (Rows "G"). Each finished batch cultivation with D-glucose was used to subsequently inoculate a batch cultivation on defined CGXII medium containing 20 g/L D-xylose (Rows "X"). (B) Average specific growth rates of cultivations using D-xylose, estimated from three independent replicate cultures. (C) Lab-scale bioreactor cultivation of strain $WMB2_{evo}$ on defined CGXII medium containing 20 g/L D-xylose. Mean values and standard deviations were estimated from two independent replicate cultures, respectively.

Table 2
Meaningful variants revealed by genome sequencing of samples from single-clone and cryo-culture ALE experiments. Variants are listed according to the sample annotation of Figs. 3B and 4C. The observed frequency of occurrence of a particular variant is given in brackets. # refers to the BX927147 accession.

Sample	Batch	μ_{avg} [h^{-1}]	Variant type	Comment
S_{F1}	1	0.04 ± 0.02	–	–
S_{F4}	4	0.07 ± 0.02	–	–
S_{F5}	5	0.10 ± 0.03	Deletion (23%) nt 3,234,237…3,234,336	In cg3388, putative transcriptional regulator
S_{F7}	7	0.16 ± 0.02	Deletion (29%) nt 3,234,237…3,234,336	In cg3388, putative transcriptional regulator
S_{E7}	7	0.10 ± 0.03	SNV G to A (17%) nt 3,234,893	Exchange A360T in cg3388, putative transcriptional regulator
S_{D7}	7	0.14 ± 0.02	SNV A to G (13%) nt 526,417	Exchange I15V in cg0587, tuf, elongation factor Tu
			SNV G to A (19%) nt 527,353	Exchange D327N in cg0587, tuf, elongation factor Tu
			SNV G to A (15%) nt 527,392	Exchange V340I in cg0587, tuf, elongation factor Tu
			SNV G to A (14%) nt 527,452	Exchange D360N in cg0587, tuf, elongation factor Tu
			SNV C to G (14%) nt 527,454	Exchange D360E in cg0587, tuf, elongation factor Tu
S_{C7}	7	0.15 ± 0.02	SNV G to A (12%) nt 527,353	Exchange D327N in cg0587. tuf. elongation factor Tu
			SNV G to A (12%) nt 527,392	Exchange V340I in cg0587, tuf, elongation factor Tu
S_{B7}	7	0.10 ± 0.02	Multiple breakpoints (45%) nt 168,365… > 168,464;	In cg0196, *iolR*, repressor of *myo*-inositol utilization genes
			SNV A to G (16%) nt 526,417	Exchange I15V in cg0587, tuf, elongation factor Tu
			SNV G to A (16%) nt 527,353	Exchange D327N in cg0587, tuf, elongation factor Tu
			SNV G to A (15%) nt 527,392	Exchange V340I in cg0587, tuf, elongation factor Tu
			SNV C to T (29%) nt 3,234,618	Exchange T268I in cg3388, putative transcriptional regulator
S_{A7}	7	0.08 ± 0.02	MNV GG to AA (98%) nt 192,844…192,845	Upstream of cg0223, *iolT1*, *myo*-inositol transporter 1
			MNV GGG to ATC (98%) nt 192,850…192,852	Upstream of cg0223, *iolT1*, *myo*-inositol transporter 1
			SNV A to G (98%) nt 192,857	Upstream of cg0223, *iolT1*, *myo*-inositol transporter 1
			SNV G to A (19%) nt 3,234,734	Exchange A307T in cg3388, putative transcriptional regulator
S_{Enr1}		0.27 ± 0.01	SNV G to A (100%) nt 3,234,078	Stop W88* in cg3388(+), putative transcriptional regulator, IclR-family
S_{Enr2}		0.27 ± 0.01	Deletion (41%) nt 168,324…168,423	In cg0196, *iolR*, repressor of *myo*-inositol utilization genes

regulator. The three amino acid exchanges T268I, A307T and A360T are located within conserved helix-turn-helix and IclR superfamily domains and probably also inactivate or modulate the DNA-binding activity of Cg3388.

In one sample also single and multiple nucleotide polymorphisms (SNV/MNV) upstream of *iolT1* (cg0223) encoding the *myo*-inositol transporter 1 were found. However, the positional distances of these SNPs/MNVs (−668 to −681 bp) to the transcriptional starts of *iolT1* (−85 bp and −113 bp) are large and it is currently unknown whether the repression of *iolT1* by IolR could be affected (Klaffl et al., 2013).

Besides genes shown or annotated to be involved in *myo*-inositol metabolism, *tuf* (cg0587) encoding the elongation factor Tu (EF-Tu) was affected in three series of the ALE experiment initiated from the six individual WMB2 clones. The prokaryotic EF-Tu is responsible for catalyzing the binding of an aminoacyl-tRNA to the ribosome and recently was also found to be involved in a first step of proofreading for maintaining a high accuracy of translation (leong et al., 2016). Here, point mutations in *tuf* resulting in the amino acid exchanges D327 N and V340I were found in all three series, suggesting some higher relevance, while exchange I15V was found in two of the three and D360 N as well as D360E in only one of the three series where *tuf* was affected. It should be mentioned that also numerous mutations in the 23S rRNA with various frequencies were found (data not shown).

4. Conclusions

In this study, a miniaturized and automated Adaptive Laboratory Evolution (ALE) approach for untargeted strain optimization was developed. The approach is highly flexible and provides access to detailed system levels studies on potential adaption strategies of microbes under different selection pressures. ALE was used to optimize D-xylose utilization in a recently developed *C. glutamicum* strain expressing the Weimberg pathway. The resulting strain $WMB2_{evo}$ currently shows the best growth performance of a *C. glutamicum* strain on defined D-xylose medium.

Acknowledgements

This work was partly funded by the German Federal Ministry of Education and Research (BMBF, Grant. No. 031L0015) as part of the project "XyloCut – Shortcut to the carbon efficient microbial pro-

duction of chemical building blocks from lignocellulose-derived D-xylose", which is embedded in the ERASysAPP framework. Further funding was received from the Innovation Lab initiative of the German Helmholtz Association to support the "Microbial Bioprocess Lab – A Helmholtz Innovation Lab."

Appendix A. Supplementary data

Supplementary data associated with this article can be found, in the online version, at http://dx.doi.org/10.1016/j.biortech.2017.05.055.

References

Abe, S., Takayama, K., Kinoshita, S., 1967. Taxonomical studies on glutamic acid producing bacteria. J. Gen. Appl. Microbiol. 13, 279–301.
Bertani, G., 1951. Studies on Lysogenesis I.: the mode of phage liberation by lysogenic *Escherichia coli*. J. Bacteriol. 62 (3), 293–300.
Bettiga, M., Bengtsson, O., Hahn-Hagerdal, B., Gorwa-Grauslund, M.F., 2009. Arabinose and xylose fermentation by recombinant *Saccharomyces cerevisiae* expressing a fungal pentose utilization pathway. Microb. Cell Fact. 8, 40.
Cheng, K.K., Lee, B.S., Masuda, T., Ito, T., Ikeda, K., Hirayama, A., Deng, L., Dong, J., Shimizu, K., Soga, T., Tomita, M., Palsson, B.O., Robert, M., 2014. Global metabolic network reorganization by adaptive mutations allows fast growth of *Escherichia coli* on glycerol. Nat. Commun. 5, 3233.
Dragosits, M., Mattanovich, D., 2013. Adaptive laboratory evolution – principles and applications for biotechnology. Microb. Cell Fact. 12 (1), 64.
Eggeling, L., Bott, M., 2005. Handbook of *Corynebacterium glutamicum*. CRC Press.
Ekman, A., Wallberg, O., Joelsson, E., Börjesson, P., 2013. Possibilities for sustainable biorefineries based on agricultural residues – a case study of potential straw-based ethanol production in Sweden. Appl. Energy 102, 299–308.
Hoffelder, M., Raasch, K., van Ooyen, J., Eggeling, L., 2010. The E2 domain of OdhA of *Corynebacterium glutamicum* has succinyltransferase activity dependent on lipoyl residues of the acetyltransferase AceF. J. Bacteriol. 192 (19), 5203–5211.
Ieong, K.W., Uzun, U., Selmer, M., Ehrenberg, M., 2016. Two proofreading steps amplify the accuracy of genetic code translation. Proc. Natl. Acad. Sci. U.S.A. 113 (48), 13744–13749.
Jantama, K., Haupt, M.J., Svoronos, S.A., Zhang, X., Moore, J.C., Shanmugam, K.T., Ingram, L.O., 2008. Combining metabolic engineering and metabolic evolution to develop nonrecombinant strains of *Escherichia coli* C that produce succinate and malate. Biotechnol. Bioeng. 99 (5), 1140–1153.
Klaffl, S., Brocker, M., Kalinowski, J., Eikmanns, B.J., Bott, M., 2013. Complex regulation of the phosphoenolpyruvate carboxykinase gene *pck* and characterization of its GntR-type regulator IolR as a repressor of *myo*-inositol utilization genes in *Corynebacterium glutamicum*. J. Bacteriol. 195 (18), 4283–4296.
Lasik, M., Nowak, J., Krzywonos, M., Cibis, E., 2010. Impact of batch, repeated-batch (with cell recycle and medium replacement) and continuous processes on the course and efficiency of aerobic thermophilic biodegradation of potato processing wastewater. Bioresour. Technol. 101 (10), 3444–3451.
Li, D., Wang, L., Zhao, Q., Wei, W., Sun, Y., 2015. Improving high carbon dioxide tolerance and carbon dioxide fixation capability of *Chlorella sp.* by adaptive laboratory evolution. Bioresour. Technol. 185, 269–275.
Mahr, R., Gätgens, C., Gätgens, J., Polen, T., Kalinowski, J., Frunzke, J., 2015. Biosensor-driven adaptive laboratory evolution of L-valine production in *Corynebacterium glutamicum*. Metab. Eng. 32, 184–194.
Meiswinkel, T.M., Gopinath, V., Lindner, S.N., Nampoothiri, K.M., Wendisch, V.F., 2013. Accelerated pentose utilization by *Corynebacterium glutamicum* for accelerated production of lysine, glutamate, ornithine and putrescine. Microb. Biotechnol. 6.
Mundhada, H., Seoane, J.M., Schneider, K., Koza, A., Christensen, H.B., Klein, T., Phaneuf, P.V., Herrgard, M., Feist, A.M., Nielsen, A.T., 2017. Increased production of L-serine in *Escherichia coli* through Adaptive Laboratory Evolution. Metab. Eng. 39, 141–150.
Portnoy, V.A., Bezdan, D., Zengler, K., 2011. Adaptive laboratory evolution–harnessing the power of biology for metabolic engineering. Curr. Opin. Biotechnol. 22 (4), 590–594.
Qin, D., Hu, Y., Cheng, J., Wang, N., Li, S., Wang, D., 2016. An auto-inducible *Escherichia coli* strain obtained by adaptive laboratory evolution for fatty acid synthesis from ionic liquid-treated bamboo hydrolysate. Bioresour. Technol. 221, 375–384.
Radek, A., Krumbach, K., Gatgens, J., Wendisch, V.F., Wiechert, W., Bott, M., Noack, S., Marienhagen, J., 2014. Engineering of *Corynebacterium glutamicum* for minimized carbon loss during utilization of D-xylose containing substrates. J. Biotechnol. 192 (Pt. A), 156–160.
Reyes, L.H., Gomez, J.M., Kao, K.C., 2014. Improving carotenoids production in yeast via adaptive laboratory evolution. Metab. Eng. 21, 26–33.
Sambrook, J., Russell, D., 2001. Molecular Cloning: a Laboratory Manual. Cold Spring Harbor Laboratory Press, Cold Spring Harbor.
Sjostrom, S.L., Huang, M., Nielsen, J., Joensson, H.N., Svahn, H.A. 2014. Micro-droplet based directed evolution outperforms conventional laboratory evolution. In: International Conference on Miniaterized Systems for Chemistry and Life Sciences (proceedings), 169–171.
Straathof, A.J.J., 2014. Transformation of biomass into commodity chemicals using enzymes or cells. Chem. Rev. 114 (3), 1871–1908.
Unthan, S., Baumgart, M., Radek, A., Herbst, M., Siebert, D., Bruhl, N., 2015a. Chassis organism from *Corynebacterium glutamicum* - a top-down approach to identify and delete irrelevant gene clusters. Biotechnol. J. 10.
Unthan, S., Grunberger, A., van Ooyen, J., Gatgens, J., Heinrich, J., Paczia, N., Wiechert, W., Kohlheyer, D., Noack, S., 2014. Beyond growth rate 0.6: what drives *Corynebacterium glutamicum* to higher growth rates in defined medium. Biotechnol. Bioeng. 111 (2), 359–371.
Unthan, S., Radek, A., Wiechert, W., Oldiges, M., Noack, S., 2015. Bioprocess automation on a Mini Pilot Plant enables fast quantitative microbial phenotyping. Microb. Cell Fact. 14 (1), 32.
Viikari, L., Vehmaanperä, J., Koivula, A., 2012. Lignocellulosic ethanol: from science to industry. Biomass Bioenergy 46, 13–24.
Wang, D., Ju, X., Zhou, D., Wei, G., 2014. Efficient production of pullulan using rice hull hydrolysate by adaptive laboratory evolution of *Aureobasidium pullulans*. Bioresour. Technol. 164, 12–19.
Wang, L., Xue, C., Wang, L., Zhao, Q., Wei, W., Sun, Y., 2016. Strain improvement of *Chlorella sp.* for phenol biodegradation by adaptive laboratory evolution. Bioresour. Technol. 205, 264–268.
Wang, Z., Wu, J., Zhu, L., Zhan, X., 2016. Activation of glycerol metabolism in *Xanthomonas campestris* by adaptive evolution to produce a high-transparency and low-viscosity xanthan gum from glycerol. Bioresour. Technol. 211, 390–397.
Yu, S., Zhao, Q., Miao, X., Shi, J., 2013. Enhancement of lipid production in low-starch mutants *Chlamydomonas reinhardtii* by adaptive laboratory evolution. Bioresour. Technol. 147, 499–507.

2.2 Discovery of a D-xylose transporter

Bioresource Technology 249 (2018) 953–961

Contents lists available at ScienceDirect

Bioresource Technology

journal homepage: www.elsevier.com/locate/biortech

The *myo*-inositol/proton symporter IolT1 contributes to D-xylose uptake in *Corynebacterium glutamicum*

Christian Brüsseler, Andreas Radek, Niklas Tenhaef, Karin Krumbach, Stephan Noack, Jan Marienhagen*

Institute of Bio- and Geosciences, IBG-1: Biotechnology, Forschungszentrum Jülich GmbH, Jülich D-52425, Germany

ARTICLE INFO

Keywords:
Corynebacterium glutamicum
D-xylose
Lignocellulosic biomass
Weimberg pathway
Isomerase pathway

ABSTRACT

Corynebacterium glutamicum has been engineered to utilize D-xylose as sole carbon and energy source. Recently, a *C. glutamicum* strain has been optimized for growth on defined medium containing D-xylose by laboratory evolution, but the mutation(s) attributing to the improved-growth phenotype could not be reliably identified. This study shows that loss of the transcriptional repressor IolR is responsible for the increased growth performance on defined D-xylose medium in one of the isolated mutants. Underlying reason is derepression of the gene for the glucose/*myo*-inositol permease IolT1 in the absence of IolR, which could be shown to also contribute to D-xylose uptake in *C. glutamicum*. IolR-regulation of *iolT1* could be successfully repealed by rational engineering of an IolR-binding site in the *iolT1*-promoter. This minimally engineered *C. glutamicum* strain bearing only two nucleotide substitutions mimics the IolR loss-of-function phenotype and allows for a high growth rate on D-xylose-containing media (μ_{max} = 0.24 ± 0.01 h^{-1}).

1. Introduction

Corynebacterium glutamicum is employed for the microbial production of amino acids such as L-glutamate and L-lysine on a large industrial scale of several million tons per year (Eggeling and Bott, 2015). In addition, engineered *C. glutamicum* strains for the production of various organic acids, alcohols and natural products such as carotenoids, stilbenes and flavonoids are available, rendering this microorganism a versatile microbial platform for a broad range of future biotechnological applications (Heider et al., 2012; Kallscheuer et al., 2016, 2017; Litsanov et al., 2012; Vogt et al., 2016).

Traditionally, D-glucose and D-fructose, mostly derived from starch hydrolysates or molasses, serve as feedstocks for large-scale productions employing *C. glutamicum* (Blombach and Seibold, 2010). With the aim to minimize competition for these hexoses between the industrial sectors of human nutrition and industrial biotechnology, *C. glutamicum* strains utilizing cellobiose, L-arabinose or D-xylose have been engineered, as these carbohydrates constitute a large portion of typical agro-waste streams (Kawaguchi et al., 2006; Kotrba et al., 2003; Radek et al., 2014; Schneider et al., 2011). In case of D-xylose, two different metabolic strategies have been implemented in *C. glutamicum* as this bacterium cannot naturally metabolize this pentose. In the isomerase pathway, D-xylose is first converted to D-xylulose by a heterologous xylose isomerase (encoded by *xylA* from either *Escherichia coli* or *Xanthomonas campestris*) and subsequently phosphorylated by an endogenous xylulokinase (encoded by *xylB*) yielding xylulose-5-phosphate (Fig. 1A) (Kawaguchi et al., 2006; Meiswinkel et al., 2013).

As this compound is an intermediate of the pentose phosphate pathway, it can be rapidly metabolized by *C. glutamicum*. Engineered strains using this pathway for D-xylose utilization allowed for the microbial synthesis of the amino acids L-lysine, L-glutamate and L-ornithine and the diamine putrescine from D-xylose (Meiswinkel et al., 2013). However, a significant fraction of the D-xylose-derived carbon is lost in the form of CO_2 during synthesis of α-ketoglutarate-derived products such as L-glutamate, lowering the overall product yield when D-xylose is metabolized by the isomerase pathway.

In contrast, the Weimberg pathway as alternative strategy for D-xylose-metabolization offers the possibility to directly convert D-xylose to the citric acid cycle intermediate and direct L-glutamate precursor α-ketoglutarate without loss of any carbon (Fig. 1B) (Johnsen et al., 2009; Stephens et al., 2007; Weimberg, 1961). In this pathway D-xylose is first oxidized by a xylose dehydrogenase (encoded by *xylB*) yielding D-xylonolactone, which is subsequently hydrolyzed by a D-xylonolactonase (encoded by *xylC*) to D-xylonate. In the two following reaction steps two molecules of water are successively eliminated by a D-xylonate dehydratase (encoded by *xylD*) and a 2-keto-3-deoxyxylonate dehydratase (encoded by *xylX*) yielding α-ketoglutarate semialdehyde. Finally, this compound is oxidized to α-ketoglutarate by a α-ketoglutarate

* Corresponding author.
E-mail address: j.marienhagen@fz-juelich.de (J. Marienhagen).

https://doi.org/10.1016/j.biortech.2017.10.098
Received 1 October 2017; Received in revised form 30 October 2017; Accepted 31 October 2017
Available online 01 November 2017
0960-8524/ © 2017 Elsevier Ltd. All rights reserved.

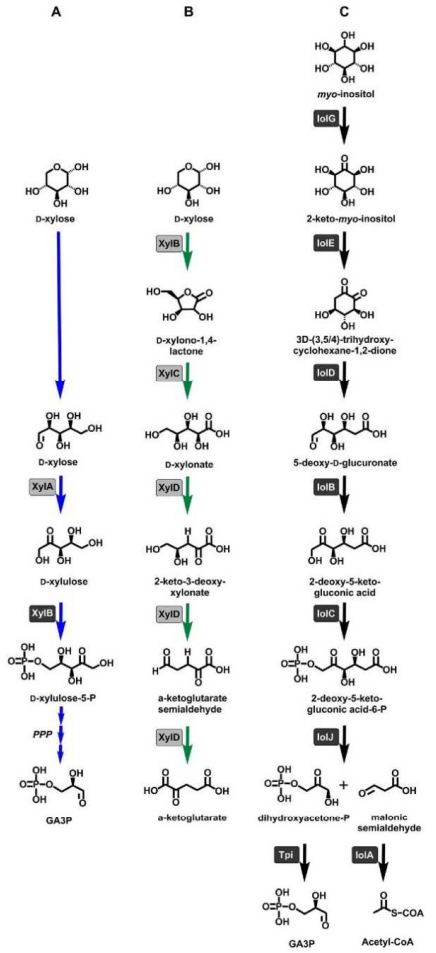

Fig. 1. Schematic overview of the isomerase pathway (A); the Weimberg pathway (B); and the *myo*-inositol pathway (C) highlighting the chemical similarities between substrates and intermediates. Heterologous enzymes required in *C. glutamicum* for establishing the respective pathway are highlighted in grey, whereas endogenous enzymatic functions of *C. glutamicum* are highlighted in black. Abbreviations: (A): XylA, xylose isomerase; XylB, xylulokinase; PPP, pentose phosphate pathway; (B) XylB, xylose dehydrogenase; XylC, D-xylonolactonase; XylD, D-xylonate dehydratase; XylX, 2-keto-3-deoxy xylonate dehydratase; XylA, α-ketoglutarate semialdehyde dehydrogenase; (C): IolG, inositol 2-dehydrogenase, IolE, 2-keto-*myo*-inositol dehydratase; IolD, epi-inositol hydrolase; IolB, 5-deoxy-glucuronate isomerase; IolC, 5-keto-2-deoxygluconokinase; IolJ, 5-keto-2-deoxy-D-gluconate-6 phosphate aldolase; Tpi, triosephosphate isomerase; IolA, methylmalonate-semialdehyde dehydrogenase.

semialdehyde dehydrogenase (encoded by *xylA*). Establishing this five-step pathway, originally discovered in *Pseudomonas fragi* and later also in *Haloferax volcanii* and *Caulobacter crescentus*, could be achieved by heterologous expression of the *xylXABCD*-operon from *C. crescentus* in *C. glutamicum* (Radek et al., 2014). Presence and activity of the Weimberg pathway enabled growth of *C. glutamicum* pEKEx3-*xylXABCD*$_{Cc}$ on D-xylose as sole carbon and energy source with $\mu_{max} = 0.07 \pm 0.01\,h^{-1}$ (Radek et al., 2014).

Recently, a *C. glutamicum* strain with a plasmid bearing the five genes of the Weimberg pathway as codon-optimized versions for expression in *C. glutamicum* and organized as a synthetic operon was subjected to an adaptive laboratory evolution experiment to improve growth on D-xylose as sole carbon and energy source (Radek et al., 2017). The best two strains allowed for growth at a maximum growth rate of $\mu_{max} = 0.26 \pm 0.02\,h^{-1}$ and genome sequencing of these strains revealed several mutations potentially contributing to improved growth on D-xylose, but a detailed analysis has not been performed yet.

In this study, we present a detailed characterization of one of these two *C. glutamicum* strains bearing a large deletion in the *iolR* gene, which encodes for a repressor involved in *myo*-inositol catabolism, and investigate its impact on D-xylose uptake in different *C. glutamicum* strains. Furthermore, we describe the rational reengineering of a *C. glutamicum* strain mimicking the *iolR* loss-of-function mutation.

2. Materials and methods

2.1. Bacterial strains, plasmids, media, and growth conditions

All used bacterial strains and plasmids are listed in Table 1. *Escherichia coli* DH5α was used for cloning purposes and was grown aerobically on a rotary shaker (170 rpm) at 37 °C in 5 mL Lysis Broth (LB) medium (Bertani, 1951) or on LB agar plates (LB medium with 1.8% [wt/vol] agar). All *C. glutamicum* strains are derived from *C. glutamicum* ATCC 13032 (Abe et al., 1967) and were routinely precultivated aerobically in Brain Heart infusion (BHI) medium (Difco Laboratories, Detroit, USA) on a rotary shaker (170 rpm) at 30 °C. These cultures were used to inoculate main cultures in defined CGXII medium (Keilhauer et al., 1993) supplemented with different mixtures of D-glucose and D-xylose as carbon and energy source. If supplementation of antibiotics for the cultivation of strains harboring pK19*mobsacB* was required, kanamycin was added to final concentrations of 25 μg mL^{-1} (*C. glutamicum*) or 50 μg mL^{-1} (*E. coli*). For the cultivation of engineered *C. glutamicum* strains utilizing the Weimberg- or Isomerase pathway for D-xylose metabolization, spectinomycin was supplemented to a final concentration of 100 μg mL^{-1}. Induction of gene expression was achieved by adding isopropyl β-D-thiogalactoside (IPTG) to a final concentration of 1 mM. In general, growth of bacterial strains, cultivated in baffled shake flasks, was followed by measuring the optical density at 600 nm (OD_{600}).

Microtiter plate cultivations of *C. glutamicum* were carried out in 48-well flowerplates (m2p-labs GmbH, Baesweiler, Germany) using a BioLector (m2p-labs GmbH) embedded in a liquid handling station (JANUS working station, Perkin Elmer, Waltham MA, USA) for automated sampling and sample processing. The cultivation settings were always kept at 1300 rpm, 95% humidity and 30 °C. Depending on the experiment, online signals for biomass (backscatter; gain 15), dissolved oxygen (pO_2; gain 35) and pH (gain 35) were collected. Plates were covered with a gas permeable sealing foil (m2p-labs GmbH) to prevent contaminations and to allow for a uniform gas exchange. Medium preparation and inoculation were performed manually under a sterile bench.

2.2. Plasmid and strain construction

All enzymes were purchased from Thermo Scientific (Schwerte, Germany) and synthetic genes were obtained as codon-optimized

Table 1
Strains and plasmids used in this study.

Strain or plasmid	Relevant characteristics[a]	Source or reference
C. glutamicum strains		
ATCC13032 (WT)	biotin auxotroph wild-type strain	Abe et al. (1967)
ISO	*C. glutamicum* ATCC 13032 pEKEx3-*xylA*$_{Xc}$-*xylB*$_{Cg}$	Radek et al. (2014)
WMB2	*C. glutamicum* ATCC 13032 pEKEx3-*xylXABCD*$_{Cc}$-opt	Radek et al. (2017)
WT Δ*iolR*	*C. glutamicum* ATCC 13032 with in-frame deletion of *iolR* (cg0196)	Klaffl et al. (2013)
ISO Δ*iolR*	Derivative of *C. glutamicum* ISO with in-frame deletion of *iolR* (cg0196)	This study
WMB2 Δ*iolR*	Derivative of *C. glutamicum* WMB2 with in-frame deletion of *iolR* (cg0196)	This study
WMB2 Δ*iolR* Δ*iolA*	Derivative of *C. glutamicum* WMB2 Δ*iolR* with in-frame deletion of *iolA* (cg0199)	This study
WMB2 Δ*iolR* Δ*iolE*	Derivative of *C. glutamicum* WMB2 Δ*iolR* with in-frame deletion of *iolE* (cg0203)	This study
WMB2 Δ*iolR* Δ*iolT1*	Derivative of *C. glutamicum* WMB2 Δ*iolR* with in-frame deletion of *iolT1* (cg0223)	This study
WMB2 Δ*iolR* Δ*iolP*	Derivative of *C. glutamicum* WMB2 Δ*iolR* with in-frame deletion of *iolP* (cg0206)	This study
WMB2 Δ*iolR* Δ*oxiA*	Derivative of *C. glutamicum* WMB2 Δ*iolR* with in-frame deletion of *oxiA* (cg0207)	This study
WMB2 Δ*iolR* Δ*iolT2*	Derivative of *C. glutamicum* WMB2 Δ*iolR* with in-frame deletion of *iolT2* (cg3387)	This study
WMB2 P_{O6} *iolT1*	Derivative of *C. glutamicum* WMB2 with two point mutations in the promotor of *iolT1*, relative to the start codon at position −113 (A → G) and −112 (C → G) respectively	This study
E. coli strains		
DH5α	F⁻ Φ80*lacZ*ΔM15 Δ(*lacZ*YA-*arg*F) U169 *rec*A1 *end*A1 *hsd*R17 (r_K^-, m_K^+) *pho*A *sup*E44 λ– *thi*-1 *gyr*A96 *rel*A1	Invitrogen (Karlsruhe, Germany)
Plasmids		
pEKEx3	Spec^r; *C. glutamicum/E. coli* shuttle vector for regulated gene expression; (P_{tac}, *lacI*^{q}, pBL1 *oriVCg*, pUC18 *oriVEc*)	Gande et al. (2007)
pEKEx3-*xylA*$_{Xc}$-*xylB*$_{Cg}$	Spec^r; pEKEx3 derivative for the regulated expression of *xylA*$_{Xc}$ of *X. campestris* and *xylB*$_{Cg}$ of *C. glutamicum*	Meiswinkel et al. (2013)
pEKEx3-*xylXABCD*$_{Cc}$-opt	Spec^r; pEKEx3 derivative for the regulated expression of *xylXABCD*$_{Cc}$ of *C. crescentus*	Radek et al. (2017)
pk19*mobsacB* Δ*iolR*	Kan^r; plasmid for in-frame deletion of *iolR* (cg0196)	Klaffl et al. (2013)
pk19*mobsacB* Δ*iolA*	Kan^r; plasmid for in-frame deletion of *iolA* (cg0199)	This study
pk19*mobsacB* Δ*iolE*	Kan^r; plasmid for in-frame deletion of *iolE* (cg0203)	This study
pk19*mobsacB* Δ*iolT1*	Kan^r; plasmid for in-frame deletion of *iolT1* (0223)	This study
pk19*mobsacB* Δ*iolP*	Kan^r; plasmid for in-frame deletion of *iolP* (cg0206)	This study
pk19*mobsacB* Δ*oxiA*	Kan^r; plasmid for in-frame deletion of *oxiA* (cg0207)	This study
pk19*mobsacB* Δ*iolT2*	Kan^r; plasmid for in-frame deletion of *iolT2* (cg3387)	This study
pk19*mobsacB* P_{O6} *iolT1*	Kan^r; plasmid for introducing two point mutations in the promotor region of *iolT1*, relative to the start codon at position -113 (A → G) and -112 (C → G), respectively	This study

[a] Kan^r, kanamycin resistance; Spec^r, spectinomycin resistance.

versions for expression in *C. glutamicum* from LifeTechnologies (Darmstadt, Germany). All oligonucleotides were synthesized by Eurofins genomics (Ebersfeld, Germany) and are listed in Table 2. For molecular cloning, standard protocols for PCR, DNA restriction, DNA ligation or Gibson cloning were used (Gibson et al., 2009; Sambrook and Russel, 2001). Verification of the constructed plasmids was performed by restriction analysis, colony PCR or DNA sequencing at Eurofins Genomics (Ebersberg, Germany). *E. coli* DH5α was transformed using the RbCl-method, whereas *C. glutamicum* was routinely transformed by electroporation (Eggeling and Bott, 2005; Hanahan, 1983).

In-frame deletions of *iolR*, *iolA*, *iolE*, *iolT1*, *iolP*, *oxiA*, *iolT2* and substitution of two successive nucleotides in the *iolT1*-promoter in *C. glutamicum* ATCC 13032 were performed by two-step homologous recombination using the plasmids pk19*mobsacB* Δ*iolR*, pk19*mobsacB* Δ*iolA*, pk19*mobsacB* Δ*iolE*, pk19*mobsacB* Δ*iolT1*, pk19*mobsacB* Δ*iolP*, pk19*mobsacB* Δ*oxiA*, pk19*mobsacB* Δ*iolT2* and pk19*mobsacB* P_{O6} *iolT1*, respectively, as previously described (Schäfer et al., 1994).

2.3. GC-TOF-MS analysis

Prior to analysis, 130 µL aliquots of extracted samples were shock frozen in liquid nitrogen, subsequently lyophilized overnight in a LT-105 freeze drier (Martin Christ Gefriertrocknungsanlagen, Osterode am Harz, Germany) and then stored at −20 °C. Dried samples were subsequently derivatized with 50 µL MeOX (20 mg mL^{-1} *O*-methylhydroxylamine in pyridine) for 90 min at 30 °C and 600 rpm in an Eppendorf Thermomixer followed by an incubation with additional 80 µL of MSTFA (*N*-acetyl-*N*-(trimethylsilyl)-trifluoroacetamide) for 90 min at 40 °C and 600 rpm. Derivatized metabolites were analyzed using an Agilent 6890N gas chromatograph (Agilent, Waldbronn, Germany) coupled to a Waters Micromass GCT Premier high resolution time-of-flight mass spectrometer (Eschborn, Germany). The system was controlled by Waters MassLynx 4.1 software. Injections were performed by a Gerstel MPS 2 (Mülheim an der Ruhr, Germany) controlled by Maestro software. 1 µL samples were injected into a split/splitless injector at 280 °C at varying split modes. The GC was equipped with a 30 m Agilent EZ-Guard VF-5ms + 10 m guard column (Agilent, Waldbronn, Germany). Constant helium flow was set to 1 mL min^{-1}. The GC temperature program starts at 60 °C with a hold time of 2 min, followed by a temperature ramp of +12 °C min^{-1} up to the final temperature of 300 °C and hold time of 8 min. The total run time for each analysis was 30 min. The transfer line temperature was set to 300 °C. The TOF-MS was operated in positive electron impact $[EI]^+$ mode at an electron energy of 70 eV. Ion source temperature was set to 180 °C. The MS was tuned and calibrated with the mass fragmentation pattern of Heptacosa (heptacosafluorotributylamine). During analysis, the accurate masses were corrected to a single point lock mass of CPFB (chloropentafluoro-benzene) as an external reference at 201.9609 *m/z*. Data acquisition was performed in centroid mode with a scan rate of 0.09 s and an interscan delay of 0.01 s, which means 10 scans s^{-1}. For identification of known metabolites, a baseline noise subtracted fragment pattern was compared to the in-house database JuPoD and the commercial database NIST11 (National Institute of Standards and Technology, Gaithersburg, USA). Unknown peaks were identified by structural combination of elemental compositions and verified by comparison to a virtual derivatization and fragmentation of the predicted structure.

2.4. Quantification of C_5 and C_6 sugars

For following substrate concentrations over time, either an enzymatic assay (Megazyme, Wickow, Ireland) or an LC-MS-based method was used. Quantification of D-xylose by the enzymatic assay was

Table 2
DNA-oligonucleotides used in this study.

Name	DNA Sequence (5′-3′)
Construction of pk19mobsacB ΔiolA (cg0199)	
IolA_check_fw	CGCCCGGGTGTGGATGGTGTGCTGG
IolA_check_rev	GAAAGCTCCTTCTGCTGCTTCGGCC
IolA_fw_fw	TGCATGCCTGCAGGTCGACTAACCCTAGTGCGCATCAAC
IolA_fw_rev	TACTCCCGGGCATATGGGTTTGTGGTTCAGACATG
IolA_rev_fw	ACCACAAACCCATATGCCCGGGAGTACTGGATCCGGTGGCATTAACCTCGGT
IolA_rev_rev	TTGTAAAACGACGGCCAGTGTTCACCTGGGGTGATTAC
Construction of pk19mobsacB ΔiolE (cg0203)	
IolE_check_fw	CGTTCTCGTGCATGGGCTATGAAAT
IolE_check_rev	ACTTCACTTCAACGGAGACAACTCG
IolE_fw_fw	TGCATGCCTGCAGGTCGACTCAACACTGAGCTGGTCAC
IolE_fw_rev	TACTCCCGGGCATATGAGGTACAGAAGTGGTCATG
IolE_rev_fw	TTCTGTACCTCATATGCCCGGGAGTACTGGATCCATCTTCGGCTGCACCCACTTC
IolE_rev_rev	TTGTAAAACGACGGCCAGTGGTGCAGGCCGCGGAGCAT
Construction of pk19mobsacB ΔiolT1 (cg0223)	
IolT1_check_fw	GATTGTTCTACGAATGCCCACTTCG
IolT1_check_rev	GGGACGATTCTCGTAGTCGGAGGGG
IolT1_fw_fw	TGCATGCCTGCAGGTCGACTTGGTCGATCGACGTCTCG
IolT1_fw_rev	TACTCCCGGGCATATGAATGAAGGTACTAGCCATCTTG
IolT1_rev_fw	TACCTTCATTCATATGCCCGGGAGTACTGGATCCTTCAACAAGGACATCCGAAAAG
IolT1_rev_rev	TTGTAAAACGACGGCCAGTGTGACAGTTCTTGGACTGG
Construction of pk19mobsacB ΔiolP (cg0206)	
IolP_check_fw	CAACATCAAGCGCATCATCCAGTTG
IolP_check_rev	GCGTTGGTTGGGCCTTCTGGAAGGT
IolP_fw_fw	TGCATGCCTGCAGGTCGACTATTTCGTGGAAAACGGTATTG
IolP_fw_rev	TACTCCCGGGCATATGCATGGCGTCGATGTCCAA
IolP_rev_fw	CGACGCCATGCATATGCCCGGGAGTACTGGATCCCGCGACGGCGGTGCCCGA
IolP_rev_rev	TTGTAAAACGACGGCCAGTGAAGGAATCAGGTTCGATCAGGTCTAGTCGCAGG
Construction of pk19mobsacB ΔoxiA (cg0207)	
OxiA_check_fw	AAGTGCTGCGGTGGTATGCGGTTTT
OxiA_check_rev	CTTGCGCGGGCGAGGAACTAACTCG
OxiA_fw_fw	TGCATGCCTGCAGGTCGACTCAACATTAGCGGGTGCCA
OxiA_fw_rev	TACTCCCGGGCATATGTCCGATTCGAATAGTCATGTTTTTATAC
OxiA_rev_fw	TCGAATCGGACATATGCCCGGGAGTACTGGATCCAGCGCTGCGGAAAAACGC
OxiA_rev_rev	TTGTAAAACGACGGCCAGTGTCCATGAGGTCAGTTCAGTAAGAG
Construction of pk19mobsacB ΔiolT2 (cg3387)	
IolT2_check_fw	TGTTTACGCCAAGCCCTAACAAGCC
IolT2_check_rev	CTTCGGCTGCAAGCACTGCGTTGAT
IolT2_fw_fw	TGCATGCCTGCAGGTCGACTTCAGAATGAGTATTTGGCCC
IolT2_fw_rev	TACTCCCGGGCATATGGGCCTTGATGTCCGTCATG
IolT2_rev_fw	CATCAAGGCCCATATGCCCGGGAGTACTGGATCCGCAGCATTCACCGGCCAG
IolT2_rev_rev	TTGTAAAACGACGGCCAGTGTTCAGATCAACACCGGTTGTTTTG
Construction of pk19mobsacB P_{O6} iolT1	
P_{O6}IolT1_check_fw	TACGAATGCCCACTTCGCACCCTT
P_{O6}IolT1_check_rev	CAACTCATTACGGCCAGCCAGTGAGC
P_{O6}IolT1_fw_fw	TGCATGCCTGCAGGTCGACTGAAAAATTGATCAGCAAACACC
P_{O6}IolT1_fw_rev	GGCAGACACGATATCCCCCGTCAATCGTACATAGGGAA
P_{O6}IolT1_rev_fw	CGGGGGATATCGTGTCTGCCACGATTAAAG
P_{O6}IolT1_rev_rev	TTGTAAAACGACGGCCAGTGGAGTCCAAGAAGCACACG

performed via monitoring of the increased NADH level measured at 340 nm which was formed during the oxidation of D-xylose by a D-xylose dehydrogenase (XDH) (Peterson and Young, 1968; Radek et al., 2014).

Quantification by LC-MS was performed using an ultra-high-performance LC (uHPLC) 1290 Infinity system coupled to a 6130 quadrupole MS system (Agilent, Waldbronn, Germany). Separation was achieved by using a Luna (NH_2) Amino column (100 Å pore size, 150 mm by 2 mm; Phenomenex, Torrance, CA, USA) at 60 °C. For elution, acetonitrile and water was used in an isocratic composition of 80% and 20% respectively. The mass spectrometer was operated in the negative electrospray ionization (ESI) and fragmented molecules were detected in the selected-ion-monitoring (SIM) mode. Data acquisition and analysis was performed using the ChemStation Edition Open Lab software (Version A.01.04; Agilent, Waldbronn, Germany).

3. Results and discussion

3.1. Deletion of iolR improves growth via the Weimberg pathway on D-xylose

Adaptive laboratory evolution of *C. glutamicum* ATCC 13032 pEKEx3-*xylXABCD*$_{Cc}$-opt (WMB2), engineered for the plasmid-based expression of the codon-optimized *xylXABCD*-operon from *C. crescentus*, yielded the strain *C. glutamicum* WMB2$_{evo}$ with the highest reported growth rate of 0.26 ± 0.02 h^{-1} on D-xylose as sole carbon and energy source (Radek et al., 2017). Genome sequencing identified a larger deletion of 98 base pairs from position 133 to 232 relative to the start codon in the open-reading frame of the *iolR*-gene, which encodes for the transcriptional regulator IolR. In *C. glutamicum*, this GntR-type regulator is responsible for the repression of the *iol*-genes involved in uptake and degradation of *myo*-inositol (Klaffl et al., 2013). Structural similarity between D-xylose and the cyclic polyol *myo*-inositol in

aqueous solution led to the assumption that this particular *iolR* mutation is responsible for improved growth of *C. glutamicum* $WMB2_{evo}$ in D-xylose containing media (Fig. 1C). For this reason, the *iolR* gene was deleted in the genetic background of the *C. glutamicum* wild type, yielding *C. glutamicum* WT Δ*iolR*. Based on this strain, a D-xylose utilizing *C. glutamicum* Δ*iolR* variant employing the Weimberg pathway was constructed by introducing the plasmid pEKEx3_*xylXABCD*$_{Cc}$-opt. Comparative cultivation of the resulting strain *C. glutamicum* WMB2 Δ*iolR* and *C. glutamicum* WMB2 on D-xylose containing substrate mixtures in a BioLector microbioreactor system revealed interesting differences (Fig. 2A, B). In defined CGXII medium containing a mixture of 10 g L^{-1} D-glucose and 30 g L^{-1} D-xylose, growth of the reference strain *C. glutamicum* WMB2 is characterized by the same three distinct growth phases as previously described for the very similar strain *C. glutamicum* WMB (Radek et al., 2014) (Fig. 2A). This strain carries the same Weimberg pathway encoding operon, which was simply isolated from *C. crescentus* by PCR and thus not codon-optimized for an expression in *C. glutamicum*.

The strain first consumed D-glucose and D-xylose in parallel in the first twelve hours, but only D-glucose utilization contributes to biomass formation (μ_{max} = 0.31 ± 0.03 h^{-1}). At this stage, D-xylose was only converted to the Weimberg pathway intermediate D-xylonate, which accumulated in the medium (data not shown). In the second growth phase, when D-glucose was depleted, D-xylose served as main carbon and energy source (μ_{max} = 0.04 ± 0.01 h^{-1}) and formation of D-xylonate continues. Accumulation of this organic acid led to the characteristic drop of the pH in this growth phase. After 27 h of cultivation, when both sugars were depleted, biomass formation continues at a very low growth rate of only 0.01 h^{-1}. In this third growth phase D-xylonate was taken up and further metabolized by the Weimberg pathway, which was reflected by an increase of pH. In direct comparison, growth of *C. glutamicum* WMB2 Δ*iolR* in medium containing 10 g L^{-1} D-glucose and 30 g L^{-1} D-xylose was characterized by a slightly elongated lag-phase in comparison to the strain having no deletion of *iolR* (Fig. 2A). Although the second growth phase is much less pronounced and much shorter, three distinct growth phases could be also detected for *C. glutamicum* WMB2 Δ*iolR* when taking the course of pH over time into consideration. Growth on D-glucose was comparable (μ_{max} = 0.31 ± 0.01 h^{-1}) to *C. glutamicum* WMB2, but the second growth phase, accompanied by the characteristic sharp drop of pH, set in after 14.5 h of cultivation and lasted only for 2.5 h. However, the growth rate of *C. glutamicum* WMB2 Δ*iolR* at this stage appeared to be almost unchanged compared to the growth rate during growth on D-glucose, which hints at an increased D-xylose uptake- or consumption rate. The third growth phase started after 17 h of cultivation, 10 h earlier compared to the cultivation of the reference strain *C. glutamicum* WMB2, which was also reflected by an increase of pH due to the onset of D-xylonate consumption. However, the growth rate of *C. glutamicum* WMB2 Δ*iolR* in this third growth phase is only slightly increased in comparison to the reference strain (μ_{max} = 0.02 ± 0.01 h^{-1}).

The observed positive effect of the *iolR*-deletion on D-xylose consumption and growth was much more pronounced during cultivation of *C. glutamicum* WMB2 Δ*iolR* in defined CGXII medium containing solely 40 g L^{-1} D-xylose as sole carbon and energy source (Fig. 2B). On this medium, the strain exhibited a biphasic growth behavior and was characterized by a shorter lag-phase compared to the reference strain. During the first growth phase *C. glutamicum* WMB2 Δ*iolR* reached a maximum specific growth rate of 0.28 ± 0.03 h^{-1}, which was twice as high as the growth rate of *C. glutamicum* WMB2 (μ_{max} = 0.13 h^{-1}). Again, growth in this phase was accompanied by a drastic drop of pH due to the extracellular accumulation of the Weimberg pathway intermediate D-xylonate. After 23 h of cultivation, the growth rate of *C. glutamicum* WMB2 Δ*iolR* dropped drastically (μ_{max} = 0.02 ± 0.01 h^{-1}), and the pH increased, indicating uptake and further metabolization of D-xylonate. In addition, deletion of *iolR* appeared to also have a pronounced positive effect on overall biomass formation during the cultivation on solely D-xylose containing defined medium. According to the backscatter measurements, this strain produced twice as much biomass as the reference strain *C. glutamicum* WMB2 within 25 h of cultivation.

3.2. Deletion of iolR also improves growth via the isomerase pathway on D-xylose

Motivated by the drastic effect of the *iolR*-deletion on a *C. glutamicum* strain utilizing D-xylose via the Weimberg pathway, the question whether absence of the transcriptional regulator has a similar effect on a strain employing the isomerase pathway needed to be answered. For this purpose, *C. glutamicum* WT Δ*iolR* was transformed with the plasmid pEKEx3_*xylA*$_{Xc}$-*xylB*$_{Cg}$ yielding the strain *C. glutamicum* ISO Δ*iolR*. At first glance, *C. glutamicum* ISO Δ*iolR* did not appear to show the same characteristic bi-phasic growth behavior of the reference strain *C. glutamicum* ISO on defined CGXII medium containing a mixture of 10 g L^{-1} D-glucose and 30 g L^{-1} D-xylose (Fig. 2C) (Radek et al., 2014). Instead, the strain reached the final biomass already after 18 h (μ_{max} = 0.27 ± 0.01 h^{-1}). However, similar to growth of *C. glutamicum* WMB2 Δ*iolR* in the same media, two different growth phases become apparent when one also considers the course of pH over the cultivation time. The pH dropped from 7.2 (12 h) to 6.9 (18 h) due to accumulation of D-xylonate in the culture medium. A significant change in the growth rate was not observable for *C. glutamicum* ISO Δ*iolR*. In contrast, growth of the reference strain *C. glutamicum* ISO was characterized by a distinct second growth phase (μ_{max} = 0.09 h^{-1}) and a slowly flattening pH, both indicating slower D-xylose-metabolization (Fig. 2C). In addition, the observation, that the *C. glutamicum* ISO strain reached the final biomass only at the end of the cultivation time of 40 h, 22 h after *C. glutamicum* ISO Δ*iolR*, indicated, that deletion of *iolR* has the same positive effect on D-xylose utilization as observed for *C. glutamicum* WMB2 Δ*iolR* employing the Weimberg pathway. Cultivation of *C. glutamicum* ISO Δ*iolR* and the reference strain *C. glutamicum* ISO in defined CGXII medium with 40 g L^{-1} D-xylose as sole carbon and energy source underpinned this assumption as the strain devoid of any *iolR*-activity grows on average 1.6 times faster compared to the reference strain (*C. glutamicum* ISO Δ*iolR*: μ_{avg} = 0.13 h^{-1} ± 0.01 h^{-1} vs. *C. glutamicum* ISO: μ_{avg} = 0.08 h^{-1} ± 0.02 h^{-1}) (Fig. 2D).

3.3. The glucose permease IolT1 contributes to D-xylose uptake in C. glutamicum

The observed effect of the *iolR*-deletion on D-xylose utilization via the Weimberg pathway and the isomerase pathway in *C. glutamicum* stimulated further investigations for uncovering the underlying physiological consequences of the absence of the transcriptional repressor IolR. A previously conducted transcriptome analysis of *C. glutamicum* ATCC 13032 Δ*iolR* identified 22 genes showing an at least 3-fold change in their transcript levels in comparison to the *C. glutamicum* ATCC 13032 wild type (Klaffl et al., 2013). Among these genes are several protein encoding genes involved in *myo*-inositol utilization, which could potentially contribute to D-xylose/D-xylonate transport or metabolization since substrates and intermediates of both pathways are chemically similar (Fig. 1B and C): The gene products of *oxiA* (cg0207, *myo*-inositol dehydrogenase OxiA) and *iolA* (cg0199, aldehyde dehydrogenase IolA) oxidize malonic semialdehyde and *myo*-inositol, respectively, which are similar to D-xylose and α-ketoglutarate semialdehyde, respectively; the 2-keto-*myo*-inositol dehydratase IolE (encoded by *iolE*, cg0203) could also catalyze the dehydration of the Weimberg pathway intermediates D-xylonate or 2-keto-3-deoxy-xylonate; and gene products of *iolP* (cg0206, efflux carrier IolP) and *iolT1* (cg0223, glucose permease/*myo*-inositol transporter IolT1) could participate in the uptake of D-xylose (Weimberg pathway/isomerase pathway). Among these candidates, *iolT1* stood out as the previously conducted adaptive laboratory evolution experiments yielded several *C. glutamicum* variants with enhanced D-xylose utilization capabilities

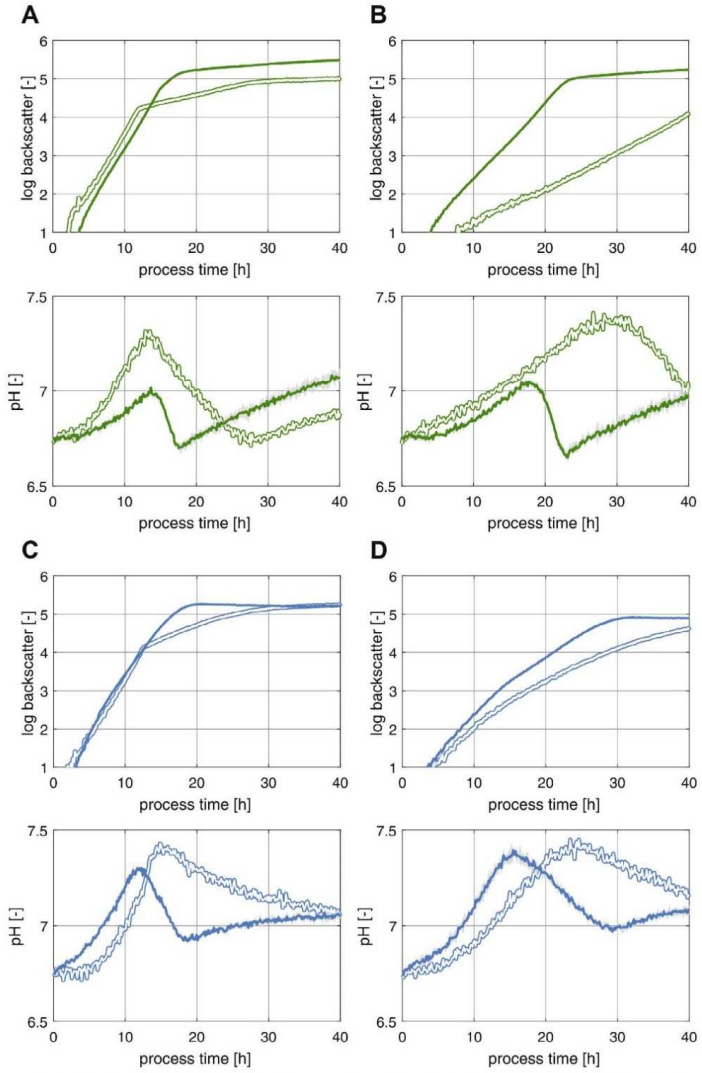

Fig. 2. Microbioreactor cultivations of *C. glutamicum* WMB2 (solid green), *C. glutamicum* WMB2 Δ*iolR* (green bordered), *C. glutamicum* ISO (solid blue), and *C. glutamicum* ISO Δ*iolR* (blue bordered). Biomass formation (as log backscatter, upper graphs) and pH (lower graphs) was followed over process time, respectively. All strains were cultivated in defined CGXII medium either containing a mixture of 10 g l^{-1} D-glucose and 30 g l^{-1} D-xylose (A, C) or solely 40 g l^{-1} D-xylose (B, D) as carbon and energy source. All data represent mean values from three biological replicates.(For interpretation of the references to colour in this figure legend, the reader is referred to the web version of this article.)

bearing mutations upstream of the *iolT1*-open reading frame (Radek et al., 2017). Furthermore, previous studies showed that IolT1 of *C. glutamicum* is capable of transporting the polyol *myo*-inositol and the hexoses D-glucose and D-fructose, rendering it also a potential permease for the pentose D-xylose (Bäumchen et al., 2009; Ikeda et al., 2011). All five genes were individually deleted in-frame in the genetic background of the *C. glutamicum* WMB2 Δ*iolR* variant to assess the contribution to the observed improved D-xylose utilization. This *C. glutamicum* strain was chosen, as the effect on growth of the *iolR*-deletion was most prominent in *C. glutamicum* strains utilizing D-xylose via the heterologous Weimberg pathway. All constructed strains were cultivated on defined CGXII medium containing 40 g L^{-1} D-xylose as sole carbon and energy source in comparison to the reference strain *C. glutamicum* WMB2 Δ*iolR* and growth of each strain was followed over time. Whereas *C. glutamicum* double-deletion mutants devoid of *iolA*, *iolE*, *iolP*, or *oxiA* exhibited the same growth behavior as the reference strain, was growth of *C. glutamicum* WMB2 Δ*iolR* Δ*iolT1* very similar to *C. glutamicum* WMB2 (Fig. 2B), indicating that the glucose permease IolT1 contributes to D-xylose transport in this bacterium.

Subsequently, *C. glutamicum* WMB2 Δ*iolR* Δ*iolT1* and *C. glutamicum* WMB2 Δ*iolR* were cultivated in parallel in the BioLector system in defined CGXII medium with 40 g L^{-1} D-xylose as sole carbon and energy source and the D-xylose concentration of both cultivations was monitored over time (Fig. 3). *C. glutamicum* WMB2 Δ*iolR* with deregulation of the *iolT1*-expression consumed D-xylose much more rapidly compared to *C. glutamicum* WMB2 Δ*iolR* Δ*iolT1* lacking the IolT1 permease. In addition, *C. glutamicum* WMB2 Δ*iolR* consumed virtually all of the available pentose in the culture medium within 30 h (0.70 ± 0.12 g L^{-1} D-xylose, residual concentration). In contrast, more than 75% of D-xylose was not consumed by *C. glutamicum* WMB2 Δ*iolR* Δ*iolT1* after the same time of cultivation (27.36 ± 0.24 g L^{-1} D-xylose, residual concentration). This showed that IolT1 indeed participates in the uptake of D-xylose in *C. glutamicum* and that the improved growth of the *C. glutamicum* WMB2 Δ*iolR* strain can be attributed to the deregulation of the *iolT1* gene. In principle, deregulation of other genes under IolR-control could also contribute to the observed increased D-xylose metabolization. However, this appears to be unlikely when considering that *C. glutamicum* WMB2 and *C. glutamicum* WMB2 Δ*iolR* Δ*iolT1* show the same growth rate under identical growth conditions. To date, the mode of D-xylose uptake in *C. glutamicum* is not fully understood. Only a recent study showed that a strain with an in-frame deletion of the *ptsG* gene encoding the glucose-specific EII permease of the phosphotransferase system is markedly impaired in its ability to utilize D-xylose via the isomerase pathway (Wang et al., 2014). Participation of IolT1 in D-xylose transport in *C. glutamicum* was unknown and the xylose-proton symporter XylE of *E. coli*, sharing 31% identity to IolT1 of *C. glutamicum*, is the only related permease for which the capability for transporting D-xylose has been experimentally confirmed (Davis and Henderson, 1987). Interestingly, the *xylE* gene coding for this permease was successfully introduced to *C. glutamicum* for increasing D-xylose uptake in the context of xylonate microbial production (Yim et al., 2017). In case of *Saccharomyces cerevisiae*, naturally also not able to utilize D-xylose, it could be shown that the hexose transporters Hxt4, Hxt5, Hxt7 and Gal2 of the 18 know hexose transporters can also facilitate the transport of D-xylose (Hamacher et al., 2002). Very recently, the gene for the arabinose-proton symporter AraE from *Bacillus subtilis* could be functionally expressed in *S. cerevisiae* (Kim et al., 2017). This genetic modification significantly enhanced xylitol production from D-xylose using this microorganism. Similarly, the arabinose-proton symporter (also named) AraE from *C. glutamicum* ATCC 31831 improved D-xylose uptake at lower substrate concentrations in *C. glutamicum* ATCC 13032, but this permease shares no significant similarities to IolT1 (Gopinath et al., 2011; Sasaki et al., 2009). However, in addition to IolT1, *C. glutamicum* does also possess the very similar permease IolT2 (56% identity to IolT1), which is known to also facilitate the uptake of *myo*-inositol, D-glucose and D-fructose similar to IolT1 (Bäumchen et al., 2009; Krings et al., 2006, Lindner et al., 2011). Due to the close similarity and the overlapping specificities of both permeases, IolT2 could also be involved in D-xylose uptake in *C. glutamicum*. To answer this question, the corresponding gene *iolT2* (although *iolT2* expression is known to be not under control of IolR) was deleted in background of the *C. glutamicum* WMB2 Δ*iolR* strain and the resulting strain *C. glutamicum* WMB2 Δ*iolR* Δ*iolT2* was compared to the reference strain *C. glutamicum* WMB2 Δ*iolR* regarding growth in defined CGXII medium containing 40 g L^{-1} D-xylose as sole carbon and energy source. *C. glutamicum* WMB2 Δ*iolR* Δ*iolT2* showed the same growth behavior as the control strain and all other double deletion mutants (except for *C. glutamicum* WMB2 Δ*iolR* Δ*iolT1*), indicating that the permease IolT2 does not contribute to D-xylose uptake under the experimental conditions tested.

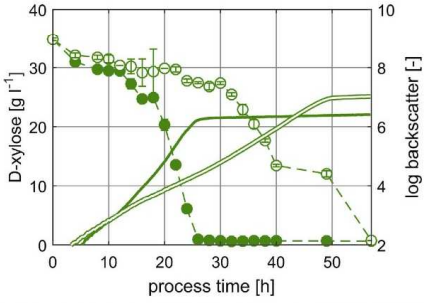

Fig. 3. Growth of *C. glutamicum* WMB2 Δ*iolR* and *C. glutamicum* WMB2 Δ*iolR* Δ*iolT1* in defined CGXII medium with 40 g L^{-1} D-xylose as sole carbon and energy source. Growth and D-xylose consumption of *C. glutamicum* WMB2 Δ*iolR* (solid green lines and filled circles, respectively) and *C. glutamicum* WMB2 Δ*iolR* Δ*iolT1* (green bordered line and empty circles, respectively) are shown. The data represent mean values from three biological replicates. (For interpretation of the references to colour in this figure legend, the reader is referred to the web version of this article.)

3.4. Rational engineering of the iolT1 promoter for repealing IolR-regulation mimics deletion of iolR

Based on these findings it can be concluded that expression of *iolT1* is highly desired in D-xylose utilizing *C. glutamicum* strains for improving growth in D-xylose-rich media. However, negative physiological effects as consequence of a deregulation of any of the other 21 IolR-controlled genes in a *C. glutamicum* WMB2 Δ*iolR* strain background can never be excluded. Thus, a *C. glutamicum* strain with a simple deletion of *iolR* does not represent a suitable platform strain for future strain constructions. For this reason, a precise engineering of the *iolT1*-promoter to repeal IolR-regulation while maintaining wild-type IolR-regulation of the other 21 IolR-controlled genes is preferred. A previous study identifying IolR as repressor of genes involved in *myo*-inositol catabolism of *C. glutamicum* also determined a consensus DNA binding motif of this regulator and identified two IolR-binding sites in the promoter of *iolT1* (Klaffl et al., 2013). In context of this present work, the IolR-binding site proximal to the transcriptional start site was disabled by substituting two successive and highly conserved nucleotides at position −29 and −28 (A → G and C → G, respectively) relative to the transcriptional start site of *iolT1* (Fig. 4A).

The resulting strain designated as *C. glutamicum* P_{O6} *iolT1* was subsequently transformed with the pEKEx3-*xylXABCD*$_{Cc}$-opt plasmid to confer D-xylose utilization capabilities via the Weimberg pathway (*C. glutamicum* WMB2 P_{O6} *iolT1*). This strain was cultivated in the BioLector microbioreactor system using defined CGXII medium containing either a D-glucose/D-xylose mixture (10 g L^{-1} D-glucose and 30 g L^{-1} D-xylose) or solely D-xylose (40 g L^{-1} D-xylose) as sole carbon and energy sources

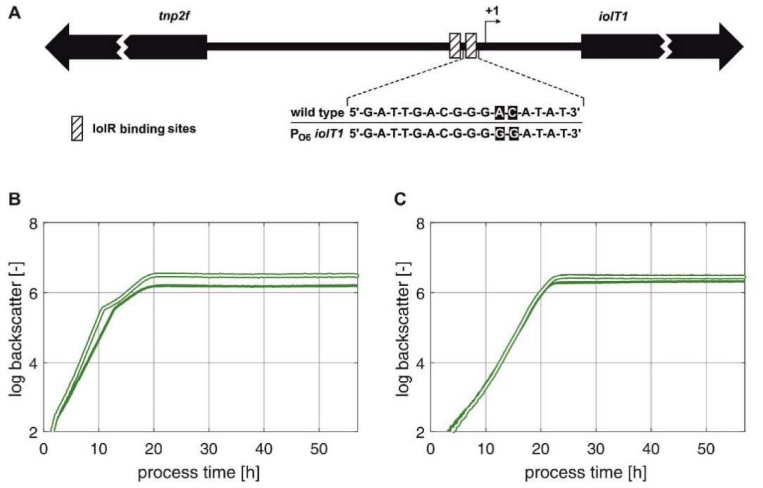

Fig. 4. Schematic representation of the intergenic region of *iolT1* and *tnp2f* on the chromosome of *C. glutamicum* (A). Both IolR-binding sites and the relevant transcriptional start site in the promoter of *iolT1* are indicated. The wild-type sequence of the proximal IolR-binding site and the same engineered sequence of the *C. glutamicum* WMB2 P_{O6}-*iolT1* strain are displayed. Growth of *C. glutamicum* WMB2 Δ*iolR* (solid green) and *C. glutamicum* WMB2 P_{O6} *iolT1* (green bordered) in defined CGXII medium containing either solely 40 g L^{-1} D-xylose (B) or a mixture of 10 g L^{-1} D-glucose and 30 g L^{-1} D-xylose (C) as carbon and energy source. The data represent mean values from three biological replicates. (For interpretation of the references to colour in this figure legend, the reader is referred to the web version of this article.)

(Fig. 4B and C). *C. glutamicum* WMB2 P_{O6} *iolT1* resembled the growth behavior of the direct control strain *C. glutamicum* WMB2 Δ*iolR* on D-xylose, indicating that mutation of only one of the IolR-binding site efficiently prohibits repression of *iolT1* expression by IolR in this strain (μ_{max} = 0.24 ± 0.01 h^{-1} for both strains) (Fig. 4B). On the D-glucose/D-xylose mixture, *C. glutamicum* WMB2 P_{O6} *iolT1* outperformed the control strain with deletion of the *iolR* gene regarding growth (Fig. 4C): In the first growth phase, in which both sugars are taken up simultaneously, *C. glutamicum* WMB2 P_{O6} *iolT1* exhibited an average growth rate of μ_{avg} = 0.21 ± 0.01 h^{-1} compared to μ_{avg} = 0.18 ± 0.01 h^{-1} as observed for *C. glutamicum* WMB2 Δ*iolR*. In the second growth phase, when D-glucose was depleted and only D-xylose was consumed, the growth rate of *C. glutamicum* WMB2 P_{O6} *iolT1* was still slightly higher compared to the control strain (μ_{avg} = 0.13 ± 0.01 h^{-1} and μ_{avg} = 0.12 ± 0.01 h^{-1}, respectively).

4. Conclusions

Loss of the transcriptional repressor IolR in *C. glutamicum* strains either employing the isomerase- or the Weimberg pathway improves growth on defined D-xylose containing media. Reason for this is an increased expression of *iolT1*, which encodes a permease contributing to D-xylose uptake in this bacterium. Introduction of two point mutations into the proximal IolR-binding site of the *iolT1*-promoter mimics the IolR loss-of function phenotype and allows for high growth rates on D-xylose containing media. This minimally engineered strain represents an excellent starting point for developing D-xylose metabolizing *C. glutamicum* strains for the production of valuable small compounds.

Acknowledgements

This work was funded by the German Federal Ministry of Education and Research (BMBF, Grant. No. 031L0015) as part of the project "XyloCut – Shortcut to the carbon efficient microbial production of chemical building blocks from lignocellulose-derived D-xylose", which is embedded in the ERASysAPP framework.

Appendix A. Supplementary data

Supplementary data associated with this article can be found, in the online version, at http://dx.doi.org/10.1016/j.biortech.2017.10.098.

References

Abe, S., Takayama, K.I., Kinoshita, S., 1967. Taxonomical studies on glutamic acid-producing bacteria. J. Gen. Appl. Microbiol. 13, 279–301.
Bäumchen, C., Krings, E., Bringer, S., Eggeling, L., Sahm, H., 2009. *Myo*-inositol facilitators IolT1 and IolT2 enhance D-mannitol formation from D-fructose in *Corynebacterium glutamicum*. FEMS Microbiol. Lett. 290, 227–235.
Bertani, G., 1951. Studies on Lysogenesis. I. The mode of phage liberation by lysogenic *Escherichia coli*. J. Bacteriol. 62, 293–300.
Blombach, B., Seibold, G.M., 2010. Carbohydrate metabolism in *Corynebacterium glutamicum* and applications for the metabolic engineering of L-lysine production strains. Appl. Microbiol. Biotechnol. 86, 1313–1322.
Davis, E.O., Henderson, P.J.F., 1987. The cloning and DNA sequence of the gene *xylE* for xylose-proton symport in *Escherichia coli* K12. J. Biol. Chem. 262, 13928–13932.
Eggeling, L., Bott, M., 2005. Handbook of Corynebacterium glutamicum. Taylor & Francis, Boca Raton.
Eggeling, L., Bott, M., 2015. A giant market and a powerful metabolism: L-lysin provided by *Corynebacterium glutamicum*. Appl. Microbiol. Biotechnol. 99, 3387–3394.
Gande, R., Dover, L.G., Krumbach, K., Besira, G.S., Sahm, H., Oikawa, T., Eggeling, L., 2007. The two carboxylases of *Corynebacterium glutamicum* essential for fatty acid and mycolic acid synthesis. J. Bacteriol. 189, 5257–5264.
Gibson, D.G., Young, L., Chuang, R.Y., Venter, J.C., Hutchison III, C.A., Smith, H.O., 2009. Enzymatic assembly of DNA molecules up to several hundred kilobases. Nat. Methods 6, 343–345.
Gopinath, V., Meiswinkel, T.M., Wendisch, V.F., Nampoothiri, M.K., 2011. Amino acid production from rice straw and wheat bran hydrolysates by recombinant pentose-utilizing *Corynebacterium glutamicum*. Appl. Microbiol. Biotechnol. 92, 985–996.
Hamacher, T., Becker, J., Gárdonyi, M., Hahn-Hägerdal, B., Boles, E., 2002. Characterization of the xylose-transporting properties of yeast hexose transporters and their influence on xylose utilization. Microbiology 148, 2783–2788.
Hanahan, D., 1983. Studies on transformation of *Escherichia coli* with plasmids. J. Mol.

Biol. 166, 557–580.
Heider, S.A.E., Peters-Wendisch, P., Wendisch, V.F., 2012. Carotenoid biosynthesis and overproduction in *Corynebacterium glutamicum*. BMC Microbiol. 12, 198.
Ikeda, M., Mizuno, Y., Awane, S.I., Hayashi, M., Mitsuhashi, S., Takeno, S., 2011. Identification and application of a different glucose uptake system that functions as an alternative to the phosphotransferase system in *Corynebacterium glutamicum*. Appl. Microbiol. Biotechnol. 90, 1443–1451.
Johnsen, U., Dambeck, M., Zaiss, H., Fuhrer, T., Soppa, J., Sauer, U., Schönheit, P., 2009. D-xylose degradation pathway in the halophilic archaeon *Haloferax volcanii*. J. Biol. Chem. 284, 27290–27303.
Kallscheuer, N., Vogt, M., Steanzel, A., Gätgens, J., Bott, M., Marienhagen, J., 2016. Construction of a *Corynebacterium glutamicum* platform strain for the production of stilbenes and (2S)-flavanones. Metab. Eng. 38, 47–55.
Kallscheuer, N., Vogt, M., Bott, M., Marienhagen, J., 2017. Functional expression of plant-derived O-methyltransferase, flavanone 3-hydroxylase, and flavonol synthase in *Corynebacterium glutamicum* for production of pterostilbene, kaempferol, and quercetin. J. Biotechnol. 258, 190–196.
Kawaguchi, H., Vertès, A.A., Okino, S., Inui, M., Yukawa, H., 2006. Engineering of a xylose metabolic pathway in *Corynebacterium glutamicum*. Appl. Environ. Microbiol. 72, 3418–3428.
Keilhauer, C., Eggeling, L., Sahm, H., 1993. Isoleucine synthesis in *Corynebacterium glutamicum*: molecular analysis of the *ilvB-ilvN-ilvC* operon. J. Bacteriol. 175, 5595–5603.
Kim, H., Lee, H.S., Park, H., Lee, D.H., Boles, E., Chung, D., Park, Y.C., 2017. Enhanced production of xylitol from xylose by expression of *Bacillus subtillis* arabinose: H^+ symporter and *Scheffersomyces stipites* xylose reductase in recombinant *Saccharomyces cerevisiae*. Enzyme Microb. Technol. 107, 7–14.
Klaffl, S., Brocker, M., Kalinowski, J., Eikmanns, B.J., Bott, M., 2013. Complex regulation of the phosphoenolpyruvate carboxykinase gene *pck* and characterization of its GntR-type regulator lolR as a repressor of *myo*-inositol utilization genes in *Corynebacterium glutamicum*. J. Bacteriol. 195, 4283–4296.
Kotrba, P., Inui, M., Yukawa, H., 2003. A single V317A or V317M substitution in enzyme II of a newly identified β-glucoside phosphotransferase and utilization system of *Corynebacterium glutamicum* R extends its specificity towards cellobiose. Microbiology 149, 1569–1580.
Krings, E., Krumbach, K., Bathe, B., Kelle, R., Wendisch, V.F., Sahm, H., Eggeling, L., 2006. Characterization of *myo*-inositol utilization by *Corynebacterium glutamicum*: the stimulon, identification of transporters, and influence on L-lysine formation. J. Bacteriol. 188, 8054–8061.
Lindner, S.N., Seibold, G.M., Henrich, A., Krämer, R., Wendisch, V.F., 2011. Phosphotransferase system-independent glucose utilization in *Corynebacterium glutamicum* by inositol permeases and glucokinases. Appl. Environ. Microbiol. 77, 3571–3581.
Litsanov, B., Kabus, A., Brocker, M., Bott, M., 2012. Efficient aerobic succinate production from glucose in minimal medium with *Corynebacterium glutamicum*. Microbiol. Biotechnol. 5, 116–128.
Meiswinkel, T.M., Gopinath, V., Lindner, S.N., Nampoothiri, K.M., Wendisch, V.F., 2013. Accelerated pentose utilization by *Corynebacterium glutamicum* for accelerated production of lysine, glutamate, ornithine and putrescine. Microb. Biotechnol. 6, 131–140.
Peterson, J.I., Young, D.S., 1968. Evaluation of the Hexokinase/Glucose-6-phosphate dehydrogenase method of determination of glucose in urine. Anal. Biochem. 23, 301–316.
Radek, A., Krumbach, K., Gätgens, J., Wendisch, V.F., Wiechert, W., Bott, M., Noack, S., Marienhagen, J., 2014. Engineering of *Corynebacterium glutamicum* for minimized carbon loss during utilization of D-xylose containing substrates. J. Biotechnol. 192, 156–160.
Radek, A., Tenhaef, N., Müller, M.F., Brüsseler, C., Wiechert, W., Marienhagen, J., Polen, Tino, Noack, S., 2017. Miniaturized and automated adaptive laboratory evolution: Evolving *Corynebacterium glutamicum* towards an improved D-xylose utilization. Bioresour. Technol. http://dx.doi.org/10.1016/j.biortech.2017.05.055. **Ahead of print.**
Sambrook, J., Russel, D., 2001. Molecular Cloning: A Laboratory Manual, 3rd ed. Cold Spring Harbor Laboratory Press, Cold Spring Harbor N.Y.
Sasaki, M., Jojima, T., Kawaguchi, H., Inui, M., Yukawa, H., 2009. Engineering of pentose transport in *Corynebacterium glutamicum* to improve simultaneous utilization of mixed sugars. Appl. Microbiol. Biotechnol. 85, 105–115.
Schäfer, A., Tauch, A., Jäger, W., Kalinowski, J., Thierbach, G., Pühler, A., 1994. Small mobilizable multi-purpose cloning vectors derived from the *Escherichia coli* plasmids pK18 and pK19: selection of defined deletions in the chromosome of *Corynebacterium glutamicum*. Gene 145, 69–73.
Schneider, J., Niermann, K., Wendisch, V.F., 2011. Production of the amino acids L-glutamate, L-lysine, L-ornithine and L-arginine from arabinose by recombinant *Corynebacterium glutamicum*. J. Biotechnol. 154, 191–198.
Stephens, C., Christen, B., Fuchs, T., Sundaram, V., Watanabe, K., Jenal, U., 2007. Genetic analysis of a novel pathway for D-xylose metabolism in *Caulobacter crescentus*. J. Bacteriol. 189, 2181–2185.
Vogt, M., Brüsseler, C., Ooyen, J.V., Bott, Michael, Marienhagen, J., 2016. Production of 2-methyl-1-butanol and 3-methyl-1-butanol in engineered *Corynebacterium glutamicum*. Metab. Eng. 38, 436–445.
Wang, C., Cai, H., Zhou, Z., Zhang, K., Chen, Z., Chen, Y., Wan, H., Ouyang, P., 2014. Investigation of *ptsG* gene in response to xylose utilization in *Corynebacterium glutamicum*. J. Ind. Microbiol. Biotechnol. 41, 1249–1258.
Weimberg, R., 1961. Pentose oxidation by *Pseudomonas fragi*. J. Biol. Chem. 236, 629–635.
Yim, S.S., Choi, J.W., Lee, S.H., Jeon, E.J., Chung, W.J., Jeong, K.J., 2017. Engineering of *Corynebacterium glutamicum* for consolidated conversion of hemicellulosic biomass into xylonic acid. Biotechnol. J Ahead of print.

2.3 Growth-decoupled production of D-xylonate

Bioresource Technology 268 (2018) 332–339

Contents lists available at ScienceDirect

Bioresource Technology

journal homepage: www.elsevier.com/locate/biortech

Production of D-xylonic acid using a non-recombinant *Corynebacterium glutamicum* strain

Niklas Tenhaef[a,b,1], Christian Brüsseler[a,b,1], Andreas Radek[a,b], René Hilmes[a,b], Pornkamol Unrean[c], Jan Marienhagen[a,b], Stephan Noack[a,b,*]

[a] Institute of Bio- and Geosciences, IBG-1: Biotechnology, Forschungszentrum Jülich GmbH, Jülich D-52425, Germany
[b] Bioeconomy Science Center (BioSC), Forschungszentrum Jülich GmbH, Jülich D-52425, Germany
[c] National Center for Genetic Engineering and Biotechnology, Pathum Thani, Thailand

ARTICLE INFO

Keywords:
D-Xylonate
Corynebacterium glutamicum
D-Xylose
Lignocellulosic biomass
Sugarcane bagasse
Sequential hydrolysis and fermentation

ABSTRACT

It was found that *Corynebacterium glutamicum* Δ*iolR* devoid of the transcriptional regulator IolR accumulates high amounts of D-xylonate when cultivated in the presence of D-xylose. Detailed analyses of constructed deletion mutants revealed that the putative *myo*-inositol 2-dehydrogenase IolG also acts as D-xylose dehydrogenase and is mainly responsible for D-xylonate oxidation in this organism. Process development for D-xylonate production was initiated by cultivating *C. glutamicum* Δ*iolR* on defined D-xylose/D-glucose mixtures under batch and fed-batch conditions. The resulting yield matched the theoretical maximum of 1 mol mol^{-1} and high volumetric productivities of up to 4 g L^{-1} h^{-1} could be achieved. Subsequently, a novel one-pot sequential hydrolysis and fermentation process based on optimized medium containing hydrolyzed sugarcane bagasse was developed. Cost-efficiency and abundance of second-generation substrates, good performance indicators, and enhanced market access using a non-recombinant strain open the perspective for a commercially viable bioprocess for D-xylonate production in the near future.

1. Introduction

D-xylonate is a C5 sugar acid with the potential of being a relevant chemical building block in a future bio-based economy. The largest potential lies in its proposed capability to replace or complement D-gluconate, which is currently produced at a scale of 100,000 t per year and finds numerous applications in the production of pharmaceuticals, food, solvents, dyes, concrete and other products (Climent et al., 2011; Toivari et al., 2012).

Most commercial-scale bioprocesses for production of bulk chemicals rely on D-glucose as main carbon substrate, but its supply can lead to competition with food industries for arable land (Ekman et al., 2013; Viikari et al., 2012). In contrast, second generation feedstocks, which are available as lignocellulosic waste material from agriculture and forest industries are highly abundant. Lignocellulosic biomass is composed of up to 40% hemicellulose, whose key building block is D-xylose (Straathof, 2014). This pentose represents an alternative source of D-xylonate as this acid could be obtained from D-xylose by oxidation.

Microbial production of D-xylonate from purified D-xylose or lignocellulosic biomass has been achieved employing several non-recombinant and recombinant organisms. Prominent examples for the first group include *Gluconobacter oxydans* (Buchert et al., 1986) and *Pseudomonas putida* (Hardy et al., 1993), both of which have the natural capability to oxidize D-xylose to D-xylonate. Functional introduction of a heterologous xylose dehydrogenase from *Caulobacter crescentus* or *Trichoderma reesei* also enabled D-xylonate production employing other microorganisms such as *Escherichia coli* (Liu et al., 2012), *Saccharomyces cerevisiae* (Toivari et al., 2010) and *Corynebacterium glutamicum* (Yim et al., 2017). Notably, xylose dehydrogenase-mediated oxidation of D-xylose does not directly yield D-xylonate, but D-xylonolactone as precursor molecule. Subsequent conversion of D-xylonolactone to D-xylonate either occurs spontaneously through chemical hydration or by enzymatic catalysis using a lactonase (Buchert et al., 1986; Nygard et al., 2014). While achieving competitive productivities and titers, the use of recombinant organisms for large-scale production of D-xylonate (and other bulk chemicals) can significantly affect process economics due to potential plasmid losses during long-term production or additional cost when operating a facility under the regulatory framework for recombinant organisms. On the other hand, microorganisms having the natural capability of producing D-xylonate are often characterized

* Corresponding author at: Institute of Bio- and Geosciences, IBG-1: Biotechnology, Forschungszentrum Jülich GmbH, Jülich D-52425, Germany.
E-mail address: s.noack@fz-juelich.de (S. Noack).
[1] These authors contributed equally to this work.

https://doi.org/10.1016/j.biortech.2018.07.127
Received 2 July 2018; Received in revised form 24 July 2018; Accepted 25 July 2018
Available online 26 July 2018
0960-8524/ © 2018 Elsevier Ltd. All rights reserved.

by low resistance to growth inhibitors present in lignocellulosic substrates, allowing only for low product yields (Turkia et al., 2010). Alternatively, lignocellulosic substrates would have to be purified prior to cultivation, rendering many processes uneconomically (Toivari et al., 2010).

Naturally, *C. glutamicum* cannot utilize D-xylose as sole carbon and energy source, but in recent years the isomerase pathway and the Weimberg pathway (WMB) as oxidative strategies for D-xylose metabolization could be functionally implemented into this organism (Meiswinkel et al., 2013; Radek et al., 2014). In the course of the studies for establishing the Weimberg pathway it was found that loss of the transcriptional regulator IolR in an evolved strain variant, termed *C. glutamicum* WMB2$_{evo}$, drastically increased the growth rate in D-xylose containing media (Radek et al., 2017). Detailed analysis of a constructed Δ*iolR* strain revealed that the *myo*-inositol/proton symporter IolT1, whose gene is under control of IolR, contributes to D-xylose uptake, ultimately leading to the observed improved growth phenotype (Brüsseler et al., 2018). This "Δ*iolR*-effect" could be mimicked by re-engineering of the *iolT1*-promoter to abolish any IolR-regulation as the resulting strain *C. glutamicum* WMB2 P_{O6} *iolT1* exhibited the same growth rate as *C. glutamicum* WMB2 Δ*iolR*.

This study reports on the application of *C. glutamicum* Δ*iolR* for the production of D-xylonate. Detailed characterization of this strain revealed that *C. glutamicum* carries an endogenous xylose dehydrogenase activity mainly responsible for the observed high productivities of this strain. Key performance indicators of the novel, non-recombinant production strain were evaluated by performing lab-scale bioreactor experiments on defined D-xylose containing media. Furthermore, the high potential for an economic production process of D-xylonate by enzymatic hydrolyzation of pretreated sugarcane bagasse and subsequent conversion of the resulting D-xylose-rich substrate to D-xylonate by *C. glutamicum* Δ*iolR* is shown.

2. Material and methods

2.1. Bacterial strains, media and growth conditions

All bacterial strains used are listed in Table 1. *E. coli* DH5α was used for cloning purposes and was grown aerobically at 37 °C either on Lysogeny Broth (LB) (Bertani, 1951) agar plates (with 1.8% (w v^{-1}) agar) or in 5 mL LB medium on a rotary shaker at 170 rpm.

All *C. glutamicum* strains are derived from *C. glutamicum* ATCC 13032 (Abe et al., 1967) and were grown aerobically at 30 °C, either on Brain Heart infusion (BHI) (Difco Laboratories, Detroit, USA) agar plates (with 1.8% (w v^{-1}) agar) or in 5 mL BHI medium on a rotary shaker at 170 rpm. If supplementation of antibiotics for the cultivation of strains harboring the cloning and construction vector pK19*mobsacB* was required, kanamycin was added to a final concentration of 25 μg mL^{-1} (*C. glutamicum*) or 50 μg mL^{-1} (*E. coli*). For the cultivation of strains harboring the expression vector pEKEx3, spectinomycin was supplemented to a final concentration of 100 μg mL^{-1}. Regulated gene expression was induced by adding isopropyl β-D-thiogalactoside (IPTG) to a final concentration of 1 mmol L^{-1}.

2.2. Plasmid and strain construction

All constructed plasmids are listed in Table 1. Oligonucleotides were synthesized by Eurofins genomics (Ebersfeld, Germany). See Supplementary Information for more details. For molecular cloning, standard protocols for PCR, DNA restriction or Gibson cloning were used (Gibson et al., 2009; Sambrook and Russell, 2001). Verification of the constructed plasmids was performed by restriction analysis, colony PCR or via DNA sequencing at Eurofins Genomics.

E. coli DH5α was transformed using the RbCl-method, whereas *C. glutamicum* was routinely transformed by electroporation with an additional heat shock for 6 min at 46 °C (Eggeling and Bott, 2005; Hanahan, 1983).

In-frame deletions of the open reading frames of *iolA*, *iolB*, *iolP*, *iolG*, *gntP*, *oxiA* or *iolH* in the genome of *C. glutamicum* were performed by two-step homologous recombination using the plasmids pk19*mobsacB* Δ*iolA*, pk19*mobsacB* Δ*iolB*, pk19*mobsacB* Δ*iolP*, pk19*mobsacB* Δ*iolG*, pk19*mobsacB* Δ*gntP*, pk19*mobsacB* Δ*oxiA* and pk19*mobsacB* Δ*iolH*, respectively, as previously described (Schäfer et al., 1994). Verification of the constructed strains was performed by colony PCR or DNA sequencing.

2.3. Shake flask cultivations

BHI-precultures in test tubes were inoculated with single colonies and incubated for 8 h at 30 °C on a rotary shaker at 170 rpm. This culture was then used to inoculate a second pre-culture in 500 mL baffled shake flasks with 50 mL of defined CGXII medium (Keilhauer et al., 1993) and a mixture of 10 g L^{-1} D-glucose and 30 g L^{-1} D-xylose as carbon and energy sources. The second pre-culture was incubated 15 h at 30 °C on a rotary shaker at 130 rpm. Finally, the main culture was inoculated to an OD_{600} of 1 in 50 mL defined CGXII medium and a mixture of 10 g L^{-1} D-glucose and 30 g L^{-1} D-xylose as carbon and energy sources. Incubation was done for 56 h at 30 °C on a rotary shaker at 130 rpm. During cultivations, samples were taken for measuring the cell densities and for preparing supernatant samples for quantification of D-xylose and D-xylonate. For complementation experiments, 1 mmol L^{-1} IPTG was added to induce plasmid-based gene expression.

2.4. Cultivation in defined CGXII media

Defined CGXII medium (Keilhauer et al., 1993) was used, containing per liter of deionized water 1 g K_2HPO_4, 1 g KH_2PO_4, 5 g urea, 13.25 mg $CaCl_2{\cdot}2\ H_2O$, 0.25 g $MgSO_4{\cdot}7\ H_2O$, 10 mg $FeSO_4{\cdot}7\ H_2O$, 10 mg $MnSO_4{\cdot}H_2O$, 0.02 mg $NiCl_2{\cdot}6\ H_2O$, 0.313 mg $CuSO_4{\cdot}5\ H_2O$, 1 mg $ZnSO_4{\cdot}7\ H_2O$, 0.2 mg biotin, 3,4-dihydroxybenzoate (PCA), 0.02% (v v^{-1}) antifoam AF204, 20 g D-glucose and 30 g D-xylose. Initial total medium volume of fed-batch cultivations was 0.9 L. Some media components were added sterile after autoclaving (D-xylose, D-glucose, PCA, trace elements, AF204). All chemicals were purchased from Sigma-Aldrich (Steinheim, Germany).

Batch and fed-batch cultivations were performed as biological duplicates using a parallel cultivation platform (Eppendorf/DASGIP, Jülich, Germany) with an initial working volume of 1.2 L. A pH of 7 was held constant during the cultivation by feeding 5 M H_3PO_4 and 5 M NH_4OH on demand. Temperature and air flow were set to 30 °C and 0.5 vvm, respectively. Aerobic process conditions were maintained by controlling the stirrer speed (400–1200 rpm) to achieve a dissolved oxygen concentration (DO) of at least 30%. Online measurements were taken for pH (405-DPAS-SC-K80/225, Mettler Toledo), DO (Visiferm DO 225, Hamilton) and exhaust gas composition (GA4, DASGIP AG). Inoculation was done from an exponential growing preculture using CGXII defined medium (20 g L^{-1} D-glucose) to a final OD_{600} of 2. Precultures were inoculated from cryocultures. Cryocultures were prepared as described previously (Unthan et al., 2014). If a fed-batch process was done, feed was added using a peristaltic pump. Feed was started after D-glucose was consumed, indicated by a sudden raise of the dissolved oxygen concentration. As feed, a solution of 100 g L^{-1} D-glucose in deionized water was used and the feed rate was set to 7.5 mL h^{-1}. Feeding was performed for 17 h resulting in a final working volume of 1.33 L.

2.5. Media development for utilization of sugarcane bagasse

Media development for utilization of sugarcane bagasse was done by cultivation of *C. glutamicum* in a 96-well deep well plate with 2 mL square-shaped wells. Each well was filled with 1 mL of the respective media variant. Each media variant was tested in triplicates.

Table 1
Strains and plasmids used in this study.

Strain or plasmid	Relevant characteristics[a]	Source or reference
C. glutamicum strains		
ATCC 13032 (WT)	biotin auxotroph wild-type strain	Abe et al. (1967)
P_{O6} *iolT1*	*C. glutamicum* WT with two point mutations in the promotor of *iolT1*, relative to the start codon at position -113 (A → G) and -112 (C → G), respectively.	This study
Δ*iolR*	*C. glutamicum* WT with in-frame deletion of *iolR* (cg0196)	Klaffl et al. (2013)
Δ*iolR*Δ*iolA*	*C. glutamicum* WT Δ*iolR* with in-frame deletion of *iolA* (cg0199)	This study
Δ*iolR*Δ*iolB*	*C. glutamicum* WT Δ*iolR* with in-frame deletion of *iolB* (cg0201)	This study
Δ*iolR*Δ*iolG*	*C. glutamicum* WT Δ*iolR* with in-frame deletion of *iolG* (cg0204)	This study
Δ*iolR*Δ*iolH*	*C. glutamicum* WT Δ*iolR* with in-frame deletion of *iolH* (cg0205)	This study
Δ*iolR*Δ*iolP*	*C. glutamicum* WT Δ*iolR* with in-frame deletion of *iolP* (cg0206)	This study
Δ*iolR*Δ*oxiA*	*C. glutamicum* WT Δ*iolR* with in-frame deletion of *oxiA* (cg0207)	This study
Δ*iolR*Δ*gntP*	*C. glutamicum* WT Δ*iolR* with in-frame deletion of *gntP* (cg3216)	This study
Δ*iolR*Δ*iolG*Δ*oxiA*	*C. glutamicum* WT Δ*iolR*Δ*iolG* double mutant with additional in-frame deletion of *oxiA* (cg0207)	This study
Δ*iolR*Δ*gntP*Δ*iolP*	*C. glutamicum* WT Δ*iolR*Δ*gntP* double mutant with additional in-frame deletion of *iolP* (cg0206)	This study
$WMB2_{evo}$	*C. glutamicum* pEKEx3-*xylXABCD*$_{Cc}$-opt	Radek et al. (2017)
E. coli strains		
DH5α	F^- Φ80*lacZ*ΔM15 Δ (*lacZYA-argF*)U169 *rec*A1 *end*A1 *hsd*R17 (r_K^-, m_K^+) *pho*A *sup*E44 λ–*thi*-1 *gyr*A96 *rel*A1	Invitrogen (Karlsruhe, Germany)
Plasmids		
pEKEx3	Spec^r; *C. glutamicum/E. coli* shuttle vector for regulated gene expression; (P_{tac}, lacI^q, pBL1 *ori*VCg, pUC18 *ori*VEc)	Gande et al. (2007)
pEKEx3-*iolG*	Spec^r; pEKEx3 derivative for the plasmid-based expression of *iolG* (cg0204) of *C. glutamicum*	This study
pk19*mobsacB* Δ*iolA*	Kan^r; plasmid for in-frame deletion of *iolA* (cg0199)	Brüsseler et al. (2018)
pk19*mobsacB* Δ*iolB*	Kan^r; plasmid for in-frame deletion of *iolB* (cg0201)	This study
pk19*mobsacB* Δ*iolG*	Kan^r; plasmid for in-frame deletion of *iolG* (cg0204)	This study
pk19*mobsacB* Δ*iolH*	Kan^r; plasmid for in-frame deletion of *iolH* (cg0205)	This study
pk19*mobsacB* Δ*iolP*	Kan^r; plasmid for in-frame deletion of *iolP* (cg0206)	Brüsseler et al. (2018)
pk19*mobsacB* Δ*oxiA*	Kan^r; plasmid for in-frame deletion of *oxiA* (cg0207)	Brüsseler et al. (2018)
pk19*mobsacB* Δ*gntP*	Kan^r; plasmid for in-frame deletion of *gntP* (cg3216)	This study
pk19*mobsacB* P_{O6} *iolT1*	Kan^r; plasmid for introducing two point mutations in the promotor region of *iolT1*, relative to the start codon at position -113 (A → G) and -112 (C → G) respectively	Brüsseler et al. (2018)

[a] Kan^r: kanamycin resistance, Spec^r: spectinomycin resistance.

Concentrations of the media components were derived from the defined CGXII medium as described above. Each media variant contained 20% (v v^{-1}) hydrolyzed bagasse. After pipetting, the plate was sealed with sterile gas-permeable sealing foil (m2p-labs, Baesweiler, Germany). The plate was incubated on a rotary shaker at 300 rpm at 30 °C. Samples were taken at 19 h and 4 days, and the optical density was determined at 600 nm using a spectrophotometer (Infinite M200, Tecan Group Ltd., Männedorf, Switzerland).

2.6. Sequential hydrolysis and fermentation process using sugarcane bagasse

The sequential hydrolysis and fermentation process was performed in duplicates. Pretreated sugarcane bagasse was provided by the Integrative Biorefinery Laboratory, National Center for Genetic Engineering and Biotechnology (BIOTEC), Pathum Thani, Thailand. Pretreatment was done by incubation of milled sugarcane bagasse (size of 0.25–1 cm) in 0.1 mol L^{-1} H_2SO_4 at 121 °C for 30 min. Steam pretreated sugarcane bagasse was stored at −20 °C. Hydrolysis was done in the STR of a parallel cultivation platform (Eppendorf/DASGIP, Jülich, Germany) using a total volume of 600 mL, containing 180 g pretreated sugarcane bagasse, 50 mM sodium acetate and 10.4 mL enzyme mix Cellic CTec2 (Novozymes, Bagsværd, Denmark). pH was adjusted to 5 using 4 M KOH. Hydrolysis was performed for 72 h at 50 °C with constant stirring (400 rpm). Supplements necessary for cultivation were then added without opening the STR by using a peristaltic pump. As supplements 8 g ammonium chloride, 2 g K_2HPO_4 and 0.2 mg biotin solved in 200 mL deionized water were added. pH was adjusted to 7 by adding 5 M NH_4OH using a syringe. Inoculation was done from an exponential growing preculture using CGXII defined medium (20 g L^{-1} D-glucose) to a final OD_{600} of 0.5. Precultures and cultivations were performed as described above.

2.7. Biomass, substrate, and product quantification

Cell dry weight (CDW) was determined gravimetrically as described previously (Limberg et al., 2017). 2 mL cultivation broth were collected in a weighted reaction tube, spun down in a tabletop centrifuge at 13,000 rpm for 10 min and resuspended in 0.9% (w v^{-1}) NaCl. After an additional centrifugation step the supernatant was removed by decantation. The cell pellet was dried at 80 °C for 24 h followed by gravimetric CDW determination.

For substrate and product quantification, the supernatants were filtered through a cellulose-acetate syringe filter (0.2 µm, DIA-Nielsen, Düren, Germany).

Separation of D glucose and D xylonate was realized via an isocratic exchange method on a HPLC system (Agilent 1100 Infinity, Agilent Technologies, Santa Clara, CA). The method used an Organic Acid Resin HPLC Column 300 × 8 mm (CS Chromatography, Düren, Germany) as stationary phase, 0.1 M H_2SO_4 with a flow rate of 0.6 mL min^{-1} as mobile phase, a column temperature of 80 °C and in injection volume of 10 µL. Detection of D-glucose was performed by using a Refractive Index Detector at 35 °C. D-xylonate was detected using UV light absorption at 215 nm with a Diode Array Detector. Concentrations were determined by applying an external standard in a weighted linear regression approach. Measurement errors were estimated by error propagation analysis.

For quantification of D-xylose an enzymatic assay (Xylose Assay Kit, Megazymes, Wickow, Ireland) was used. All pipetting steps were done by using a Freedom Evo 200 automated liquid handling system (Tecan Group Ltd., Männedorf, Switzerland). NADH increase was monitored at 340 nm by an integrated plate reader (Infinite M200, Tecan Group Ltd., Männedorf, Switzerland).

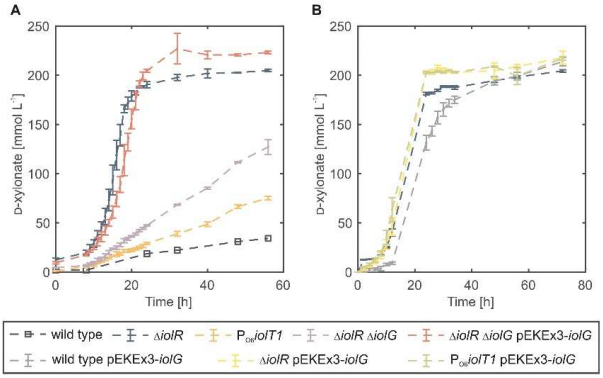

Fig. 1. Accumulation of D-xylonate during shake flask cultivations of different *C. glutamicum* strains in defined CGXII medium containing 10 g L^{-1} D-glucose and 30 g L^{-1} D-xylose. (A) Selected strains showing differential production phenotypes for D-xylonate. For all strains except wild type, the data represent mean values and standard deviations obtained from three independent cultures. (B) Strains with plasmid-based overexpression of *iolG* and strain Δ*iolR* as reference. The data represent mean values and standard deviations obtained from three independent cultures.

3. Results and discussion

3.1. An endogenous xylose dehydrogenase enables the oxidation of D-xylose in C. glutamicum

During growth studies of *C. glutamicum* Δ*iolR* on media containing D-glucose and D-xylose it could be observed that this strain accumulates high amounts of extracellular D-xylonate (205 mmol L^{-1} after 56 h, Fig. 1A). Further experiments showed that the *C. glutamicum* wild type, as well as the *C. glutamicum* P_{O6} *iolT1* variant, in which the IolR-mediated repression of *iolT1* expression is abolished, accumulates D-xylonate under the same cultivation conditions. However, in contrast to *C. glutamicum* Δ*iolR*, both strains accumulated D-xylonate to a much lower extend (34 mmol L^{-1} and 75 mmol L^{-1} after 56 h, Fig. 1A, respectively). This observation indicates that loss of IolR does not only have an impact on D-xylose import due to increased expression of the *iolT1* gene encoding the *myo*-inositol/proton symporter IolT1, but additionally appears to also affect either *i*) D-xylose oxidation; *ii*) D-xylonate export; or *iii*) both. Since IolR acts as repressor of at least 22 genes in *C. glutamicum*, which are for the most part associated with *myo*-inositol catabolism, several genes could be involved (Klaffl et al., 2013).

In case loss of IolR-mediated gene repression positively affects D-xylonate export, the gluconate permease GntP (encoded by *gntP*) represents a possible candidate as the similar gluconate permease of *Pseudomonas putida* is known to be involved in D-xylonate transport (Meijnen et al., 2009). Furthermore, the putative *myo*-inositol permease IolP (encoded by *iolP*) as second transporter protein whose expression is IolR-controlled, might contribute to D-xylonate export. With the aim to find out whether one or both of the permeases are capable of exporting D-xylonate in *C. glutamicum*, corresponding genes were individually deleted in *C. glutamicum* Δ*iolR*. In addition to *C. glutamicum* Δ*iolR*Δ*gntP* and *C. glutamicum* Δ*iolR*Δ*iolP*, also the triple mutant *C. glutamicum* Δ*iolR*Δ*iolP*Δ*gntP* was constructed as both permeases might complement each other. All strains were cultivated in defined CGXII medium with 10 g L^{-1} D-glucose and 30 g L^{-1} D-xylose as carbon and energy sources and compared to *C. glutamicum* Δ*iolR* and *C. glutamicum* P_{O6} *iolT1* with regard to growth and extracellular D-xylonate accumulation. However, as these experiments showed no difference between these strains and the control strains regarding D-xylonate formation, none of the permeases appears to be involved in D-xylonate transport in *C. glutamicum* (see Supplementary Information for more details).

D-xylose oxidation to D-xylonolactone is usually catalyzed by dehydrogenases (Stephens et al., 2007; Weimberg, 1961). In total five genes, either encoding known dehydrogenases or putative enzymes exhibiting a high sequence similarity to dehydrogenases, are under the transcriptional control of IolR. Namely, *iolA* (cg0199, aldehyde dehydrogenase), *iolB* (cg0201, 5-deoxy-glucuronate isomerase), *iolG* (cg0204, *myo*-inositol dehydrogenase), *oxiA* (cg0207, *myo*-inositol dehydrogenase) and *iolH* (cg0205, *myo*-inositol catabolism protein). Again, these genes were deleted in *C. glutamicum* Δ*iolR* and the resulting strain variants analyzed with respect to their ability to accumulate D-xylonate. All strains showed the same growth behavior as the control strains but whereas, deletion of *iolA*, *iolB*, *oxiA*, and *iolH* had no effect on D-xylonate formation (see Supplementary Information for more details), did loss of *iolG* result in a decreased overall D-xylonate concentration in the culture medium (Fig. 1A). After 24 h of cultivation, a concentration of 47 mmol L^{-1} D-xylonate was observed for *C. glutamicum* Δ*iolR*Δ*iolG*, compared to 190 mmol L^{-1} for strain *C. glutamicum* Δ*iolR*. The final titer was decreased by 38%.

In order to validate the contribution of *iolG* to D-xylonate formation in *C. glutamicum*, its deletion was complemented by plasmid-based expression of *iolG* in *C. glutamicum* Δ*iolR*Δ*iolG*. During growth and production experiments, the resulting strain *C. glutamicum* Δ*iolR*Δ*iolG* pEKEx3-*iolG* accumulated nearly the same amount of D-xylonate as *C. glutamicum* Δ*iolR* (223 mmol L^{-1} after 56 h, Fig. 1A). These experiments revealed that the *myo*-Inositol 2-dehydrogenase IolG is mainly responsible for the D-xylose oxidation observed in *C. glutamicum* Δ*iolR*. Interestingly, this dehydrogenase shows only 15% sequence identity when compared to the best-described xylose dehydrogenase XylB of *Caulobacter crescentus*. However, *C. glutamicum* Δ*iolR*Δ*iolG* was still capable of oxidizing D-xylonate, which indicates that at least one additional endogenous enzyme contributes to D-xylose oxidation in *C. glutamicum*. However, considering that *C. glutamicum* ATCC 13032 possesses more than 100 dehydrogenases of which one more might also accept D-xylose as substrate, detailed studies would have to be conducted for identifying such enzyme(s) with a D-xylose-oxidizing side-activity (Baumgart et al., 2018).

3.2. Derepression of iolG in C. glutamicum Δ*iolR* is sufficient for maximizing D-xylose oxidation

With the aim to find out if IolG-activity in *C. glutamicum* Δ*iolR* is rate-limiting for D-xylonate production, *iolG*-overexpression from the multi-copy vector pEKEx3 was implemented in the *C. glutamicum* wild type, *C. glutamicum* P_{O6} *iolT1* and *C. glutamicum* Δ*iolR*. All strains were cultivated in defined CGXII medium with 10 g L^{-1} D-glucose and

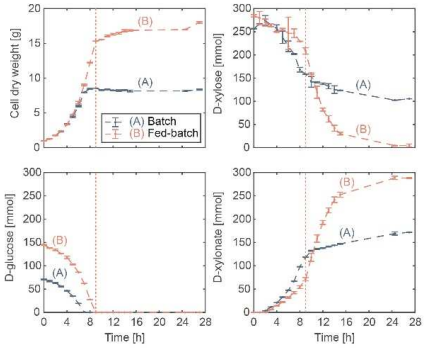

Fig. 2. Batch and fed-batch bioreactor cultivations of *C. glutamicum* Δ*iolR* for production of D-xylonate. (A) For batch cultivation, CGXII medium containing 10 g L^{-1} D-glucose and 40 g L^{-1} D-xylose was used. (B) For fed-batch cultivation, CGXII medium containing 20 g L^{-1} D-glucose and 40 g L^{-1} D-xylose was used for the initial batch phase. After consumption of D-glucose, a feed of 0.75 g h^{-1} D-glucose was introduced (as indicated by the vertical red line). Error bars show the standard deviation between two biological replicates. (For interpretation of the references to colour in this figure legend, the reader is referred to the web version of this article.)

30 g L^{-1} D-xylose as carbon and energy sources. As a result, strains with heterologous overexpression of *iolG* showed similar D-xylonate accumulation when compared to the non-recombinant strain *C. glutamicum* Δ*iolR* (Fig. 1B). Moreover, *C. glutamicum* pEKEx3-*iolG* showed a significantly lower D-xylonate formation rate in comparison to all other strains, again underlining the importance of IolT1 for the D-xylose transport in this bacterium (Brüsseler et al., 2018).

Conclusively, IolG-mediated oxidation of D-xylose to D-xylonate in *C. glutamicum* Δ*iolR* appears to be neither limited by the IolG-activity, nor by the intracellular availability of D-xylose.

3.3. Production of D-xylonate during batch and fed-batch cultivation

Process development for D-xylonate production with *C. glutamicum* Δ*iolR* was initiated by cultivating this strain on defined D-xylose/D-glucose mixtures in a parallel bioreactor system (1 L) under batch and fed-batch conditions. During batch cultivation on defined CGXII medium containing 10 g L^{-1} D-glucose as carbon and energy source and 40 g L^{-1} D-xylose for D-xylonate formation, two different phases could be distinguished (Fig. 2A and Table 2). Within the first 10 h, D-glucose was consumed completely and the cell dry weight rose to 6 g L^{-1}. In this phase, D-xylonate was produced to a titer of 9.8 ± 0.5 g L^{-1}. After consumption of D-glucose, no further increase in biomass was observed, but D-xylose was still converted into D-xylonate, notably at a much lower rate. The resulting final concentration of D-xylonate was 24.0 ± 0.01 g L^{-1} and the yield matched the theoretical maximum of 1 $mmol_{D\text{-}xylonate}$ $mmol_{D\text{-}xylose}^{-1}$. The observed higher conversion rate of D-xylose to D-xylonate when D-glucose was still available might be due to the fact that this oxidation requires NAD^+ as an electron acceptor. During assimilation of D-glucose the metabolic activities of the TCA-cycle and respiratory chain should permit an efficient recycling of this cofactor.

To achieve higher productivity of D-xylonate formation with *C. glutamicum* Δ*iolR*, a fed-batch process was employed (Fig. 2B and Table 2). This process was started with an initial batch cultivation using 20 g L^{-1} D-glucose and 40 g L^{-1} D-xylose. After depletion of the initial D-glucose, indicated by a sudden increase in the dissolved oxygen signal, a solution of 100 g L^{-1} D-glucose was fed with a rate of 7.5 mL h^{-1}. This feed resulted in a very slow biomass increase, indicating a strong carbon limitation. Most importantly, the remaining batch D-xylose was completely converted to D-xylonate. While the conversion yield remained at the theoretical maximum, the final titer was increased by nearly 50% to 35.7 ± 0.10 g L^{-1} (Fig. 2B). Especially in the D-glucose limited fed-batch phase, the volumetric productivity was greatly improved compared to the batch process (Table 2). A reason for this could be the competition of D-xylose and D-glucose for the available transporters. For example, the *myo*-inositol/protein symporter IolT1 contributes to the transport of both sugars and might block uptake of D-xylose under conditions of D-glucose excess (Brüsseler et al., 2018).

Table 2
Yield, titer and volumetric productivity of the investigated batch and fed-batch processes for production of D-xylonate with *C. glutamicum* Δ*iolR*. Standard deviations were calculated using biological duplicates.

	Batch on defined CGXII	Fed-batch on defined CGXII	Batch on hydrolyzed bagasse
Yield [$mmol_{D\text{-}xylonate}$ $mmol_{D\text{-}xylose}^{-1}$][a]	1.0 ± 0.02	1.0 ± 0.03	1.0 ± 0.03
Titer [g L^{-1}]	24.0 ± 0.01	35.7 ± 0.10	5.7 ± 0.03
Volumetric productivity [g L^{-1} h^{-1}]	0.89 ± 0.01	1.32 ± 0.01	0.24 ± 0.01
Volumetric productivity [g L^{-1} h^{-1}] (feed phase, $9 \le t \le 15$ h)	–	3.98 ± 0.03	–

[a] Molar masses of D-xylose and D-xylonate are 150.13 g mol^{-1} and 165.12 g mol^{-1}, respectively.

The fed-batch production process using *C. glutamicum* Δ*iolR* showed a higher titer and higher productivity when compared to the recently published recombinant strain *C. glutamicum* pUXE (Yim et al., 2017). In this work, the xylose dehydrogenase (encoded by *xylB*) and the xylose transporter (encoded by *xylE*) from *E. coli* were introduced to produce D-xylonate up to a titer of 20.71 g L^{-1} with a productivity of 1 g L^{-1} h^{-1} in a batch culture. Noteworthy, *C. glutamicum* pUXE bears the burden of plasmid-based gene expression.

A prominent, non-recombinant D-xylonate production organism is *Gluconobacter oxydans* (Toivari et al., 2012). Batch processes using *G. oxydans* reached D-xylonate titers up to 100 g L^{-1} and volumetric productivities of up to 2.5 g L^{-1} h^{-1}. Although product titers with *C. glutamicum* presented in this study are lower, the volumetric productivity in the feed phase outperforms all published processes employing *G. oxydans*. A possible extension of our process could be the addition of a D-xylose co-feed for an elongated production phase or the development of a continuous process using cell retention systems. Both strategies would increase the cost-efficiency of the process due to a better usage of the biocatalyst produced in the initial batch phase using D-glucose.

3.4. Utilization of hydrolyzed sugarcane bagasse in a one-pot sequential hydrolysis and fermentation process

Sugarcane bagasse is readily available as waste material from agriculture industry and contains a substantial amount of D-xylose as part of its hemicellulose fraction. D-xylose and other carbohydrates can be released by enzymatic hydrolysis and subsequently used for cultivation in a sequential hydrolysis and fermentation process.

Towards utilizing this hydrolysate in a cost-efficient manner, a novel cultivation medium was designed. To reach higher cell densities, these experiments were carried out using strain *C. glutamicum* $WMB2_{evo}$, which can utilize D-xylose as carbon and energy source (Radek et al., 2017). Other nutrient requirements are not altered in this strain and the results can be transferred directly to cultivations using *C. glutamicum* Δ*iolR*.

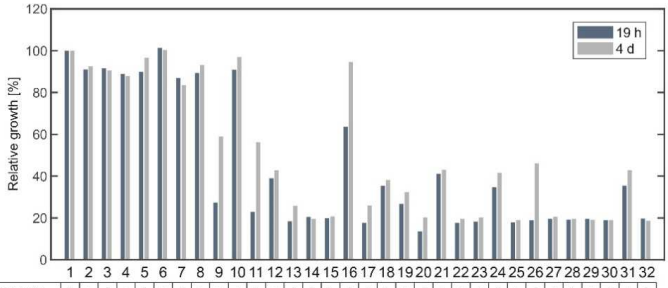

	1	2	3	4	5	6	7	8	9	10	11	12	13	14	15	16	17	18	19	20	21	22	23	24	25	26	27	28	29	30	31	32
Hydrolysate	+	+	+	+	+	+	+	+	+	+	+	+	+	+	+	+	+	+	+	+	+	+	+	+	+	+	+	+	+	+	+	+
$(NH_4)_2SO_4$	+	+	+	+	+	+	+	+	-	+	-	+	-	-	-	+	-	+	-	-	+	-	-	+	-	-	-	-	-	-	-	-
KH_2PO_4	+	+	+	+	+	+	+	+	+	+	+	-	+	-	-	+	+	-	-	+	-	+	+	-	+	-	-	-	-	-	-	-
Urea	+	+	-	+	+	+	+	+	-	-	+	-	-	+	-	-	+	-	+	-	-	-	-	-	-	+	-	-	-	-	-	-
MOPS	+	+	+	+	+	+	+	+	+	+	-	-	-	+	-	-	+	+	+	-	-	-	-	-	-	-	+	-	-	-	-	-
$MgSO_4$	+	+	+	-	+	-	-	-	+	-	-	+	+	+	+	-	-	-	-	-	-	-	-	-	-	-	-	-	+	-	-	-
$CaCl_2$	+	+	+	+	-	-	-	-	+	-	-	+	+	+	+	-	-	-	-	-	-	-	-	-	-	-	-	+	-	-	-	-
Biotin	+	-	-	-	-	+	-	-	-	-	-	-	-	-	-	-	-	-	-	-	+	+	-	-	-	-	-	-	-	+	-	-
Trace elements	+	-	-	-	-	-	+	-	-	-	-	-	-	-	-	-	-	-	-	-	-	-	+	-	-	-	-	-	-	-	+	-

Fig. 3. Media development for cultivation of *C. glutamicum* strains in hydrolyzed sugarcane bagasse. Components from the defined CGXII medium were tested in different combinations to identify their relevance for growth. For each medium variant the resulting cell density was measured photometrically (OD_{600}) after 19 h and 4 days of cultivation and related to the reference culture which included all components (No. 1). The basal medium contained 20% (v v^{-1}) hydrolyzed sugarcane bagasse (No. 32). For the concentrations of the added components the reader is referred to the Material and Methods section.

By taking the defined CGXII medium supplemented with 20% (v v^{-1}) hydrolyzed bagasse as reference (No. 1), all CGXII components were stepwise reduced and cultures were checked for remaining growth (Fig. 3). Clearly, the cheapest medium is only composed of hydrolyzed bagasse in deionized water (No. 32), but here the final cell density was decreased by 80%. The most interesting medium variants are No. 10 and No. 16, both only containing ammonium sulfate and dibasic potassium phosphate as additional growth supplements. No. 10 was also supplemented with MOPS buffer and revealed similar growth performance compared to the reference, reaching cell densities of 90% after 19 h and 97% after 4 days, respectively. No. 16 contained no MOPS buffer, which slowed down growth up to the first sampling point, probably due to pH shifts. After 4 days, the cell density in this medium reached 95% of the reference. Therefore, it can be concluded that nitrogen and phosphate are limiting components for growth of *C. glutamicum* in hydrolyzed bagasse and should be supplemented. Furthermore, for cultivations were the pH cannot be controlled by addition of acid and base, a buffer system should be used.

The resulting optimized media contained a nitrogen source (ammonium chloride), a phosphate source (dibasic potassium phosphate) and biotin. Ammonium chloride was chosen instead of ammonium sulfate for its lower market price. Moreover, additional supplementation of sulfate is not required, since pretreatment of sugarcane bagasse using sulfuric acid was performed. Further experiments also revealed that biotin, which is essential for growth of *C. glutamicum*, might not be sufficiently available in hydrolyzed bagasse and therefore was added (data not shown).

Based on these results, a one-pot process for the efficient hydrolysis and utilization of sugarcane bagasse to produce D-xylonate was developed (Fig. 4A). The sequential hydrolysis and fermentation process was initiated by setting up a stirred tank reactor with pretreated bagasse suspended in a buffer system. Here, 50 mmol L^{-1} acetate was used. Acetate is cost efficient, readily available from renewable resources, and can be consumed by *C. glutamicum* during cultivation (Gerstmeir et al., 2003). After enzymatic hydrolysis over the course of 72 h, the additional supplements as described above were added and the pH was adjusted to 7. Subsequently, cultivation of *C. glutamicum* Δ*iolR* was performed for 24 h (Fig. 4B and Table 2).

As a result, the strain completely utilized the fractions of D-glucose and acetate from the hydrolysis step for biomass formation. After depletion of these two carbon sources, oxidation of D-xylose to D-xylonate took place and a final titer of 5.7 ± 0.03 g L^{-1} was reached. Similar to the cultivations on defined CGXII-media, the product yield was at its theoretical maximum. The delayed production phase was, however, a notable difference to the cultivations using defined media. Conversion of D-xylose started after depletion of acetic acid. Presumably, the presence of this or other carbon sources impeded the uptake of D-xylose. The observation that D-xylonate was produced in this growth phase led to the assumption that other, unidentified carbon sources are present in the hydrolysate, which allow the organism to maintain redox balance after D-glucose- and acetate depletion.

In comparison to other processes using lignocellulosic hydrolysates, our cultivation process performed similar in terms of volumetric productivity (Toivari et al., 2012). The product titer was comparably low, but this can be explained by the low D-xylose-concentration in the hydrolyzed sugarcane bagasse (6 g L^{-1}), which is the decisive factor for final D-xylonate concentration. By optimizing the hydrolysis step, higher D-xylose concentrations and therefore higher product titers can be expected. A continuous culture with cell retention could also be an option for hydrolysates with low D-xylonate concentration. For other hydrolysates with higher D-xylose and lower D-glucose concentration (e.g. from an OrganoCat process (Grande et al., 2015)), a feed phase with D-glucose or another hydrolysate with high D-glucose concentration could be applied for rapid and complete conversion. This process would be similar to the fed-batch process described above.

The one-pot sequential hydrolysis and fermentation process presented here can utilize sugarcane bagasse, an abundant second-generation substrate, for the production of D-xylonate in a straightforward

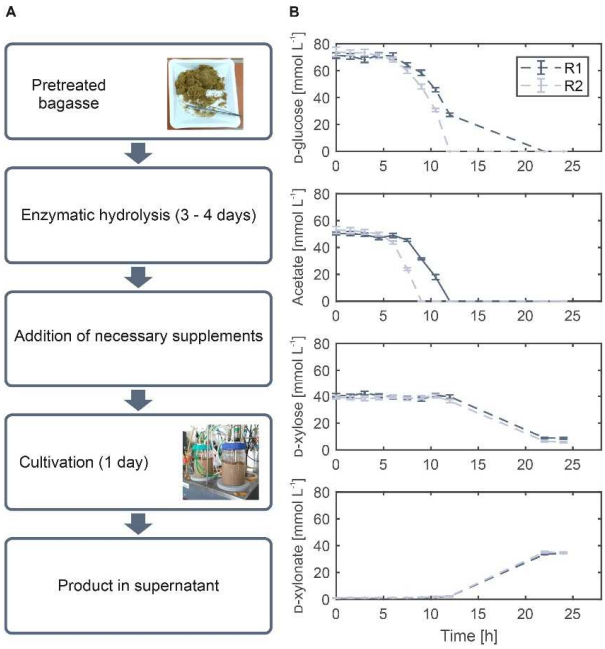

Fig. 4. Utilization of hydrolyzed bagasse for production of D-xylonate using *C. glutamicum ΔiolR*. (A) Flow chart of the experimental workflow. (B) Data from two bioreactor cultivations (biological replicates) using media containing hydrolyzed bagasse. Error bars show the propagated error from analytical replicates.

and cost-effective manner. In an industrial application, the downstream processing of D-xylonate must be considered. Ethanol precipitation has been described as a method of purifying D-xylonate from the cultivation medium (Buchert et al., 1986), but also *in situ* product removal by extraction represents an interesting option (Li et al., 2016).

4. Conclusions

In this study, it was discovered that *C. glutamicum ΔiolR* accumulates large amounts of D-xylonate when cultivated in D-xylose-containing media. A detailed analysis of this strain revealed that the endogenous *myo*-inositol dehydrogenase IolG is mainly responsible for the oxidation of D-xylose in *C. glutamicum*. D-xylonate production with *C. glutamicum ΔiolR* is characterized by a high volumetric productivity and maximum product yield under batch and fed-batch process conditions applying defined D-xylose/D-glucose mixtures and hydrolyzed bagasse, respectively. With this non-recombinant strain a highly profitable bioprocess to produce D-xylonate from lignocellulosic biomass as cost-efficient second-generation substrate is in reach.

Acknowledgements

This work was partly funded by the German Federal Ministry of Education and Research (BMBF, Grant. No. 031L0015) as part of the project "XyloCut – Shortcut to the carbon efficient microbial production of chemical building blocks from lignocellulose-derived D-xylose", which is embedded in the ERASysAPP framework. Further funding was obtained from the Bioeconomy Science Center (BioSC, Grant. No. 325-40000213) as part of the Focus FUND project "HyImPAct – Hybrid processes for important precursor and active pharmaceutical ingredients".

Appendix A. Supplementary data

Supplementary data associated with this article can be found, in the online version, at https://doi.org/10.1016/j.biortech.2018.07.127.

References

Abe, S., Takayama, K.I., Kinoshita, S., 1967. Taxonomical studies on glutamic acid-producing bacteria. J. Gen. Appl. Microbiol. 13 (3), 279–+.
Baumgart, M., Unthan, S., Kloss, R., Radek, A., Polen, T., Tenhaef, N., Muller, M.F., Kuberl, A., Siebert, D., Bruhl, N., Marin, K., Hans, S., Kramer, R., Bott, M., Kalinowski, J., Wiechert, W., Seibold, G., Frunzke, J., Ruckert, C., Wendisch, V.F., Noack, S., 2018. *Corynebacterium glutamicum* chassis C1*: building and testing a novel platform host for synthetic biology and industrial biotechnology. ACS Synth. Biol. 7 (1), 132–144.
Bertani, G., 1951. Studies on lysogenesis. I. The mode of phage liberation by lysogenic *Escherichia coli*. J. Bacteriol. 62 (3), 293–300.
Brüsseler, C., Radek, A., Tenhaef, N., Krumbach, K., Noack, S., Marienhagen, J., 2018. The *myo*-inositol/proton symporter IolT1 contributes to D-xylose uptake in *Corynebacterium glutamicum*. Bioresour. Technol. 249, 953–961.
Buchert, J., Viikari, L., Linko, M., Markkanen, P., 1986. Production of xylonic acid by *Pseudomonas fragi*. Biotechnol. Lett. 8 (8), 541–546.
Climent, M.J., Corma, A., Iborra, S., 2011. Converting carbohydrates to bulk chemicals and fine chemicals over heterogeneous catalysts. Green Chem. 13 (3), 520–540.

Eggeling, L., Bott, M. 2005. Handbook of *Corynebacterium glutamicum*.
Ekman, A., Wallberg, O., Joelsson, E., Börjesson, P., 2013. Possibilities for sustainable biorefineries based on agricultural residues – a case study of potential straw-based ethanol production in Sweden. Appl. Energy 102, 299–308.
Gande, R., Dover, L.G., Krumbach, K., Besra, G.S., Sahm, H., Oikawa, T., Eggeling, L., 2007. The two carboxylases of *Corynebacterium glutamicum* essential for fatty acid and mycolic acid synthesis. J. Bacteriol. 189, 5257–5264.
Gerstmeir, R., Wendisch, V.F., Schnicke, S., Ruan, H., Farwick, M., Reinscheid, D., Eikmanns, B.J., 2003. Acetate metabolism and its regulation in *Corynebacterium glutamicum*. J. Biotechnol. 104 (1–3), 99–122.
Gibson, D.G., Young, L., Chuang, R.-Y., Venter, J.C., Hutchison III, C.A., Smith, H.O., 2009. Enzymatic assembly of DNA molecules up to several hundred kilobases. Nat. Methods 6 (5), 343.
Grande, P.M., Viell, J., Theyssen, N., Marquardt, W., Domínguez de María, P., Leitner, W., 2015. Fractionation of lignocellulosic biomass using the OrganoCat process. Green Chem. 17 (6), 3533–3539.
Hanahan, D., 1983. Studies on transformation of *Escherichia coli* with plasmids. J. Mol. Biol. 166 (4), 557–580.
Hardy, G.P., de Mattos, M.J.T., Neijssel, O.M., 1993. Energy conservation by pyrroloquinoline quinol-linked xylose oxidation in *Pseudomonas putida* NCTC 10936 during carbon-limited growth in chemostat culture. FEMS Microbiol. Lett. 107 (1), 107–110.
Keilhauer, C., Eggeling, L., Sahm, H., 1993. Isoleucine synthesis in *Corynebacterium glutamicum*: molecular analysis of the *ilvB-ilvN-ilvC* operon. J. Bacteriol. 175 (17), 5595–5603.
Klafft, S., Brocker, M., Kalinowski, J., Eikmanns, B.J., Bott, M., 2013. Complex regulation of the phosphoenolpyruvate carboxykinase gene *pck* and characterization of its GntR-type regulator IolR as a repressor of *myo*-inositol utilization genes in *Corynebacterium glutamicum*. J. Bacteriol. 195 (18), 4283–4296.
Li, Q.-Z., Jiang, X.-L., Feng, X.-J., Wang, J.-M., Sun, C., Zhang, H.-B., Xian, M., Liu, H.-Z., 2016. Recovery processes of organic acids from fermentation broths in the biomass-based industry. J. Microbiol. Biotechnol 26 (1), 1–8.
Limberg, M.H., Schulte, J., Aryani, T., Mahr, R., Baumgart, M., Bott, M., Wiechert, W., Oldiges, M., 2017. Metabolic profile of 1,5-diaminopentane producing *Corynebacterium glutamicum* under scale-down conditions: Blueprint for robustness to bioreactor inhomogeneities. Biotechnol. Bioeng. 114 (3), 560–575.
Liu, H., Valdehuesa, K.N., Nisola, G.M., Ramos, K.R., Chung, W.J., 2012. High yield production of D-xylonic acid from D-xylose using engineered *Escherichia coli*. Bioresour. Technol. 115, 244–248.
Meijnen, J.P., de Winde, J.H., Ruijssenaars, H.J., 2009. Establishment of oxidative D-xylose metabolism in *Pseudomonas putida* S12. Appl. Environ. Microbiol. 75 (9), 2784–2791.
Meiswinkel, T.M., Gopinath, V., Lindner, S.N., Nampoothiri, K.M., Wendisch, V.F., 2013. Accelerated pentose utilization by *Corynebacterium glutamicum* for accelerated production of lysine, glutamate, ornithine and putrescine. Microb. Biotechnol. 6 (2), 131–140.
Nygard, Y., Maaheimo, H., Mojzita, D., Toivari, M., Wiebe, M., Resnekov, O., Gustavo Pesce, C., Ruohonen, L., Penttila, M., 2014. Single cell and in vivo analyses elucidate the effect of *xylC* lactonase during production of D-xylonate in *Saccharomyces cerevisiae*. Metab. Eng. 25, 238–247.
Radek, A., Krumbach, K., Gätgens, J., Wendisch, V.F., Wiechert, W., Bott, M., Noack, S., Marienhagen, J., 2014. Engineering of *Corynebacterium glutamicum* for minimized carbon loss during utilization of D-xylose containing substrates. J. Biotechnol. 192, 156–160.
Radek, A., Tenhaef, N., Müller, M.F., Brüsseler, C., Wiechert, W., Marienhagen, J., Polen, T., Noack, S., 2017. Miniaturized and automated adaptive laboratory evolution: Evolving *Corynebacterium glutamicum* towards an improved D-xylose utilization. Bioresour. Technol. 245, 1377–1385.
Sambrook, J., Russell, D.W., 2001. Molecular Ccloning: A Laboratory Manual, third ed. Coldspring-Harbour Laboratory Press, UK.
Schäfer, A., Tauch, A., Jäger, W., Kalinowski, J., Thierbach, G., Pühler, A., 1994. Small mobilizable multi-purpose cloning vectors derived from the *Escherichia coli* plasmids pK18 and pK19: selection of defined deletions in the chromosome of *Corynebacterium glutamicum*. Gene 145 (1), 69–73.
Stephens, C., Christen, B., Fuchs, T., Sundaram, V., Watanabe, K., Jenal, U., 2007. Genetic analysis of a novel pathway for D-xylose metabolism in *Caulobacter crescentus*. J. Bacteriol. 189 (5), 2181–2185.
Straathof, A.J.J., 2014. Transformation of biomass into commodity chemicals using enzymes or cells. Chem. Rev. 114 (3), 1871–1908.
Toivari, M.H., Nygard, Y., Penttila, M., Ruohonen, L., Wiebe, M.G., 2012. Microbial D-xylonate production. Appl. Microbiol. Biotechnol. 96 (1), 1–8.
Toivari, M.H., Ruohonen, L., Richard, P., Penttilä, M., Wiebe, M.G., 2010. *Saccharomyces cerevisiae* engineered to produce D-xylonate. Appl. Microbiol. Biotechnol. 88 (3), 751–760.
Turkia, H., Sirén, H., Pitkänen, J.-P., Wiebe, M., Penttilä, M., 2010. Capillary electrophoresis for the monitoring of carboxylic acid production by *Gluconobacter oxydans*. J. Chromatogr. A 1217 (9), 1537–1542.
Unthan, S., Grunberger, A., van Ooyen, J., Gatgens, J., Heinrich, J., Paczia, N., Wiechert, W., Kohlheyer, D., Noack, S., 2014. Beyond growth rate 0.6: What drives *Corynebacterium glutamicum* to higher growth rates in defined medium. Biotechnol. Bioeng. 111 (2), 359–371.
Viikari, L., Vehmaanperä, J., Koivula, A., 2012. Lignocellulosic ethanol: From science to industry. Biomass Bioenergy 46, 13–24.
Weimberg, R., 1961. Pentose oxidation by *Pseudomonas fragi*. J. Biol. Chem. 236, 629–635.
Yim, S.S., Choi, J.W., Lee, S.H., Jeon, E.J., Chung, W.J., Jeong, K.J., 2017. Engineering of *Corynebacterium glutamicum* for Consolidated Conversion of Hemicellulosic Biomass into Xylonic Acid. Biotechnol. J. 12 (11).

2.4 Discovery of an α-ketoglutarate semialdehyde dehydrogenase

Metabolic Engineering Communications 9 (2019) e00090

Contents lists available at ScienceDirect

Metabolic Engineering Communications

journal homepage: www.elsevier.com/locate/mec

Alone at last! – Heterologous expression of a single gene is sufficient for establishing the five-step Weimberg pathway in *Corynebacterium glutamicum*

Christian Brüsseler, Anja Späth, Sascha Sokolowsky, Jan Marienhagen *

Institute of Bio- and Geosciences, IBG-1: Biotechnology, Forschungszentrum Jülich GmbH, Jülich, D-52425, Germany

ARTICLE INFO

Keywords:
Corynebacterium glutamicum
D-xylose
Weimberg pathway
α-ketoglutarate

ABSTRACT

Corynebacterium glutamicum can grow on D-xylose as sole carbon and energy source via the five-step Weimberg pathway when the pentacistronic *xylXABCD* operon from *Caulobacter crescentus* is heterologously expressed. More recently, it could be demonstrated that the *C. glutamicum* wild type accumulates the Weimberg pathway intermediate D-xylonate when cultivated in the presence of D-xylose. Reason for this is the activity of the endogenous dehydrogenase IolG, which can also oxidize D-xylose. This raised the question whether additional endogenous enzymes in *C. glutamicum* contribute to the catabolization of D-xylose via the Weimberg pathway. In this study, analysis of the *C. glutamicum* genome in combination with systematic reduction of the heterologous *xylXABCD* operon revealed that the hitherto unknown and endogenous dehydrogenase KsaD (Cg0535) can also oxidize α-ketoglutarate semialdehyde to the tricarboxylic acid cycle intermediate α-ketoglutarate, the final enzymatic step of the Weimberg pathway. Furthermore, heterologous expression of either *xylX* or *xylD*, encoding for the two dehydratases of the Weimberg pathway in *C. crescentus*, is sufficient for enabling *C. glutamicum* to grow on D-xylose as sole carbon and energy source. Finally, several variants for the carbon-efficient microbial production of α-ketoglutarate from D-xylose were constructed. In comparison to cultivation solely on D-glucose, the best strain accumulated up to 1.5-fold more α-ketoglutarate in D-xylose/D-glucose mixtures.

1. Introduction

The Gram-positive bacterium *Corynebacterium glutamicum* has a long history in the industrial production of proteinogenic amino acids. In particular L-glutamate and L-lysine are produced at million ton-scale with this microorganism (Eggeling and Bott, 2015; Lee and Wendisch, 2017). Furthermore, *C. glutamicum* strains for more than 70 biotechnologically interesting compounds such as alcohols, organic acids or polyphenols have been engineered over the last years (Becker et al., 2018; Kallscheuer et al., 2016, 2017; Vogt et al., 2016; Wieschalka et al., 2013). However, all large-scale applications for amino acid production with *C. glutamicum* use D-glucose from starch hydrolysates or D-fructose (and sucrose) from molasses and the substrate spectrum of *C. glutamicum* variants engineered for other small molecules is also for the most part limited to these hexoses (Blombach and Seibold, 2010).

More recent studies focus on engineering *C. glutamicum* for the utilization of lignocellulose-derived pentoses D-xylose and L-arabinose as *C. glutamicum* cannot naturally catabolize these sugars (Kawaguchi et al., 2006, 2008). In case of D-xylose, two different metabolic routes have been individually added to the catabolic repertoire of *C. glutamicum*. In the Isomerase pathway, D-xylose is first converted to D-xylulose by a heterologous D-xylose isomerase (encoded by *xylA* from either *Escherichia coli* or *Xanthomonas campestris*) and subsequently phosphorylated by an endogenous D-xylulokinase (encoded by *xylB*) yielding D-xylulose-5-phosphate, which can be rapidly metabolized (Kawaguchi et al., 2006; Meiswinkel et al., 2013). Several *C. glutamicum* strains, capable of utilizing D-xylose via the Isomerase pathway have been engineered for the production of succinate, ethanol, lysine, glutamate, ornithine, putrescine and 1,5-diaminopentane (Buschke et al., 2011; Jo et al., 2017; Meiswinkel et al., 2013). In contrast, functional introduction of the *xylXABCD* operon from *Caulobacter crescentus* enabled *C. glutamicum* to grow on D-xylose as sole carbon and energy source via the five-step Weimberg pathway (Radek et al., 2014). In this pathway, D-xylose is initially oxidized to 1,4-D-xylonolactone via a xylose dehydrogenase (XylB) and subsequently hydrolyzed by a D-xylonolactonase (XylC) yielding D-xylonate (Fig. 1). Two subsequent dehydration reactions, catalyzed by a D-xylonate dehydratase (XylD) and a 2-keto-3-deoxyxylonate dehydratase (XylX), lead to

* Corresponding author.
E-mail address: j.marienhagen@fz-juelich.de (J. Marienhagen).

https://doi.org/10.1016/j.mec.2019.e00090
Received 27 January 2019; Received in revised form 29 March 2019; Accepted 29 March 2019
2214-0301/© 2019 The Authors. Published by Elsevier B.V. on behalf of International Metabolic Engineering Society. This is an open access article under the CC BY license (http://creativecommons.org/licenses/by/4.0/).

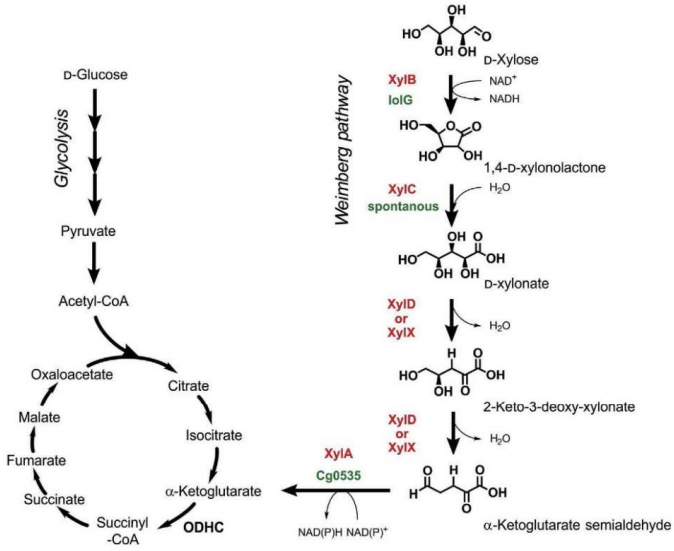

Fig. 1. Schematic overview of the metabolic connection of the Weimberg pathway to the central carbon metabolism of *C. glutamicum*. Endogenous enzymes of *C. glutamicum* catalyzing reactions of the Weimberg pathway or spontaneous chemical reactions are highlighted in green, whereas the respective heterologous enzymes originating from *C. crescentus* are highlighted in red. Abbreviations: XylB, xylose dehydrogenase; XylC, D-1,4-xylono lactonase; XylD, D-xylonate dehydratase; XylX, 2-keto-3-deoxy-D-xylonate dehydratase; XylA, α-ketoglutarate semi aldehyde dehydrogenase; IolG, *myo*-inositol-2-dehydrogenase; KsaD, α-ketoglutarate semialdehyde dehydrogenase; ODHC, α-ketoglutarate dehydrogenase complex. (For interpretation of the references to colour in this figure legend, the reader is referred to the Web version of this article.)

α-ketoglutarate semialdehyde, which is finally oxidized by an α-ketoglutarate semialdehyde dehydrogenase (XylA) to the tricarboxylic acid (TCA)-cycle intermediate α-ketoglutarate. However, *C. glutamicum* WMB1 as the first engineered strain having the Weimberg pathway allowed only for a growth rate of $\mu = 0.07\ h^{-1}$ on D-xylose containing defined medium. Adaptive laboratory evolution improved D-xylose utilization by 260 % yielding the strain *C. glutamicum* $WMB2_{evo}$ ($\mu_{max} = 0.26\ h^{-1}$) (Radek et al., 2017). Genome sequencing of this strain revealed a functional loss of the transcriptional regulator IolR, which controls the expression of 22 genes for the most part believed to be involved in *myo*-inositol metabolization (Klaffl et al., 2013). Among these genes is *iolT1* encoding for the *myo*-inositol/proton symporter IolT1, which turned out to also contribute to D-xylose uptake in *C. glutamicum* (Brüsseler et al., 2018). By rationally introducing two point mutations into the IolR-binding site of the *iolT1*-promoter yielding *C. glutamicum* P_{O6} *iolT1*, this effect could be successfully mimicked. Furthermore, an endogenously encoded D-xylose dehydrogenase (IolG) contributing to the oxidation of D-xylose in *C. glutamicum* could be identified, which was subsequently employed for the carbon efficient production of D-xylonate with *C. glutamicum* (Tenhaef et al., 2018).

These studies show that the *C. glutamicum* wild type, although not capable of D-xylose utilization via the Weimberg pathway or any other catabolic strategy by nature, does already possess individual Weimberg pathway components enabling D-xylose transport and initial D-xylose oxidation. This causes one to wonder whether there are additional endogenous enzymatic activities contributing to D-xylose utilization, which would help to reduce the number of heterologous genes required for establishing the Weimberg pathway in this bacterium.

In this study, we performed an analysis of the *C. glutamicum* genome in combination with systematic reduction of the *xylXABCD* operon to identify such enzymes. Furthermore, we exploited the Weimberg pathway for the direct conversion of D-xylose to α-ketoglutarate and could show that this represents a promising strategy for the microbial production of α-ketoglutarate with *C. glutamicum*.

2. Materials and methods

2.1. Bacterial strains, plasmids, media and growth conditions

All used bacterial strains and plasmids including their characteristics and sources are listed in Table 1. *Escherichia coli* DH5α, used for cloning purposes only, was routinely cultivated on a rotary shaker (170 rpm, 37 °C) in reaction tubes with 5 mL Lysogeny Broth (LB) medium (Bertani, 1951) or on LB agar plates (LB medium with 1.8 % [wt/vol] agar). All *C. glutamicum* strains are derived from *C. glutamicum* ATCC 13032 (Abe et al., 1967) and were aerobically cultivated on a rotary shaker either in reaction tubes (170 rpm, 30 °C) or in baffled shake flasks (130 rpm, 30 °C). As cultivation medium, brain heart infusion (BHI) medium (Difco Laboratories, Detroit, USA) or defined CGXII medium (Keilhauer et al., 1993) supplemented with different D-glucose/D-xylose mixtures were used. For plasmid propagation, kanamycin was added to final concentrations of 25 μg mL^{-1} (*C. glutamicum*) or 50 μg mL^{-1} (*E. coli*). Where appropriate, the antibiotic spectinomycin was added to a final concentration of 100 μg mL^{-1}. Induction of gene expression was achieved by isopropyl β-D-thiogalactoside (IPTG) supplementation to a final concentration of 1 mM. In general, growth of bacterial strains, cultivated in baffled shake flasks, was followed over time by measuring the optical density at 600 nm (OD_{600}). Cultivations in the microtiter plate format were performed in Flower Plates with optodes using the microbioreactor BioLector (m2plabs, Baesweiler, Germany), enabling online determination of backscatter, pH and dissolved oxygen. BioLector cultivations were routinely inoculated to an OD_{600} of 1 and incubated at 30 °C, 1300 rpm and 80 % humidity. The total culture volume was always 1 mL and the backscatter gain was set to 15.

2.2. Plasmid and strain construction

All enzymes were purchased from Thermo Scientific (Schwerte, Germany) whereas codon-optimized synthetic genes for expression in

Table 1
Strains and plasmids used in this study.

Strain or plasmid	Relevant characteristics[a]	Source or reference
***C. glutamicum* strains**		
ATCC 13032 (WT)	biotin auxotroph wild-type strain	Abe et al. (1967)
P_{O6} *iolT1*	Derivative of *C. glutamicum* ATCC 13032 with two point mutations in the promotor of *iolT1*, relative to the start codon at position −113 (A→G) and −112 (C→G) respectively	(Brüsseler et al., 2018)
P_{O6} *iolT1* Δcg0535	Derivative of *C. glutamicum* P_{O6} *iolT1* with in-frame deletion of cg0535 (*ksaD*)	This study
P_{O6} *iolT1 ΔodhA*	Derivative of *C. glutamicum* P_{O6} *iolT1* with in-frame deletion of *odhA* (cg1280)	This study
***E. coli* strains**		
DH5α	F^- Φ80*lacZ*ΔM15 Δ(*lacZYA-argF*)U169 *recA*1 *endA*1 *hsdR*17 (r_K^-, m_K^+) *pho*A *sup*E44 λ− *thi*-1 *gyr*A96 *rel*A1	Invitrogen (Karlsruhe, Germany)
BL21 (DE3)	F^- *ompT hsdSB*(r_B^- m_B^-) *gal dcm* (DE3)	Invitrogen (Karlsruhe, Germany)
***C. glutamicum* Plasmids**		
pEKEx3	Spec^r; *C. glutamicum/E. coli* shuttle vector for regulated gene expression; (P_{tac}, lacI^Q, pBL1 *oriVC*g, pUC18 *oriVEc*)	(Gande et al., 2007)
pEKEx3-*xylXABCD*$_{Cc}$-opt	Spec^r; pEKEx3 derivative for the regulated expression of *xylXABCD*$_{Cc}$ of *C. crescentus*	Radek et al. (2017)
pEKEx3-*xylXAD*$_{Cc}$-opt	Spec^r; pEKEx3 derivative for the regulated expression of *xylXAD*$_{Cc}$ of *C. crescentus*	This study
pEKEx3-*xylXD*$_{Cc}$-opt	Spec^r; pEKEx3 derivative for the regulated expression of *xylXD*$_{Cc}$ of *C. crescentus*	This study
pEKEx3-*xylX*$_{Cc}$-opt	Spec^r; pEKEx3 derivative for the regulated expression of *xylX*$_{Cc}$ of *C. crescentus*	This study
pEKEx3-*xylD*$_{Cc}$-opt	Spec^r; pEKEx3 derivative for the regulated expression of *xylD*$_{Cc}$ of *C. crescentus*	This study
pk19*mobsacB*-Δcg0535	Kan^r; plasmid for in-frame deletion of cg0535 (*ksaD*)	This study
pk19*mobsacB*-Δ*odhA*	Kan^r; plasmid for in-frame deletion of *odhA* (cg1280)	This study
***E. coli* Plasmids**		
pET-28b(+)	Kan^r; Vector for overexpression of genes in *E. coli*, adding an N-terminal hexahistidine affinity tag to the synthesized protein (pBR322 *ori*$V_{E.c.}$ P_{T7} *lacI*)	Novagen (Darmstadt, vector, Germany)
pET-28b(+)-cg0535	Kan^r; pET-28b(+) derivative for the regulated expression of cg0535 (*ksaD*) of *C. glutamicum*	This study

[a] Kan^r; Kanamycin resistance, Spec^r; Spectinomycin resistance.

C. glutamicum were obtained from Life Technologies (Darmstadt, Germany). Oligonucleotides were synthesized by Eurofins genomics (Ebersfeld, Germany) and are listed in Table 2. For molecular cloning work, standard protocols, e.g. PCR and Gibson were used (Gibson et al., 2009; Sambrook and Russel, 2001). Verification of the constructed plasmids was performed either by restriction analysis or colony PCR. DNA sequencing was conducted at Eurofins Genomics (Ebersberg, Germany). *E. coli* DH5α was routinely transformed using the RbCl-method, whereas *C. glutamicum* was always transformed by electroporation followed by an additional heat shock at 46 °C for 6 min (Eggeling and Bott, 2005; Hanahan, 1983). In-frame deletion of *odhA* and cg0535 (*kasD*) was performed by two-step homologues recombination using the plasmids pk19*mobsacB*-Δ*odhA* and pk19*mobsacB*-Δcg0535 as previously described (Schäfer et al., 1994).

2.3. Microbial production of α-ketoglutarate

For initial biomass formation, all constructed *C. glutamicum* strains were cultivated in 50 mL BHI medium with 10 g/l D-glucose in 500 mL baffled shake flasks at 130 rpm and 30 °C on a rotary shaker. Cells were harvested by centrifugation at 4000 rpm for 10 min, resuspended in defined CGXII medium with either 4 % D-glucose or a 1 % D-glucose/3 % D-xylose mixture and then further cultivated for 40 h at 130 rpm and 30 °C on a rotary shaker. For α-ketoglutarate production, defined CGXII medium with either 4 % D-glucose or a 1 % D-glucose/3 % D-xylose mixture was inoculated to an OD_{600} of 4. If appropriate, gene expression was induced by adding IPTG to a final concentration of 1 mM.

2.4. Heterologous expression of Cg0535 in E. coli and protein purification

The plasmid pET-28b(+)-cg0535 was transformed into *E. coli* BL21 for heterologous gene expression of cg0535. Cultivations for this purpose were performed in 10 mL 2xYT medium in baffled shake flasks for 15 h at 37 °C and 130 rpm on a rotary shaker. 1 mL of this culture was used to inoculate an expression culture in 100 mL 2xYT medium with 50 mg L^{-1} kanamycin and cultivated at 37 °C and 130 rpm. At an optical density of OD_{600} = 1.5, gene expression was induced by the addition of 0.5 mM IPTG and then further incubated at 18 °C and 130 rpm for 18 h. Cells were harvested by centrifugation for 30 min at 6000 rpm and the cell-free supernatant was discarded. Cell pellets were routinely stored at −80 °C if not further processed the same day. In order to avoid protein degradation, all subsequent steps for protein isolation were performed at 4 °C. Frozen cell pellets were first thawed on an ice-water mixture and resuspended in 15 mL lysis buffer (50 mM Tris-HCl pH 7.6, 100 mM NaCl, 10 mM Imidazole, 5 % Glycerin and 1 mM DTT). Crude cell extracts were obtained by using a Branson Sonifier 250 (intensity, 7; duty cycle, 40 %, 6 min; Branson Ultrasonics, Danbury, USA). After removal of the cellular debris by two centrifugation steps (30 min at 6000 rpm and 45 min at 50,000 rpm) Cg0535 was purified from the protein fraction by affinity chromatography using a GE Äkta pure chromatography system (GE Healthcare Life Sciences, Chicago, USA).

2.5. Kinetic characterization of KsaD (Cg0535)

In all dehydrogenase assays performed, the initial NAD(P)H generation due to KsaD-mediated α-ketoglutarate semialdehyde oxidation was monitored at 340 nm and 30 °C using an Shimadzu UV-1601 Spectrophotometer (Kyoto, Japan). The enzyme assays contained 0–5 mM α-ketoglutarate semialdehyde (FCH Group, Chernigiv, Ukraine, supplied by AKos Consulting & Solutions Deutschland GmbH, Steinen, Germany), 5 mM $NAD(P)^+$, 100 mM Potassium phosphate, pH 7.5. Assays were linear over time and proportional to the protein concentration used.

2.6. Quantification of D-xylose

For quantification of D-xylose, a commercial enzyme assay kit was used according to the manufacturer's instructions (Xylose Assay Kit, Megazymes, Wickow, Ireland). A set of different D-xylose concentrations served as external standards.

2.7. HPLC analysis

Identification and quantification of metabolites was performed using a High Performance Liquid Chromatography (HPLC) 1260 Infinity system (Agilent, Waldbronn, Germany). Separation was achieved by using an Organic acid H^+ column (8 %, 300 mm by 7.80 mm; Phenomenex, Torrance, CA, USA) at 80 °C with an isocratic elution program using 5 mM sulfuric acid. For detection of organic acids and D-glucose, a diode array detector (DAD) at 210 nm or a refraction index (RI) detector was used, respectively. Data acquisition and analysis was performed using the Agilent OpenLAB Data Analysis - Build 2.200.0.528 software (Agilent,

Table 2
Oligonucleotides used in this study.

Name	DNA Sequence (5′- 3′)
Construction of pEKEx3-*xylXAD*$_{Cc}$-opt	
pe3_check fw	CGGCGTTTCACTTCTGAGTTCGGC
pe3_check rev	GATATGACCATGATTACGCCAAGC
pe3_xylXAD_xylX_fw	GCCAAGCTTGCATGCCTGCATAACTAGTATAAGGAGATATAGATATGG
pe3_xylXAD_xylX_rev	TTATACTAGCTTATTACAGCAGGCCACG
pe3_xylXAD_xylA_fw	GCTGTAATAAGCTAGTATAAGGAGATATAGATATGAC
pe3_xylXAD_xylA_rev	TTATACTAGCTTATTAGGACCAGGAGTAGG
pe3_xylXAD_xylD_fw	GTCCTAATAAGCTAGTATAAGGAGATATAGATATGC
pe3_xylXAD_xylD_rev	CTGTAAAACGACGGCCAGTGTTATTAGTGGTTGTGGCG
Construction of pEKEx3-*xylXD*$_{Cc}$-opt	
pe3_check fw	CGGCGTTTCACTTCTGAGTTCGGC
pe3_check rev	GATATGACCATGATTACGCCAAGC
pe3_xylXD_xylX_fw	GCCAAGCTTGCATGCCTGCAGCTAGTATAAGGAGATATAGATATGGGCGTGTCCGAGTTC
pe3_xylXD_xylX_rev	CGGAGCGCATATCTATATCTCCTTATACTAGCTTATTACAGCAG
pe3_xylXD_xylD_fw	AGATATAGATATGCGCTCCGCACTGTCC
pe3_xylXD_xylD_rev	CTGTAAAACGACGGCCAGTGTTATTAGTGGTTGTGGCGTGGC
Construction of pk19*mobsacB*- Δcg0535 (*ksaD*)	
rsp	CACAGGAAACAGCTATGACCATG
univ	CGCCAGGGTTTTCCCAGTCACGAC
cg0535_seq_fw	AATCCACTTCTCTTGGTGTCATCGT
cg0535_seq_rev	CTTCGAGGACGCGAGTATTCATATT
cg0535_fw_fw	TGCATGCCTGCAGGTCGACTATCTACTCCCCAGAGGTTATCG
cg0535_fw_rev	CCCATTTATTTGCGGTTGCGGTGATCATG
cg0535_rev_fw	CGCAACCGCAAATAAATGGGCTGTACCTC
cg0535_rev_rev	TTGTAAAACGACGGCCAGTGCGCTAGATTTAGGCCTTG
Construction of pk19*mobsacB*-Δ*odhA* (cg1280)	
rsp	CACAGGAAACAGCTATGACCATG
univ	CGCCAGGGTTTTCCCAGTCACGAC
odhA check fw	GAAGCACACTTGTTTAGTGG
odhA check rev	CCCGTAGAGATCGGGCTGGGT
odhA fw_fw	TGCATGCCTGCAGGTCGACTCCATCGCCGCCATCCCTG
odhA fw_rev	TAAGCTGCTTCTCAGTACTAGCGCTGCTCACGG
odhA rev_fw	CGCTAGTACTGAGAAGCAGCTTATCGAC
odhA rev_rev	TTGTAAAACGACGGCCAGTGTCCATTATCGTAGGTGATG
Construction of pET-28b(+)-cg0535	
pET16b_fw	GATCCCGCGAAATTAATACG
pET16b_rv	CAAGACCCGTTTAGAGGCCCC
cg0535_fw	CTGGTGCCGCGCGGCAGCCACATGATCACCGCAACCGC
cg0535_rev	AAGCTTGTCGACGGAGCTCGTTAACGGTCTATTTCCCGAGG

Waldbronn, Germany).

3. Results

3.1. Identification of an endogenous α-ketoglutarate semialdehyde dehydrogenase activity

Presence of the endogenous dehydrogenase IolG oxidizing D-xylose to 1,4-D-xylonolactone and the observation that hydrolyzation of this lactone can occur spontaneously, indicates that heterologous expression of the xylose dehydrogenase (encoded by *xylB*) and the D-xylonolactonase (encoded by *xylC*) from *C. crescentus* might not be required for establishing the Weimberg pathway in *C. glutamicum*. Since reduction of the Weimberg pathway encoding operon has not been tried yet, a synthetic operon comprised of codon-optimized genes for 2-keto-3-desoxyxylonate dehydratase (*xylX*), xylonate dehydratase (*xylD*) and the α-ketoglutarate semialdehyde dehydrogenase (*xylA*), all originating from *C. crescentus*, was constructed. The resulting pEKEx3-*xylXAD*$_{Cc}$-opt plasmid was then transferred to *C. glutamicum* P$_{O6}$ *iolT1*, which is characterized by deregulation of the *myo*-inositol/proton symporter gene *iolT1*. Growth of the resulting strain *C. glutamicum* P$_{O6}$ *iolT1* pEKEx3-*xylXAD*$_{Cc}$-opt was compared to that of *C. glutamicum* P$_{O6}$ *iolT1* pEKEx3-*xylXABCD*$_{Cc}$-opt bearing the complete *xylXABCD* operon from *C. crescentus* (Fig. 2A). Surprisingly, growth of both strains was indistinguishable ($\mu_{max} = 0.26 \pm 0.006\ h^{-1}$, $\mu_{max} = 0.26 \pm 0.004\ h^{-1}$, respectively), indicating that heterologous expression of the xylose dehydrogenase (encoded by *xylB*) and the xylonolactonase (encoded by *xylC*) is neither necessary nor beneficial for growth of *C. glutamicum*.

Motivated by these results, we performed a genome-wide search based on sequence similarity to identify genes potentially encoding for enzymes with XylX-, XylD- or XylA-activity in *C. glutamicum* ATCC 13032. These analyses suggested that the gene cg0535 could encode for an enzyme having a α-ketoglutarate semialdehyde dehydrogenase activity. However, the predicted protein Cg0535 shares only 25 % sequence identity with XylA of *C. crescentus*. For a better assessment, secondary structures of Cg0535 and XylA were calculated and aligned using PROMALS3D (PROfile Multiple Alignment with predicted Local Structures and three-dimensional constraints) (Supplementary Fig. S1) (Pei et al., 2008). This *in silico* analysis revealed a striking resemblance between both proteins with regard to their secondary structure triggering further investigations. To the best of our knowledge, nothing about regulation and expression of cg0535 in *C. glutamicum* is known. Nonetheless, *C. glutamicum* P$_{O6}$ *iolT1* pEKEx3-*xylXD*$_{Cc}$-opt with a further reduced operon was constructed to find out whether heterologous expression of *xylA* from *C. crescentus* is required for establishing the Weimberg pathway in *C. glutamicum*. Comparative cultivation of *C. glutamicum* P$_{O6}$ *iolT1* pEKEx3-*xylXD*$_{Cc}$-opt and *C. glutamicum* P$_{O6}$ *iolT1* pEKEx3-*xylXAD*$_{Cc}$-opt revealed that *C. glutamicum* indeed does have an endogenous α-ketoglutarate semialdehyde dehydrogenase as both strains exhibited the same growth rate ($\mu_{max} = 0.26 \pm 0.008\ h^{-1}$, $\mu_{max} = 0.26 \pm 0.006\ h^{-1}$, respectively) (Fig. 2A). Subsequently, cg0535 was deleted in the genome of *C. glutamicum* P$_{O6}$ *iolT1*, yielding *C. glutamicum* P$_{O6}$ *iolT1* Δcg0535. After transformation of this strain with pEKEx3-*xylXD*$_{Cc}$-opt, the resulting strain *C. glutamicum* P$_{O6}$ *iolT1* Δcg0535 pEKEx3-*xylXD*$_{Cc}$-opt was compared to its parent strain *C. glutamicum* P$_{O6}$ *iolT1* pEKEx3-*xylXD*$_{Cc}$-opt. These experiments showed that deletion of cg0535 completely abolished growth of *C. glutamicum* P$_{O6}$ *iolT1* Δcg0535 pEKEx3*xylXD*$_{Cc}$-opt confirming that Cg0535 indeed has α-ketoglutarate semialdehyde dehydrogenase activity

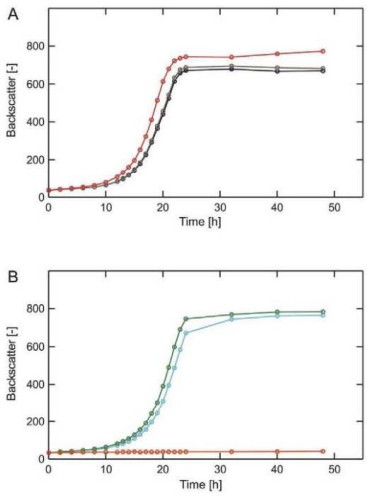

Fig. 2. Microbioreactor cultivations of *C. glutamicum* strains engineered for D-xylose utilization via the Weimberg pathway. **(A)** *C. glutamicum* P_{O6} *iolT1* pEKEx3-*xylXABCD*$_{Cc}$-*opt (black)*, *C. glutamicum* P_{O6} *iolT1* pEKEx3-*xylXAD*$_{Cc}$-*opt* (*brown*) and *C. glutamicum* P_{O6} *iolT1* pEKEx3-*xylXD*$_{Cc}$-*opt (red)*; **(B)** *C. glutamicum* P_{O6} *iolT1* pEKEx3-*xylX*$_{Cc}$-*opt (cyan)*, *C. glutamicum* P_{O6} *iolT1* pEKEx3-*xylD*$_{Cc}$-*opt* (*green*) and *C. glutamicum* P_{O6} *iolT1* pEKEX3 *(orange)*. All strains were cultivated in a BioLector microbioreactor system using defined CGXII medium with 40 g L^{-1} D-xylose as sole carbon and energy source. All data represent mean values from three biological replicates. (For interpretation of the references to colour in this figure legend, the reader is referred to the Web version of this article.)

(data not shown). The inability of the cg0535 deletion mutant to grow on D-xylose also indicates that Cg0535 appears to be the only endogenous enzyme of *C. glutamicum* significantly contributing to α-ketoglutarate semialdehyde oxidation, at last under the cultivation conditions tested.

With the aim to characterize Cg0535 in more detail, the cg0535 gene was isolated from the genome of *C. glutamicum* ATCC 13032 by PCR and cloned into the pET-28b(+)-vector for heterologous expression in *E. coli* BL21 (DE3). Gene expression in *E. coli* at 100 mL-scale and subsequent protein purification by affinity chromatography yielded 0.6 mg Cg0535 protein. Subsequently, we performed *in vitro* dehydrogenase assays using α-ketoglutarate semialdehyde as substrate and NAD or NADP as cofactors to determine selected kinetic parameters of Cg0535. These *in vitro* experiments confirmed the assumed α-ketoglutarate semialdehyde dehydrogenase activity of this enzyme and furthermore revealed a preference for the cofactor NAD as the calculated specific activity (U mg^{-1}) with NAD was three times higher compared to the activity with NADP (51.8 μmol min^{-1} mg^{-1} and 15.8 μmol min^{-1} mg^{-1}, respectively) (Supplementary Fig. S2). Therefore, depending on the cofactor used, different Michaelis constants (K_m) for α-ketoglutarate semialdehyde could be calculated (NAD, 0.87 mM; NADP, 0.21 mM). Considering these findings, we would like to introduce the designation *ksaD* (α-ketoglutarate semialdehyde dehydrogenase) for cg0535 of *C. glutamicum*.

3.2. Expression of xylD or xylX enables growth on D-xylose

Analysis of the *C. glutamicum* genome did not identify any hitherto unknown dehydratases potentially catalyzing the two subsequent dehydration reactions of the Weimberg pathway. Noteworthy, enzyme assays conducted with the dehydratases XylX and XylD of *C. cresentus* showed that both dehydratases accept D-xylonate as substrate (Dahms and Donald, 1982). Since both dehydratase substrates D-xylonate and 2-keto-3-deoxy-xylonate of the Weimberg pathway, are chemically quite similar, it makes one wonder why two separate enzymes appear to be necessary (Fig. 1). Unfortunately, no experimental data shedding more light on this interesting aspect are available for the enzymes of *C. crescentus*. However, a conducted comparison of both enzymes as part of this study revealed only a low sequence identity (18 %) and an analysis using PROMALS3D suggested two very different secondary structures (data not shown). Nevertheless, driven by curiosity, the plasmids pEKEx3-*xylX*$_{Cc}$-opt and pEKEx3-*xylD*$_{Cc}$-opt were constructed and individually introduced into *C. glutamicum* P_{O6} *iolT1*. The resulting strains *C. glutamicum* P_{O6} *iolT1* pEKEx3-*xylX*$_{Cc}$-opt and *C. glutamicum* P_{O6} *iolT1* pEKEx3-*xylD*$_{Cc}$-opt were compared with regard to growth to *C. glutamicum* P_{O6} *iolT1* pEKEx3 (Fig. 2B). As a result, both strains expressing either *xylX* or *xylD* could grow on this defined medium with D-xylose as sole carbon and energy source, whereas *C. glutamicum* P_{O6} *iolT1* could not. The growth rates of *C. glutamicum* P_{O6} *iolT1* pEKEx3-*xylX*$_{Cc}$-opt and *C. glutamicum* P_{O6} *iolT1* pEKEx3-*xylD*$_{Cc}$-opt were identical ($\mu_{max} = 0.25 \pm 0.006$ h^{-1}, $\mu_{max} = 0.25 \pm 0.004$ h^{-1}, respectively). Apparently, both dehydratases can complement for each other in *C. glutamicum* and heterologous expression of either *xylX* or *xylD* from *C. crescentus* is sufficient for enabling D-xylose utilization via the Weimberg pathway in *C. glutamicum* P_{O6} *iolT1*.

3.3. α-ketoglutarate synthesis via the Weimberg pathway

The Weimberg pathway represents a shortcut to the biotechnologically interesting TCA-cycle intermediate α-ketoglutarate without loss of carbon as compared to α-ketoglutarate synthesis starting from D-glucose (Fig. 1) (Jo et al., 2012). Nevertheless, microbial production of this dicarboxylic acid from D-xylose via the Weimberg pathway with *C. glutamicum* has not been investigated, yet. Within the TCA-cycle of *C. glutamicum*, the large multienzyme α-ketoglutarate dehydrogenase complex (ODHC) is responsible for the oxidative decarboxylation of α-ketoglutarate (Usuda et al., 1996; Bott, 2007). ODHC is comprised of three subunits: E1o (α-ketoglutarate decarboxylase, OdhA), E2 (dihydrolipoamide acetyl/succinyl-transferase, AceF) and E3 (dihydrolipoamide dehydrogenase, Lpd). It could be shown previously, that deletion of *odhA* results in the accumulation of α-ketoglutarate (Asakura et al., 2007). With the aim of establishing microbial α-ketoglutarate production from D-xylose via the Weimberg pathway in *C. glutamicum*, *odhA* was also deleted in *C. glutamicum* P_{O6} *iolT1*. Initially, the resulting strain *C. glutamicum* P_{O6} *iolT1 ΔodhA* was cultivated in defined CGXII medium supplemented with 40 g L^{-1} D-glucose as the sole carbon and energy source to find out if this is able to overproduce α-ketoglutarate from this hexose. Within 120 h, this strain accumulated 5.76 ± 0.06 g L^{-1} (39.43 ± 0.4 mM) α-ketoglutarate in the supernatant (Fig. 3). In contrast, the parent strain *C. glutamicum* P_{O6} *iolT1* without deletion of *odhA* accumulated only 0.05 ± 0.00 g L^{-1} (0.37 ± 0.03 mM) α-ketoglutarate. Subsequently, *C. glutamicum* P_{O6} *iolT1 ΔodhA* was transformed with pEKEx3-*xylXABCD*$_{Cc}$-opt to find out whether the resulting strain accumulates more α-ketoglutarate in D-glucose/D-xylose mixtures. Noteworthy, deletion of *odhA* interrupting the TCA-cycle renders cultivation on D-xylose as sole carbon and energy source impossible. Here, *C. glutamicum* P_{O6} *iolT1 ΔodhA* pEKEx3-*xylXABCD*$_{Cc}$-opt accumulated 7.92 ± 0.13 g L^{-1} (54.21 ± 0.86 mM) α-ketoglutarate in the supernatant when cultivated in defined CGXII medium with 10 g L^{-1} D-glucose and 30 g L^{-1} D-xylose (Fig. 3). In comparison to cultivation of *C. glutamicum* P_{O6} *iolT1 ΔodhA* in defined medium containing only D-glucose, the product titer could be increased 1.5-fold. Motivated by these findings, *C. glutamicum* P_{O6} *iolT1 ΔodhA* pEKEx3-*xylX*$_{Cc}$-opt and *C. glutamicum* P_{O6} *iolT1 ΔodhA* pEKEx3-*xylD*$_{Cc}$-opt were also constructed and characterized with regard to their α-ketoglutarate production capabilities on D-glucose/D-xylose mixtures. Interestingly, both strains accumulated

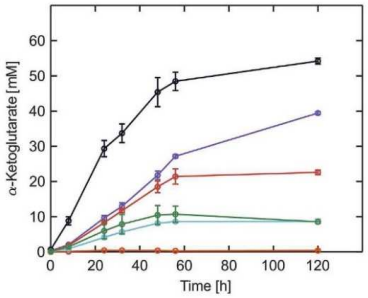

Fig. 3. Accumulation of α-ketoglutarate during shake flask cultivations of different *C. glutamicum* strains in defined CGXII medium supplemented with either 40 g L^{-1} D-glucose or a mixture of 10 g L^{-1} D-glucose and 30 g L^{-1} D-xylose. *C. glutamicum* P_{O6} *iolT1* (*orange*, 40 g L^{-1} D-glucose), *C. glutamicum* P_{O6} *iolT1 ΔodhA* (*purple*, 40 g L^{-1} D-glucose), *C. glutamicum* P_{O6} *iolT1 ΔodhA* pEKEx3-*xylXABCD*$_{Cc}$-*opt* (*black*, 10 g L^{-1} D-glucose and 30 g L^{-1} D-xylose), *C. glutamicum* P_{O6} *iolT1 ΔodhA* pEKEx3-*xylXD*$_{Cc}$-*opt* (*red*, 10 g L^{-1} D-glucose and 30 g L^{-1} D-xylose), *C. glutamicum* P_{O6} *iolT1 ΔodhA* pEKEx3-*xylX*$_{Cc}$-*opt* (*cyan*, 10 g L^{-1} D-glucose and 30 g L^{-1} D-xylose), *C. glutamicum* P_{O6} *iolT1 ΔodhA* pEKEx3-*xylD*$_{Cc}$-*opt* (*green*, 10 g L^{-1} D-glucose and 30 g L^{-1} D-xylose). The data represent mean values and standard deviations obtained from three independent cultures. (For interpretation of the references to colour in this figure legend, the reader is referred to the Web version of this article.)

much less α-ketoglutarate in the supernatant compared to the strain with the full *xylXABCD*-operon (1.27 ± 0.1 g L^{-1} (8.71 ± 0.7 mM) and 1.26 ± 0.0 g L^{-1} (8.62 ± 0.0 mM, respectively). This was somewhat surprising, as these results hint towards a limitation of the flux through the Weimberg pathway during product formation, which was not observable during growth experiments with *C. glutamicum* strains without *odhA*-deletion. Subsequent construction and characterization of *C. glutamicum* P_{O6} *iolT1 ΔodhA* pEKEx3-*xylXD*$_{Cc}$-opt, bearing the plasmid for expression of both dehydratase genes from *C. crescentus*, supports the hypothesis of a restricted flux through the Weimberg pathway in this strain background because an increased α-ketoglutarate concentration of 3.30 ± 0.09 g L^{-1} (22.61 ± 0.65 mM) could be determined in the supernatant.

4. Discussion

Functional introduction of a pathway from another organism or implementation of a novel synthetic pathway usually means addition of new enzymatic activities to the catalytic repertoire of the respective host organism. However, sometimes the "new" enzymes have overlapping substrate specificities with endogenous enzymes rendering their introduction unnecessary. This could be already shown for *C. glutamicum* R and *C. glutamicum* ATCC 13032 when establishing the two-step Isomerase pathway for D-xylose utilization as both strains already have a xylulokinase (XylB) and thus only require a heterologous gene encoding for a xylose isomerase (Kawaguchi et al., 2006). In case of *Pseudomonas* sp., it could be demonstrated that the periplasmic glucose dehydrogenase (Gcd) also contributes to D-xylose utilization via the Weimberg pathway (Köhler et al., 2015; Meijnen et al., 2009). Similarly, an enzymatic study not directly connected to growth on D-xylose revealed that the two endogenous *myo*-inositol dehydrogenases IolG1 and IolG2 of *Lactobacillus casei* BL23 can convert D-xylose to D-xylonate similar to IolG of *C. glutamicum* (Aamudalapalli et al., 2018).

The endogenous α-ketoglutarate semialdehyde dehydrogenase (KsaD) of *C. glutamicum* discovered in the context of this study is characterized by a high specific activity (51.8 μmol min^{-1} mg^{-1}), which is comparable to that of the enzyme with the same activity in *P. putida* (53 μmol min^{-1} mg^{-1}) (Adams and Rosso, 1967). In the genome of *C. glutamicum*, the open reading frame of *ksaD* overlaps with that of cg0536 encoding for a putative 5-dehydro-4-deoxyglucarate dehydratase. This finding hints towards a potential role of KsaD in a putative oxidative pathway for the utilization of sugar acids such as D-galacturonic acid or D-glucuronic acid as theses pathways require α-ketoglutarate semialdehyde dehydrogenase- and 5-dehydro-4-deoxyglucarate dehydratase activities (Richard and Hilditch, 2009; Pick et al., 2016). It sounds reasonable that *C. glutamicum* has such a catabolic pathway as these sugar derivatives typically to be found in pectin-rich fruits and vegetables such as grapes, apples, bean sprouts should be readily available in the natural habitat of this soil bacterium (Li et al., 2016).

Heterologous expression of either *xylX* or *xylD* in *C. glutamicum* P_{O6} *iolT1* enables growth in D-xylose containing media, indicating that both dehydratases from *C. crescentus* catalyze both dehydration reactions of the Weimberg pathway in *C. glutamicum*. In contrast, a *P. putida* S12 strain equipped with the Weimberg pathway from *C. crescentus* inevitably requires the expression of *xylD* whereas heterologous expression of *xylX* alone is not sufficient for enabling growth on D-xylose (Meijnen et al., 2009). In this case, it was assumed that the endogenous dehydratase PP2836 of *P. putida* S12 exhibiting 57 % sequence identity to XylX from *C. crescentus* renders heterologous *xylX* expression unnecessary. However, this is somewhat puzzling as it would mean that the two dehydratases from *C. crescentus* cannot complement for each other. Unfortunately, the importance of having both dehydratase has not been studied in *C. crescentus* as the natural source of both enzymes yet. A detailed kinetic characterization of both dehydratases could shed more light on this important aspect. Noteworthy in this context, the archaeon *Haloferax volcanii*, naturally having the Weimberg pathway, requires the activity of both dehydratases (HVO_B0038A and HVO_B0027) for growth on D-xylose containing media (Johnsen et al., 2009).

In our experiments, microbial synthesis of α-ketoglutarate from a D-glucose/D-xylose mixture with engineered *C. glutamicum* strains having the Weimberg pathway turned out to be more beneficial for product formation compared to cultivations using D-glucose as only substrate. This could be a direct consequence of the carbon efficiency of the Weimberg pathway offering a theoretical product yield of 100 %. In contrast, α-ketoglutarate synthesis from D-glucose is always accompanied by loss of carbon as CO_2 during isocitrate oxidation in the TCA-cycle, which eventually only allows for a maximum theoretical yield of 83 %. However, we could observe that reduction of the *xylXABCD*-operon also reduced final product concentrations in the constructed *odhA*-deletion strains. At this stage, we can only speculate that deletion of *odhA*, necessary for the accumulation of significant amounts of α-ketoglutarate, causes this effect as this is the only genetic difference to the other D-xylose consuming *C. glutamicum* strains evaluated in the context of *xylXABCD*-operon reduction. However, this indicates that heterologous expression of the whole pentacistronic *xylXABCD*-operon might not be necessary for growth of *C. glutamicum* in D-xylose containing defined medium, but is beneficial for product formation via the Weimberg pathway, especially in more engineered strains.

5. Conclusions

Reduction of the Weimberg pathway encoding operon from *C. crescentus* revealed that sole expression of *xylX* (2-keto-3-deoxy-xylonate-dehydratase) or *xylD* (xylonate dehydratase) is sufficient for establishing this five-step pathway in *C. glutamicum*. Reason for this is that *C. glutamicum* is already equipped with two dehydrogenases conferring the capacity to oxidize D-xylose and α-ketoglutarate semialdehyde. A lactonase converting 1,4-D-xylonolactone to D-xylonate is not required as hydrolyzation of this lactone can occur spontaneously. Conducted experiments employing the carbon efficient Weimberg pathway for the microbial synthesis of α-ketoglutarate indicate that D-xylose might represent a more suitable substrate for the production of this organic acid compared to D-glucose.

Acknowledgements

This work was funded by the German Federal Ministry of Education and Research (BMBF, Grant. No. 031L0015) as part of the project "XyloCut – Shortcut to the carbon efficient microbial production of chemical building blocks from lignocellulose-derived D-xylose", which is embedded in the ERASysAPP framework.

Appendix A. Supplementary data

Supplementary data to this article can be found online at https://doi.org/10.1016/j.mec.2019.e00090.

References

Aamudalapalli, H.B., Bertwistle, D., Palmer, D.R.J., Sanders, D.A.R., 2018. *Myo*-inositol dehydrogenase and *scyllo*-inositol dehydrogenase from *Lactobacillus casei* BL23 bind their substrates in very different orientations. BBA – Proteins and Proteomics 1866, 1115–1124.

Adams, E., Rosso, G., 1967. Alpha-ketoglutaric semialdehyde dehydrogenase of *Pseudomonas*. Properties of the purified enzyme induced by hydroxyproline and of the glucarate-induced and constitutive enzymes. J. Biol. Chem. 242, 1802–1814.

Asakura, Y., Kimura, E., Usuda, Y., Kawahara, Y., Matsui, K., Osumi, T., Nakamatsu, T., 2007. Altered metabolic flux due to deletion of *odhA* causes L-glutamate overproduction in *Corynebacterium glutamicum*. Appl. Environ. Microbiol. 73 (4), 1308–1319.

Abe, S., Takayama, K.I., Kinoshita, S., 1967. Taxonomical studies on glutamic acid-producing bacteria. J. Gen. Appl. Microbiol. 13, 279–301.

Becker, J., Rohles, C.M., Wittmann, C., 2018. Metabolically engineered *Corynebacterium glutamicum* for bio-based production of chemicals, fuels, materials, and healthcare products. Met. Eng. 50, 122–141.

Bertani, G., 1951. Studies on Lysogenesis I. The mode of phage liberation by lysogenic *Escherichia coli*. J. Bacteriol. 62, 293–300.

Blombach, B., Seibold, G.M., 2010. Carbohydrate metabolism in *Corynebacterium glutamicum* and applications for the metabolic engineering of L-lysine production strains. Appl. Microbiol. Biotechnol. 86, 1313–1322.

Bott, M., 2007. Offering surprises: TCA cycle regulation in *Corynebacterium glutamicum*. Trends Microbiol. 15 (9), 417–425.

Brüsseler, C., Radek, A., Tenhaef, N., Krumbach, K., Noack, S., Marienhagen, J., 2018. The *myo*-inositol/proton symporter IolT1 contributes to D-xylose uptake in *Corynebacterium glutamicum*. Bioresour. Technol. 249, 953–961.

Buschke, N., Schröder, H., Wittmann, C., 2011. Metabolic engineering of *Corynebacterium glutamicum* for production of 1,5-diaminopentane from hemicellulose. Biotechnol. J. 6, 306–317.

Dahms, A.S., Donald, A., 1982. D-xylo-aldonate dehydratase. Methods Enzymol. 90, 302–305.

Eggeling, L., Bott, M., 2005. Handbook of Corynebacterium glutamicum. Taylor & Francis, Boca Raton.

Eggeling, L., Bott, M., 2015. A giant market and a powerful metabolism: L-lysin provided by *Corynebacterium glutamicum*. Appl. Microbiol. Biotechnol. 99, 3387–3394.

Gande, R., Dover, L.G., Krumbach, K., Besira, G.S., Sahm, H., Oikawa, T., Eggeling, L., 2007. The two carboxylases of *Corynebacterium glutamicum* essential for fatty acid and mycolic acid synthesis. J. Bacteriol 189, 5257–5264.

Gibson, D.G., Young, L., Chuang, R.Y., Venter, J.C., Hutchison III, C.A., Smith, H.O., 2009. Enzymatic assembly of DNA molecules up to several hundred kilobases. Nat. Methods 6, 343–345.

Hanahan, D., 1983. Studies on transformation of *Escherichia coli* with plasmids. J. Mol. Biol. 166, 557–580.

Jo, J.-H., Seol, H.-Y., Lee, Y.-B., Kim, M.-H., Hyun, H.-H., Lee, H.-H., 2012. Disruption of genes for the enhanced biosynthesis of α-ketoglutarate in *Corynebacterium glutamicum*. Can. J. Microbiol. 58, 278–286.

Jo, S., Yoon, J., Lee, S.-M., Um, Y., Han, S.O., Woo, H.M., 2017. Modular pathway engineering of *Corynebacterium glutamicum* to improve xylose utilization and succinate production. J. Biotechnol. 258, 69–78.

Johnsen, U., Dambeck, M., Zaiss, H., Fuhrer, T., Soppa, J., Sauer, U., Schönheit, P., 2009. D-xylose degradation pathway in the halophilic archaeon *Haloferax volcanii*. J. Biol. Chem. 284 (40), 27290–27303.

Kallscheuer, N., Vogt, M., Stenzel, A., Gätgens, J., Bott, M., Marienhagen, J., 2016. Construction of a *Corynebacterium glutamicum* platform strain for the production of stilbenes and (2*S*)-flavanones. Metab. Eng. 38, 47–55.

Kallscheuer, N., Vogt, M., Bott, M., Marienhagen, J., 2017. Functional expression of plant-derived *O*-methyltransferase, flavone 3-hydroxylase, and flavonol synthase in *Corynebacterium glutamicum* for production of pterostilbene, kaempferol, and quercetin. J. Biotechnol. 258, 190–196.

Kawaguchi, H., Vertes, A.A., Okino, S., Inui, M., Yukawa, H., 2006. Engineering of a xylose metabolic pathway in *Corynebacterium glutamicum*. Appl. Environ. Microbiol. 72, 3418–3428.

Kawaguchi, H., Sasaki, M., Vertes, A.A., Inui, M., Yukawa, H., 2008. Engineering of an L-arabinose metabolic pathway in *Corynebacterium glutamicum*. Appl. Microbiol. Biotechnol. 77, 1053–1062.

Keilhauer, C., Eggeling, L., Sahm, H., 1993. Isoleucine synthesis in *Corynebacterium glutamicum*: molecular analysis of the *ilvB-ilvN-ilvC* operon. J. Bacteriol. 175, 5595–5603.

Klaffl, S., Brocker, M., Kalinowski, J., Eikmanns, B.J., Bott, M., 2013. Complex regulation of the phosphoenolpyruvate carboxykinase gene *pck* and characterization of its GntR-type regulator IolR as a repressor of *myo*-inositol utilization genes in *Corynebacterium glutamicum*. J. Bacteriol. 195, 4283–4296.

Köhler, K.A.K., Blank, L.M., Frick, O., Schmid, A., 2015. D-Xylose assimilation via the Weimberg pathway by solvent-tolerant *Pseudomonas taiwanensis* VLB120. Environ. Microbiol. 17 (1), 156–170.

Lee, J.-H., Wendisch, V.F., 2017. Production of amino acids – genetic and metabolic engineering approaches. Bioresour. Technol. 245, 1575–1587.

Li, Y., Sun, L., Feng, J., Wu, R., Xu, Q., Zhang, C., Chen, N., Xie, X., 2016. Efficient production of α-ketoglutarate in the *gdh* deleted *Corynebacterium glutamicum* by novel double-phase pH and biotin control strategy. Bioproc. Biosyst. Eng. 39, 967–976.

Meijnen, J.P., de Winde, J.H., Ruijssenaars, H.J., 2009. Establishment of oxidative D-xylose metabolism in *Pseudomonas putida* S12. Appl. Environ. Microbiol. 75 (9), 2784–2791.

Meiswinkel, T.M., Gopinath, V., Lindner, S.N., Madhavan Nampoothiri, K., Wendisch, V.F., 2013. Accelerated pentose utilization by *Corynebacterium glutamicum* for accelerated production of lysine, glutamate, ornithine and putrescine. Microb. Biotechnol. 6 (2), 131–140.

Pei, J., Kim, B.-H., Grishin, N.V., 2008. PROMALS3D: a tool for multiple protein sequence and structure alignments. Nucleic Acids Res. 36 (7), 2295–2300.

Pick, A., Beer, B., Hemmi, R., Momma, R., Schmid, J., Miyamoto, K., Sieber, V., 2016. Identification and characterization of two new 5-keto-4-deoxy-D-glucarate dehydratases/decarboxylases. BMC Biotechnol. 16, 80.

Radek, A., Krumbach, K., Gätgens, J., Wendisch, V.F., Wiechert, W., Bott, M., Noack, S., Marienhagen, J., 2014. Engineering of *Corynebacterium glutamicum* for minimized carbon loss during utilization of D-xylose containing substrates. J. Biotechnol. 192, 156–160.

Radek, A., Tenhaef, N., Müller, M.F., Brüsseler, C., Wiechert, W., Marienhagen, J., Polen, Tino, Noack, S., 2017. Miniaturized and automated adaptive laboratory evolution: evolving *Corynebacterium glutamicum* towards an improved D-xylose utilization. Bioresour. Technol. 245, 1377–1385.

Richard, P., Hilditch, S., 2009. D-galacturonic acid catabolism in microorganisms and its biotechnological relevance. Appl. Microbiol. Biotechnol. 82, 597–604.

Sambrook, J., Russel, D., 2001. Molecular Cloning: A Laboratory Manual, third ed. Cold Spring Harbor Laboratory Press. Cold Spring Harbor N.Y.

Schäfer, A., Tauch, A., Jäger, W., Kalinowski, J., Thierbach, G., Pühler, A., 1994. Small mobilizable multi-purpose cloning vectors derived from the *Escherichia coli* plasmids pK18 and pK19: selection of defined deletions in the chromosome of *Corynebacterium glutamicum*. Gene 145, 69–73.

Tenhaef, N., Brüsseler, C., Radek, A., Hilmes, R., Unrean, P., Marienhagen, J., Noack, S., 2018. Production of D-xylonic acid using a non-recombinant *Corynebacterium glutamicum* strain. Bioresour. Technol. 268, 332–339.

Usuda, Y., Tujimoto, N., Abe, C., Asakura, Y., Kimura, E., Kawahara, Y., Kurahashi, O., Matsui, H., 1996. Molecular cloning of the *Corynebacterium glutamicum* ('*Brevibacterium lactofermentum*' AJ12036) *odhA* gene encoding a novel type of 2-oxoglutarate dehydrogenase. Microbiology 142, 3347–3354.

Vogt, M., Brüsseler, C., Ooyen, J. v., Bott, M., Marienhagen, J., 2016. Production of 2-methyl-1-butanol and 3-methyl-1-butanol in engineered *Corynebacterium glutamicum*. Metab. Eng. 38, 436–445.

Wieschalka, S., Blombach, B., Bott, M., Eikmanns, B.J., 2013. Bio-based production of organic acids with *Corynebacterium glutamicum*. Microb. Biotechnol. 6 (2), 87–102.

3. References

Abe, S., Takayama, K. I., Kinoshita, S. 1967. Taxonomical studies on glutamic acid-producing bacteria. *J. Gen. Appl. Microbiol.* 13, 279 – 301

Acatech (German academy of engineering sciences). 2012. Biotechnologische Energieumwandlung in Deutschland. Stand, Kontext, Perspektiven [Internet]. 06/21/2012 [cited on 02/05/2019]. URL: https://www.acatech.de/Publikation/biotechnologische-energieumwandlung-in-deutschland-stand-kontext-perspektiven/

Anderson, R. L., Wood, W. A. 1962. Purification and properties of L-xylulokinase. *J. Biol. Chem.* 237, 1029

Asakura, Y., Kimura, E., Usuda, Y., Kawahara, Y., Matsui, K., Osumi, T., Nakamatsu, T. 2007. Altered metabolic flux due to deletion of *odhA* causes L-glutamate overproduction in *Corynebacterium glutamicum. Appl. Environ. Microbiol.* 73 (4), 1308 – 1319

Banerjee, S., Archana, A., Satyanarayana, T. 1994. Xylose metabolism in a thermophilic mould *Malbranchea pulchella* var. sulfurea TMD-8. *Curr. Microbiol.* 29, 349 – 352

Bar-On, Y. M., Phillips, R., Milo, R. 2018. The biomass distribution on earth. *PNAS.* 115 (25), 6506 – 6511

Becker, J., Zelder, O., Häfner, S., Schröder, H., Wittmann, C. (2011) From zero to hero — design-based systems metabolic engineering of *Corynebacterium glutamicum* for L-lysine production. *Met. Eng.* 13, 159 – 168.

Becker, J., Rohles, C. M., Wittmann, C. 2018. Metabolically engineered *Corynebacterium glutamicum* for bio-based production of chemicals, fuels, materials, and healthcare products. *Met. Eng.* 50, 122 – 141

BGR (Federal Institute for Geosciences and Raw Materials). 2017. BGR Energiestudie 2017 – Daten und Entwicklungen der deutschen und globalen Energieversorgung (21). [Internet]. December 2017 [cited on 02/05/2019]. URL: https://www.bgr.bund.de/DE/Themen/Energie/Downloads/energiestudie_2017.pdf?__blob=publicationFile&v=5

Blombach, B., Seibold, G. M. 2010. Carbohydrate metabolism in *Corynebacterium glutamicum* and applications for the metabolic engineering of L-lysine production strains. *Appl. Microbiol. Biotechnol.* 86, 1313 – 1322

Bolen, P. L., Roth, K. A., Freer, S. N. 1986. Affinity purifications of aldose reductase and xylitol dehydrogenase from the xylose-fermenting yeast *Pachysolen tannophilus. Appl. Environ. Microbiol.* 52 (4), 660 – 664

Bott, M. 2007. Offering surprises: TCA cycle regulation in *Corynebacterium glutamicum*. *Trends Microbiol.* 15 (9), 417 – 425

Bruinenberg, P. M., Peter, H. M., van Dijken, J. P., Scheffers, W. A. 1983. The role of redox balances in the anaerobic fermentation of xylose by yeasts. *Eur. J. Appl. Microb. Biotech.* 18, 287 – 292

Chen, W. P. 1980. Glucose isomerase (a review). *Process. Biochem.* 15, 30 – 41

Climent, M. J., Corma, A., Iborra, S., 2011. Converting carbohydrates to bulk chemicals and fine chemicals over heterogenous catalysts. *Green Chem*. 13 (3), 520 – 540

Dahms, A. S., Donald, A. 1982. D-xylo-aldonate dehydratase. *Meth. Enzymol*. 90, 302 – 305

Eggeling, L., Bott, M. 2005. Handbook of *Corynebacterium glutamicum*. Taylor & Francis, Boca Raton

Eggeling, L., Bott, M. 2015. A giant market and a powerful metabolism: L-lysin provided by *Corynebacterium glutamicum*. *Appl. Microbiol. Biotechnol*. 99, 3387 – 3394

FAO (Food and Agriculture Organization). 2018. World Food and Agriculture – Statistical Pocketbook 2018. Rome. 1 – 254. License: CC BY-NC-SA 3.0 IGO

FitzPatrick, M., Champagne, P., Cunningham, M. F., Whitney, R. A. 2010. A biorefinery processing perspective: Treatment of lignocellulosic materials for the production of value-added products. *Bioresour. Technol*. 101, 8915 – 8922

Gao, J., Hou, H., Zhai, Y., Woodward, A., Vardoulakis, S., Kovats, S., Wilkinson, P., Li, L., Song, X., Xu, L., Meng, B., Liu, X., Wang, J., Zhao, J., Liu, Q. 2018.

Greenhouse gas emissions reduction in different economic sectors: Mitigation measures, health co-benefits, knowledge gaps, and policy implications. *Environm. Pollut.* 240, 683 – 698

Harhangi, H. R., Akhmanova, A. A., Emmens, R., Van der Drift, C., de Laat, W. T., van Dijken, J. P., Jetten, M. S., Pronk, J. T., Op den Camp, H. J. 2003. Xylose metabolism in the anaerobic fungus *Piromyces sp*. Strain E2 follows the bacterial pathway. *Arch. Microbiol*. 180 (2), 134 – 141

IEA (International Energy Agency). 2018. World energy statistics 2018 [Internet]. September 2018 [cited on 02/05/2019]. URL: https://webstore.iea.org/world-energy-statistics-2018

Ieong, K. W., Uzun, U., Selmer, M., Ehrenberg, M., 2016. Two proofreading steps amplify the accuracy of genetic code translation. PNAS 113 (48) 13744 – 13749

Ikeda, M. (2006) Towards bacterial strains overproducing L-tryptophan and other aromatics by metabolic engineering. *Appl. Microbiol. Biotechnol*. 69, 615

Jo, J-H., Seol, H-Y., Lee, Y-B., Kim, M-H., Hyun, H-H., Lee, H-H. (2012). Disruption of genes for the enhanced biosynthesis of α-ketoglutarate in *Corynebacterium glutamicum*. *Can. J. Microbiol.* 58, 278 – 286

Johnsen, U., Dambeck, M., Zaiss, H., Fuhrer, T., Soppa, J., Sauer, U., Schönheit, P. 2009. D-xylose degradation pathway in the halophilic archaeon *Haloferax volcanii*. *J. Biol. Chem*. 284 (40), 27290 – 27303

Kalinowski, J., Bathe, B., Bartels, D., Bischoff, N., Bott, M., Burkovski, A., Dusch, N., Eggeling, L., Eikmanns, B. J., Gaigalat, L., Goesmann, A., Hartmann, M., Huthmacher, K., Kramer, R., Linke, B., McHardy, A. C., Meyer, F., Mockel, B., Pfefferle, W., Puhler, A., Rey, D. A., Ruckert, C., Rupp, O., Sahm, H., Wendisch, V. F., Wiegrabe, I., Tauch, A. 2003. The complete *Corynebacterium glutamicum* ATCC 13032 genome sequence and its impact on the production of L-aspartate-derived amino acids and vitamins. *J. Biotechnol.*104, 5 – 25

Kallscheuer, N., Vogt, M., Stenzel, A., Gätgens, J., Bott, M., Marienhagen, J., 2016. Construction of a *Corynebacterium glutamicum* platform strain for the production of stilbenes and (2S)-flavanones. *Metab. Eng.* 38, 47 – 55

Kallscheuer, N., Vogt, M., Bott, M., Marienhagen, J., 2017. Functional expression of plant derived *O*-methyltransferase, flavone 3-hydroxylase, and flavonol synthase in *Corynebacterium glutamicum* for production of pterostilbene, kaemperol, and quercetin. *J. Biotechnol.* 258, 190 – 196

Kawaguchi, H., Vertes, A. A., Okino, S., Inui, M., Yukawa, H. (2006) Engineering of a xylose metabolic pathway in *Corynebacterium glutamicum*. *Appl. Environ. Microbiol.* 72, 3418 – 3428

Kawaguchi, H., Sasaki, M., Vertes, A. A., Inui, M., Yukawa, H. (2008) Engineering of an L-arabinose metabolic pathway in *Corynebacterium glutamicum*. *Appl. Microbiol. Biotechnol.* 77, 1053 – 1062

Kinoshita, S., Nakayama, K., Akita, S. 1957. Taxonomical study of glutamic acid accumulating bacteria, *Micrococcus glutamicus Nov-Sp. Agr. Chem. Soc. Japan* 22 (3), 176 – 185

Klaffl, S., Brocker, M., Kalinowski, J., Eikmanns, B. J., Bott, M. 2013. Complex regulation of the phosphoenolpyruvate carboxykinase gene *pck* and characterization of its GntR-type regulator IolR as a repressor of *myo*-inositol utilization genes in *Corynebacterium glutamicum*. *J. Bacteriol*. 195, 4283 – 4296

Langeveld, J. W. A., Dixon, J., Jaworski, J. F. 2010. Development perspectives of the biobased economy: A review. *Crop Sci*. 50, 142 – 151

Mosier, N., Wyman, C., Dale, B., Elander, R., Lee, Y. Y., Holtzapple, M., Ladisch, M. 2005. Features of promising technologies for pretreatment of lignocellulosic biomass. *Bioresour. Technol*. 96, 673 – 686

NOAA (National Centers for Environmental Information) State of the Climate: Global Climate Report for Annual 2017, published online January 2018, retrieved on February 05, 2019 from URL: https://www.ncdc.noaa.gov/sotc/global/201713

IPCC (Intergovernmental Panel on Climate Change). 2014. Climate change 2014: Synthesis report. Contribution of working groups I, II and III to the fifth assessment report of the intergovernmental panel on climate change. [Core Writing Team, R. K. Pachauri and L. A. Meyer (eds)] *IPCC, Geneva Switzerland,* 1 – 151

Pátek, M., Nešvera, J. (2013) Promoters and plasmid vectors of *Corynebacterium glutamicum*. In *Corynebacterium glutamicum* Biology and Biotechnology, Volume 23 of the series Microbiology Monographs, Springer, pp. 51-88

Patrick, J. W., Lee, N. 1968. Purification and properties of an L-arabinose isomerase from *Escherichia coli. J. Biol. Chem.* 243 (16), 4312 – 4318

Radek, A., Krumbach, K., Gätgens, J., Wendisch, V. F., Wiechert, W., Bott, M., Noack, S., Marienhagen, J. 2014. Engineering of *Corynebacterium glutamicum* for minimized carbon loss during utilization of D-xylose containing substrates. *J. Biotechnol.* 192, 156 – 160

Rizzi, M., Erlemann, P., Bui-Thahn, N-A., Dellweg, H. 1988. Xylose fermentation by yeasts. 4. Purification and kinetic studies of xylose reductase from *Pichia stipites. Appl. Microbiol. Biotechnol.* 29, 148 – 154

Rizzi, M., Harwart, K., Erlemann, P., Bui-Thahn, N-A., Dellweg, H. 1989. Purification and properties of the NAD^+ xylitol-dehydrogenase from the yeast *Pichia stipitis. J. Ferment. Bioeng.* 67, 20 – 24

Rubin, E. M. 2008. Genomics of cellulosic biofuels. *Nature* 454, 841 – 845

Sahm, H., Eggeling, L., de Graaf, A. A. 2000. Pathway analysis and metabolic engineering in *Corynebacterium glutamicum*. *Biol. Chem.* 381, pp. 899 – 910

Sanders, J., Scott, E., Weusthuis, R., Mooibroek, H. 2007. Bio-refinery as the bio-inspired process to bulk chemicals. *Macromol. Biosci*. 7, 105 – 117

Stephens, C., Christen, B., Fuchs, T., Sundaram, V., Watanabe, K., Jenal, U. 2007. Genetic analysis of a novel pathway for D-xylose metabolism in *Caulobacter crescentus. J. Bacteriol.* 189 (5), 2181 – 2185

Toivari, M. H., Nygard, Y., Penttila, M., Ruohonen, L., Wiebe, M. G., 2012. Microbial D-xylonate production. *Appl. Microbiol. Biotechnol*. 96 (1), 1 – 8

Usuda, Y., Tujimoto, N., Abe, C., Asakura, Y., Kimura, E., Kawahara, Y., Kurahashi, O., Matsui, H. 1996. Molecular cloning of the *Corynebacterium glutamicum* (‘*Brevibacterium lactofermentum*’ AJ12036) *odhA* gene encoding a novel type of 2-oxoglutarate dehydrogenase. *Microbiology* 142, 3347 – 3354

Vogt, M., Brüsseler, C., Ooyen, J. v. Bott, M., Marienhagen, J. 2016. Production of 2-methyl-1-butanol and 3-methyl-1-butanol in engineered *Corynebacterium glutamicum. Metab. Eng.* 38, 436 – 445

Vongsuvanlert, V., Tani, Y. 1988. Purification and characterization of xylose isomerase of a methanol yeast, *C. boidinii*, which is involved in sorbitol production from glucose. *Agric. Biol. Chem.* 52, 1817 – 1824

Wang, V. W., Jeffries, T. 1990. Purification and properties of xylitol dehydrogenase from the xylose-fermenting *Candida shehatae. Appl. Biochem. Biotechnol.* 26, 197 – 206

Weimberg, R. 1961. Pentose oxidation by *Pseudomonas fragi. J. Biol. Chem.* 236, 629 – 635

Wendisch, V., Eberhardt, D., Herbst, M., Jensen, J. (2014) Biotechnological Production of Amino acids and nucleotides. In: Biotechnological production of natural ingredients for food industry, Bentham Science eBooks, pp. 60 – 163.

Wieschalka, S., Blombach, B., Bott, M., Eikmanns, B. J. 2013. Bio-based production of organic acids with *Corynebacterium glutamicum. Microb. Biotechnol.* 6 (2), 87 – 102

4. Appendix

4.1 Authors‘ Contributions

1.) Radek, A., Tenhaef, N., Müller, M. F., Brüsseler, C., Wiechert, W., Marienhagen, J., Polen, T., Noack, S. (2017). Miniaturized and automated adaptive laboratory evolution: Evolving *Corynebacterium glutamicum* towards an improved D-xylose utilization. *Bioresource Technology*, 245: 1377-1385.

CB analyzed the genome sequencing data together with TP, constructed the plasmid and strains and wrote 10 % of the manuscript. AR developed the automated and miniaturized ALE approach and wrote 45 % of the manuscript. NT applied the new ALE method to the D-xylose utilizing strains and wrote 45 % of the manuscript. MM performed lab-scale bioreactor cultivations. WW and JM contributed to manuscript preparation. SN conceived the study and revised the manuscript.

Overall contribution CB: 20 %

2.) Brüsseler, C., Radek, A., Tenhaef, N., Krumbach, K., Noack, S., Marienhagen, J. (2018). The *myo*-inositol/proton symporter IolT1 contributes to D-xylose uptake in *Corynebacterium glutamicum*. *Bioresource Technology*, 249: 953-961.

CB constructed the plasmids and strains, performed the cultivation experiments of strains using the Weimberg pathway for D-xylose utilization and wrote the manuscript. AR, NT and KK characterized the *iolR*-deletion strains and analyzed the GC-TOF-MS and HPLC data. SN contributed to the figure preparation and revised the manuscript together with JM.

Overall contribution CB: 80 %

3.) Tenhaef, N*., Brüsseler, C*., Radek, A., Hilmes, R., Pornkamol, U., Marienhagen, J., Noack, S. (2018). Production of D-xylonic acid using a non-recombinant *Corynebacterium glutamicum* strain. *Bioresource Technology*, 268: 332-339.

*Shared first coauthorship

CB performed HPLC analysis, constructed the plasmids and strains, performed shake-flask cultivations and wrote 50 % of the manuscript. NT (shared first author) performed the media development for utilization of sugarcane bagasse in *Corynebacterium glutamicum*, performed the sequential hydrolysis and fermentation process using sugarcane bagasse and wrote 50 % of the manuscript. AR performed lab-scale bioreactor cultivations. RH constructed the in-frame deletion plasmid for the gluconate permease (*gntP*), the plasmid for the complementation of the *myo*-inositol-2-dehydrogenase (*iolG*) and contributed to shake-flask cultivations. UP performed pretreatment of bagasse. JM and SN revised the manuscript.

Overall contribution CB: 40 %

Brüsseler, C., Späth, A., Sokolowsky, S., Marienhagen, J. (2019). Alone at last! – Heterologous expression of a single gene is sufficient for establishing the five-step Weimberg pathway in *Corynebacterium glutamicum*. Submitted to *Metabolic Engineering Communications*

CB performed the literature and database search, conducted the sequence comparison and prediction of the secondary structures, constructed the strains and plasmids, performed microbioreactor cultivations, analyzed the enzyme kinetic data and wrote the manuscript. AS contributed to cloning work and performed shake-flask cultivations. SS carried out the protein purification and performed the enzyme assay. JM revised the manuscript.

Overall contribution CB: 90 %

4.2 Patent application

1.) Brüsseler, C., Tenhaef, N., Marienhagen, J., Noack, S. (26.02.2018). Patentanmeldung PT 0.3143: „Verfahren zur verbesserten fermentativen Herstellung von D-Xylonat unter Verwendung coryneformer Bakterien“

Danksagung

Bei **Herrn Prof. Dr. Michael Bott** bedanke ich mich für die Überlassung dieses spannenden Projektes, das stetige Interesse am Fortgang meiner Arbeit sowie für die Übernahme des Erstgutachtens.

Prof. Dr. Karl-Erich Jaeger danke ich für die Übernahme des Zweitgutachtens und die Bereitschaft, die Arbeit als Mentor zu begleiten.

Besonders bedanken möchte ich mich bei **Prof. Dr. Jan Marienhagen** für die stets informativen und motivierenden Diskussionen, die Unterstützung beim Schreiben von Publikationen und die engagierte Betreuung der Arbeit.

Dr. Michael Vogt möchte ich für die hervorragende Betreuung und Einarbeitung zu Beginn meiner Zeit im Institut und die Unterstützung in der Anfangszeit dieses Projektes danken.

Anja Späth und **René Hilmes** danke ich für die sehr gute Mitarbeit an diesem Projekt, die vielen wichtigen Daten, Schlussfolgerungen und den damit verbundenen wertvollen Beitrag für diese Doktorarbeit.

Dr. Nicolai Kallscheuer danke ich für die vielen intensiven Diskussionen, Hilfestellungen und das ständige Interesse am Fortgang dieses Projektes.

Der gesamten Arbeitsgruppe „**Synthetische Zellfabriken**“ danke ich für die tolle Arbeitsatmosphäre und die ständige Hilfsbereitschaft untereinander.

Bei **Dr. Stephan Noack, Niklas Tenhaef, Prof. Dr. Gunnar Lidén, Dr. Lisa Wasserstrom, Celina Tufvegren, Dr. Henrik Almqvist, Dr. Jinrui Zhang, Prof. Dr. Marie Francoise Gorwa Grauslund, Prof. Dr. Aljoscha Wahl** bedanke ich mich für die schönen Projektmeetings, den regen Austausch und der guten Zusammenarbeit.

Dem gesamten **Institut für Biotechnologie und Geowissenschaften (IBG-1)** danke ich für das tolle Miteinander und der ständigen Hilfsbereitschaft bei administrativen und fachlichen Fragestellungen.

Mein größter Dank gilt **meiner Familie** für ihre ständige Unterstützung in jeder Lebenslage.

Erklärung

Ich versichere an Eides Statt, dass die Dissertation von mir selbständig und ohne unzulässige fremde Hilfe unter Beachtung der „Grundsätze zur Sicherung guter wissenschaftlicher Praxis an der Heinrich-Heine-Universität Düsseldorf“ erstellt worden ist. Die Dissertation wurde in der vorgelegten oder ähnlichen Form noch bei keiner anderen Institution eingereicht. Ich habe bisher keine erfolglosen Promotionsversuche unternommen.

Jülich, den 25.02.2019

Christian Brüsseler

Band / Volume 184
Translation Initiation with 70S Ribosomes: A Single Molecule Study
C. Remes (2018), iv, 113 pp
ISBN: 978-3-95806-358-7

Band / Volume 185
Scanning tunneling potentiometry at nanoscale defects in thin films
F. Lüpke (2018), iv, 144 pp (untersch. Pag.)
ISBN: 978-3-95806-361-7

Band / Volume 186
Inelastic neutron scattering on magnetocaloric compounds
N. Biniskos (2018), iii, 92 pp
ISBN: 978-3-95806-362-4

Band / Volume 187
Magnetic Order and Excitation in Frustrated Pyrochlore 5d - Transition Metal Oxides
E. Feng (2018), iv, 182 pp
ISBN: 978-3-95806-365-5

Band / Volume 188
Finite-Difference Time-Domain Simulations Assisting to Reconstruct the Brain's Nerve Fiber Architecture by 3D Polarized Light Imaging
M. Menzel (2018), ix, 296 pp
ISBN: 978-3-95806-368-6

Band / Volume 189
Characterization of the cell-substrate interface using surface plasmon resonance microscopy
E. M. Kreysing (2018), xiii, 260 pp
ISBN: 978-3-95806-369-3

Band / Volume 190
Scattering! Soft, Functional and Quantum Materials
Lecture Notes of the 50th IFF Spring School 2019
11 – 22 March 2019, Jülich, Germany
ed. by M. Angst, T. Brückel, S. Förster, K. Friese, R. Zorn (2019),
ca 1000 pp
ISBN: 978-3-95806-380-8

Band / Volume 191
Absolute scale off-axis electron holography of thin dichalcogenide crystals at atomic resolution
F. Winkler (2019), xxiii, 187 pp
ISBN: 978-3-95806-383-9

Band / Volume 192
High-resolution genome and transcriptome analysis of *Gluconobacter oxydans* 621H and growth-improved strains by next-generation sequencing
A. Kranz (2019), III, 182 pp
ISBN: 978-3-95806-385-3

Band / Volume 193
Group IV (Si)GeSn Light Emission and Lasing Studies
D. Stange (2019), vi, 151 pp
ISBN: 978-3-95806-389-1

Band / Volume 194
Construction and analysis of a spatially organized cortical network model
J. Senk (2019), 245 pp
ISBN: 978-3-95806-390-7

Band / Volume 195
Large-scale Investigations of Non-trivial Magnetic Textures in Chiral Magnets with Density Functional Theory
M. Bornemann (2019), 143 pp
ISBN: 978-3-95806-394-5

Band / Volume 196
Neutron scattering
Experimental Manuals of the JCNS Laboratory Course held at Forschungszentrum Jülich and at the Heinz-Maier-Leibnitz Zentrum Garching
edited by T. Brückel, S. Förster, G. Roth, and R. Zorn (2019),
ca 150 pp
ISBN: 978-3-95806-406-5

Band / Volume 197
Topological transport in non-Abelian spin textures from first principles
P. M. Buhl (2019), vii, 158 pp
ISBN: 978-3-95806-408-9

Band / Volume 198
Shortcut to the carbon-efficient microbial production of chemical building blocks from lignocellulose-derived D-xylose
C. Brüsseler (2019), X, 62 pp
ISBN: 978-3-95806-409-6

Weitere ***Schriften des Verlags im Forschungszentrum Jülich*** unter
http://wwwzb1.fz-juelich.de/verlagextern1/index.asp

Schlüsseltechnologien / Key Technologies
Band / Volume 198
ISBN 978-3-95806-409-6

Mitglied der Helmholtz-Gemeinschaft

JÜLICH
Forschungszentrum